

NO-A100 012

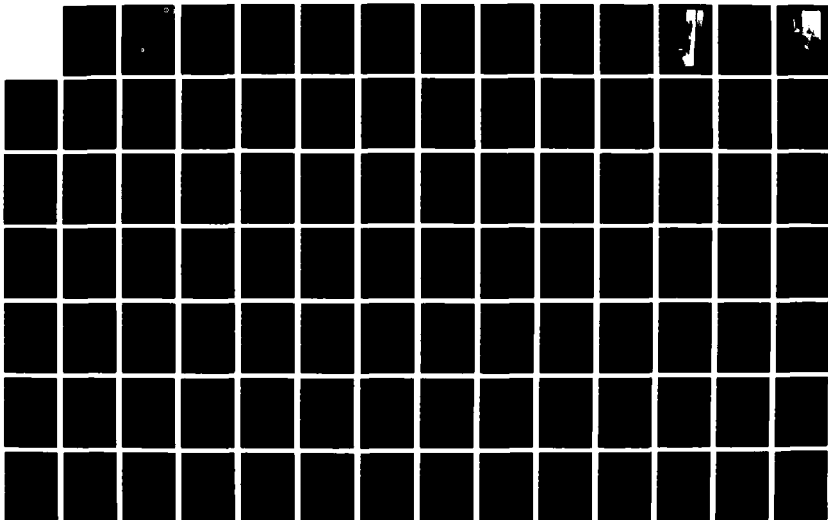
VECTOR ELECTRIC FIELDS MEASURED IN A LIGHTNING  
ENVIRONMENT(U) NAVAL RESEARCH LAB WASHINGTON DC  
R V ANDERSON ET AL. 07 APR 87 NRL-NR-5899

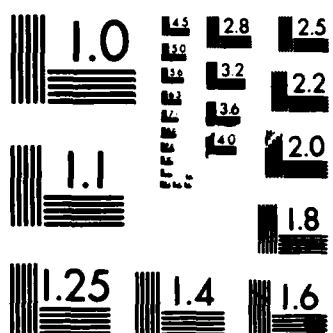
1/2

UNCLASSIFIED

F/G 4/1

NL





MICROCOPY RESOLUTION TEST CHART  
NATIONAL BUREAU OF STANDARDS 1963-A



2

NRL Memorandum Report 5899

# Vector Electric Fields Measured in a Lightning Environment

R.V. ANDERSON AND J.C. BAILEY

*Atmospheric Physics Branch  
Space Sciences Division*

April 7, 1987

AD-A180 012

DTIC  
ELECTE  
APR 30 1987  
S D

AD-A180012

SECURITY CLASSIFICATION OF THIS PAGE

## REPORT DOCUMENTATION PAGE

1a REPORT SECURITY CLASSIFICATION UNCLASSIFIED			1b RESTRICTIVE MARKINGS		
2a SECURITY CLASSIFICATION AUTHORITY			3 DISTRIBUTION/AVAILABILITY OF REPORT		
1b DECLASSIFICATION/DOWNGRADING SCHEDULE			Approved for public release; distribution unlimited.		
4 PERFORMING ORGANIZATION REPORT NUMBER(S) NRL Memorandum Report 5899			5 MONITORING ORGANIZATION REPORT NUMBER(S)		
6a NAME OF PERFORMING ORGANIZATION Naval Research Laboratory	6b OFFICE SYMBOL (If applicable) Code 4110	7a NAME OF MONITORING ORGANIZATION			
6c ADDRESS (City, State, and ZIP Code) Washington, DC 20375-5000			7b ADDRESS (City, State, and ZIP Code)		
8a NAME OF FUNDING/SPONSORING ORGANIZATION Office of Naval Research	8b OFFICE SYMBOL (If applicable)	9 PROCUREMENT INSTRUMENT IDENTIFICATION NUMBER			
8c ADDRESS (City, State, and ZIP Code) Arlington, VA 22217		10 SOURCE OF FUNDING NUMBERS			
		PROGRAM ELEMENT NO 61153N	PROJECT NO RR033-03-042	TASK NO	WORK UNIT ACCESSION NO
11 TITLE (Include Security Classification) Vector Electric Fields Measured in a Lightning Environment					
12 PERSONAL AUTHOR(S) Anderson, R.V. and Bailey, J.C.					
13a TYPE OF REPORT	13b TIME COVERED FROM TO	14 DATE OF REPORT (Year, Month, Day) 1987 April 7		15 PAGE COUNT 105	
16 SUPPLEMENTARY NOTATION					
17 COSATI CODES			18 SUBJECT TERMS (Continue on reverse if necessary and identify by block number)		
FIELD	GROUP	SUB-GROUP			
19 ABSTRACT (Continue on reverse if necessary and identify by block number)					
<p>The measurement of vector electric fields from an aircraft which is struck by lightning can provide information on lightning initiation and triggering processes. Calibration of the aircraft to determine geometric field enhancements and to separate the vector components, although difficult, has been accomplished. Data from 31 strikes in the summer of 1985 are presented in three formats. The raw fields measured at the four field meters are presented both to indicate proper operation and because strikes to the wing tips may be strongly related to the local field at the wing tips. The three cartesian vector components of field and the aircraft voltage (with respect to its immediate environment) are next shown followed finally by an azimuth-elevation-magnitude presentation which appears useful for triggering studies.</p>					
20 DISTRIBUTION/AVAILABILITY OF ABSTRACT <input checked="" type="checkbox"/> UNCLASSIFIED/UNLIMITED <input type="checkbox"/> SAME AS RPT <input type="checkbox"/> DTIC USERS			21 ABSTRACT SECURITY CLASSIFICATION UNCLASSIFIED		
2a NAME OF RESPONSIBLE INDIVIDUAL R.V. Anderson			22b TELEPHONE (Include Area Code) (202) 767-3350		22c OFFICE SYMBOL Code 4110

## CONTENTS

BACKGROUND .....	1
INSTALLATION .....	2
CONCLUSIONS .....	5
ACKNOWLEDGMENTS .....	6
REFERENCES .....	6

Accession For	
NTIS CRA&I	<input checked="" type="checkbox"/>
DTIC TAB	<input type="checkbox"/>
Unannounced	<input type="checkbox"/>
Justification .....	
By .....	
Distribution / .....	
Availability Codes	
Dist	Available / or Special
A-1	



## VECTOR ELECTRIC FIELDS MEASURED IN A LIGHTNING ENVIRONMENT

### BACKGROUND

The lack of reliable quantitative data on lightning strikes to an aircraft in flight prompted the creation of the Direct Strike project, a joint effort of the USAF/FDL, FAA/ACT, NRL, and NASA/KSC with French participation by ONERA as well. An FAA research aircraft, a Convair CV-580, N-49, was hardened for lightning exposure and instrumented to measure and record electric field, field derivative, strike current, current flow in the skin of the aircraft, and turbulence. These installations and participants are shown in the table below, and a more detailed discussion is provided by Rasch and Glynn (1985).

### DIRECT STRIKE PROJECT ORGANIZATION

AGENCY	PARTICIPANTS	MEASUREMENTS
FAA/ACT	N. Rasch M. Glynn D. Lawrence J. Terry	Provision of CV-580 aircraft Aircraft modification and installation Turbulence (vertical) measurement Pilots and maintenance
AFWL/FDL	P. Rustan H. Burket J. Reazer (T/SSI)	Direct current shunts field change (D) Surface current change (B) Photography of aircraft surface
NRL	R. Anderson J. Bailey	Vector electric field Aircraft electric potential

Manuscript approved December 18, 1986.

ONERA	P. Laroche J. P. Moreau	Five electric field meters Surface current change (1 sensor) Field Change (1 sensor)
NASA/KSC USAF/CCAFS		Aircraft refueling Radar tracking Aircraft controller

This aircraft is shown in Figure 1. There were two primary objectives in the program. First, the characteristics of lightning which strikes an aircraft in flight were unknown, with lightning specifications of necessity inferred from a few ground measurements; hence, the current, energy, and waveform of lightning attachment to aircraft were needed for the development of realistic standards. Second, the statistical fact that aircraft in flight are far more likely to be struck than the same aircraft on the ground leads to the hypothesis that a triggering process exists in which the aircraft in flight induces strikes which otherwise would not have occurred. Therefore the second primary objective of the program was to obtain data in the immediate pre- and post-strike period with which to assess this triggering hypothesis. This report is presented as a catalog of available observations from the 1985 campaign for the use of co-workers in the field. Consequently, analysis and conclusions are not presented here but will appear in subsequent reports.

#### INSTALLATION

The measurement of an ambient vector field from an isolated vehicle such as an aircraft requires that four independent unknowns be determined. In addition to the three spatial

components of the field, the vehicle net charge (or equivalently its voltage) is an unknown which affects all field measurements made on the aircraft. Consequently at least four field meters are required in a complete installation. There are geometric considerations which can define optimum sites for field meter locations (see companion report, Bailey and Anderson). These optimum locations are not readily determinable, however, and may not be physically viable for a field meter installation. The four meters therefore were installed at positions as near as possible to reasonable estimates of the optimum locations. These positions were on the two wing tips (P and S), the belly centerline near the nose (F), and the belly centerline near the tail (T) as indicated in Figure 2. Details of the meters and the data recording system are given in the companion report. A typical wing tip installation is shown in Figure 3, and the vector coordinate system attached to the aircraft is seen in Figure 4. The calibration of the aircraft geometry and the separation of the vector components is described in the companion report. The result of this work is the calibration matrix:

$$\begin{aligned}
 E_x &= .0086 E_p + .0086 E_s + .181 E_f - .212 E_t \\
 E_y &= .019 E_p - .019 E_s \\
 E_z &= .024 E_p + .024 E_s - .168 E_f - .080 E_t \\
 V &= .352 E_p + .352 E_s - .065 E_f + .076 E_t
 \end{aligned}$$

where  $E_x$ ,  $E_y$ ,  $E_z$  and the vector components of the external field in the coordinate system of Figure 3,  $V$  is the aircraft



potential, and  $E_p$ ,  $E_s$ ,  $E_f$ ,  $E_t$  are the fields in units of volts per meter at the meter location.

The fields measured at the four meters are plotted in Figures 5-35. The sign convention is that of classical physics ( $E = -\text{grad } V$ ) where a positive field is the result of net positive surface charge density on the aircraft skin at the meter location. Ten seconds of data are shown in each figure, and the exact time of the center is given at the top. In most cases the lightning strike is exactly at this center, but there are a few in which this is not true. In these cases the lightning leaves an unmistakable signature; so there is no ambiguity. Gaps in the plots represent fields which were outside of the linear operating range of the instruments. These direct field values are used as inputs to the calibration matrix, they are useful for triggering analysis by showing the actual field at specific locations, and they are useful in assessment of system operation.

The next group of thirty figures (Figures 36-65) show the cartesian field vector components and the aircraft potential relative to its environment. Only thirty are given because the meter at the starboard wing tip failed during the flight of 29 June. The polarities of the field components are in accordance with the coordinate axes shown in figure 4 where the positive  $x$ ,  $y$ , and  $z$  axes are forward, left, and upward. The time axes are identical to the first set of curves. As mentioned in the companion report, the aircraft potential is shown in preference to charge since it is more accurately known and is equally useful.

The final set of curves (Figures 66-95), show the vector field in the angular azimuth-elevation-magnitude coordinate system defined in Figure 4. It should be noted that this is not a standard polar spherical system, but it is chosen to facilitate interpretation. Initial analysis indicates that this presentation, by giving the field as magnitude and direction, is more easily interpreted in a search for evidence of triggering.

## CONCLUSIONS

There are 31 occasions on which lightning was known to strike the aircraft during the 1985 campaign. Some data is available for each of these events. It was found that data quality improved as experience was obtained and appropriate operating conditions were experimentally determined. The instrument system demonstrated a high level of reliability with only one sensor failure in the entire period.

The accuracy of the data depends on direction and on the ratio of vehicle charge to field. Analysis indicated that the worst case error is of the order  $\pm 20\%$  with many values (most notably the y component) much better than this. A detailed error analysis is contained in the companion report. Work on analysis of this data is continuing; so further conclusions including an assessment of the triggering hypothesis will appear in subsequent reports.

## ACKNOWLEDGMENTS

It is a pleasure to acknowledge the significant contributions of others to the success of the effort. The FAA Atlantic City Technical Center provided the aircraft, modification work, and pilots. Messrs. M. Glynn and N. Rasch provided an invaluable contribution in coordinating the entire effort. Jesse Terry and the other pilots provided skill, responsiveness, and safety without which the project could not have existed. The Air Force Flight Dynamics Laboratory provided extensive instrumentation, funding for flight expenses and the enthusiasm of Maj. P. L. Rustan and 1st Lt Harry Burket. Radar control from PAFB and NASA/KSC as well as essential ground support also were essential to the success of the mission.

## REFERENCES

- J. C. Bailey and R. V. Anderson, "Experimental Calibration of a Vector Electric Field Meter Measurement System on an Aircraft", NRL Memorandum Report 5900, January 1987.
- N. O. Rasch and M. S. Glynn, "Survey of Lightning Hazard and Low Altitude Direct Lightning Strike Program", 10th International Aerospace and Ground Conference on Lightning and Static Electricity, P. Contensou, Chm., les editions de physique, 91944 Les Ulis Cedex, France, pp 247-252.



Fig. 1 — Photograph of CV-580 aircraft

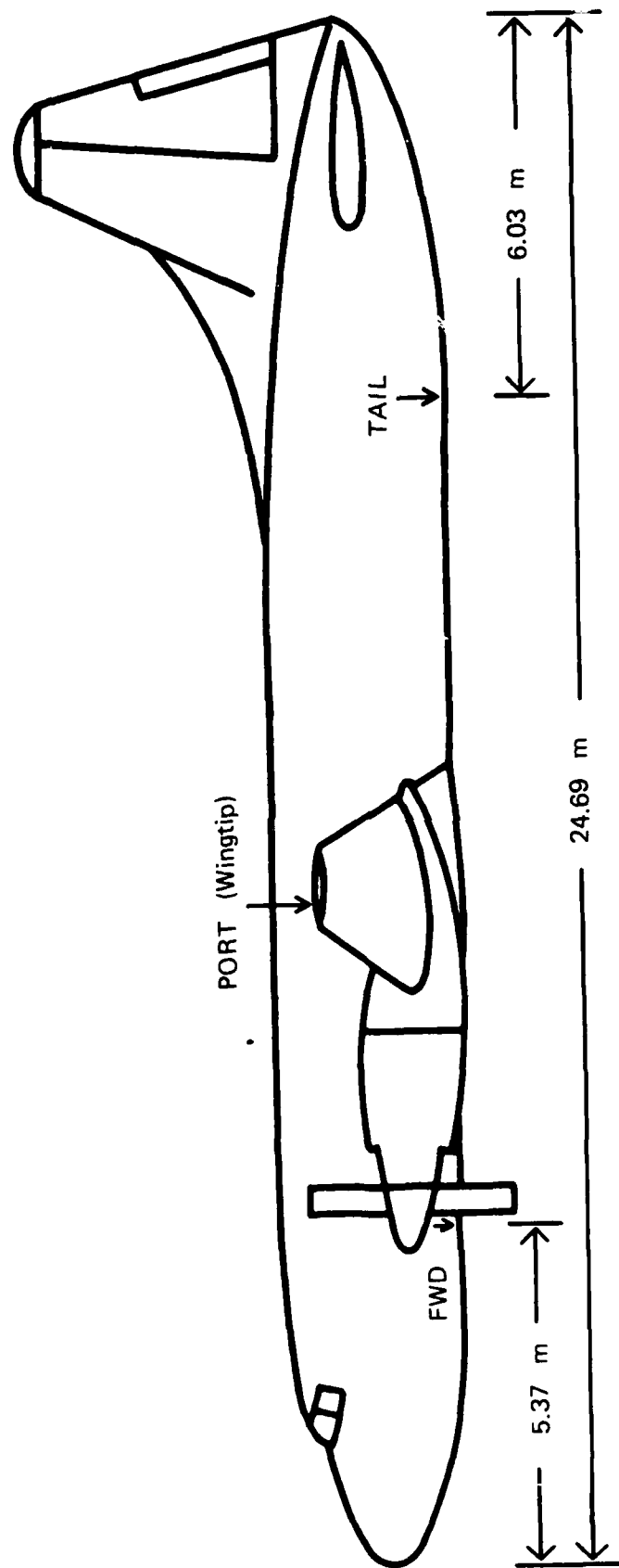


Fig. 2 — Field meter locations on the aircraft



Fig. 3 — Photograph of wing tip field meter installation

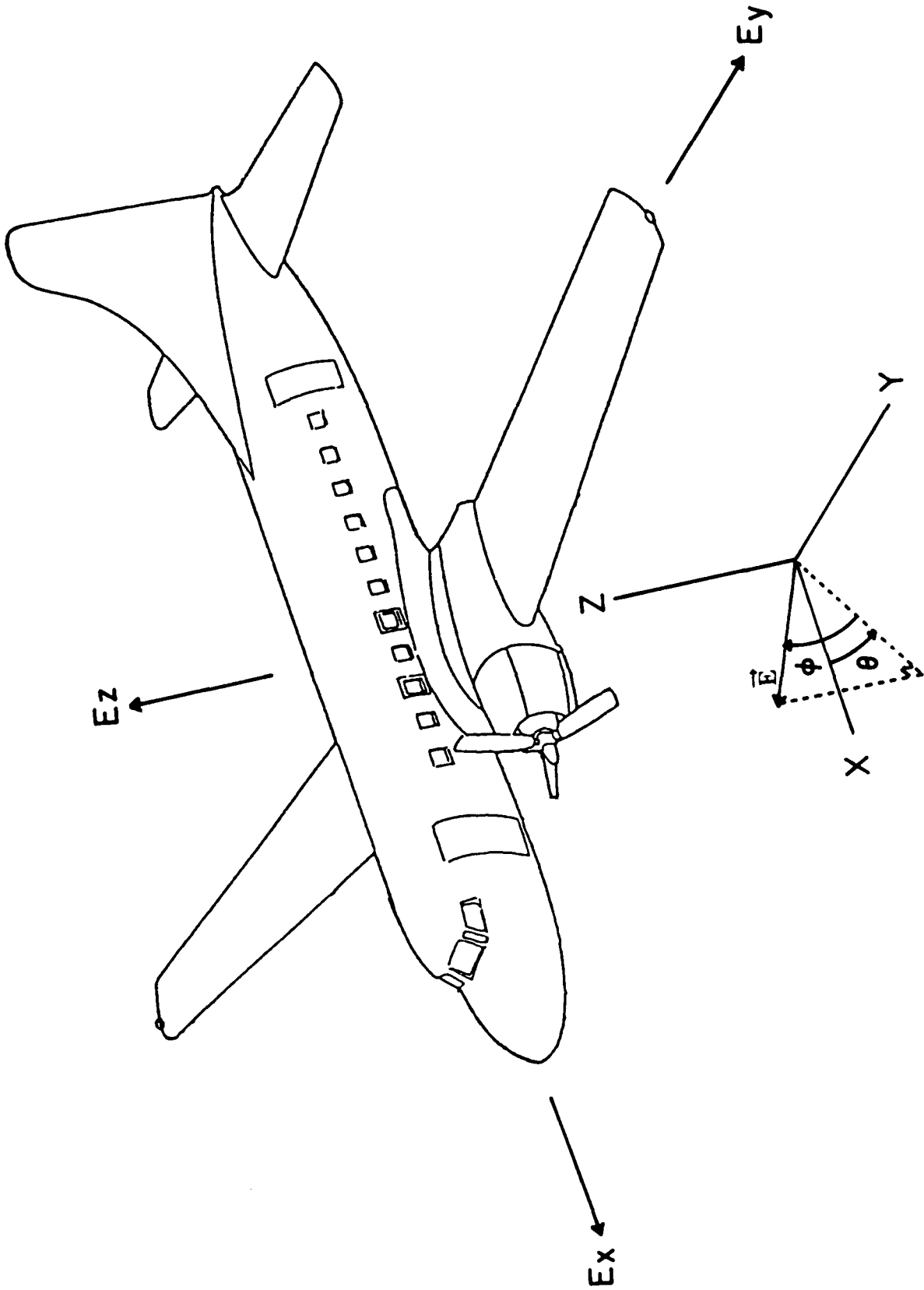


Fig. 4 — Aircraft-based coordinate systems. Cartesian coordinates shown on aircraft drawing and angular system in diagram below.

JUNE2185L3

2021:49.34

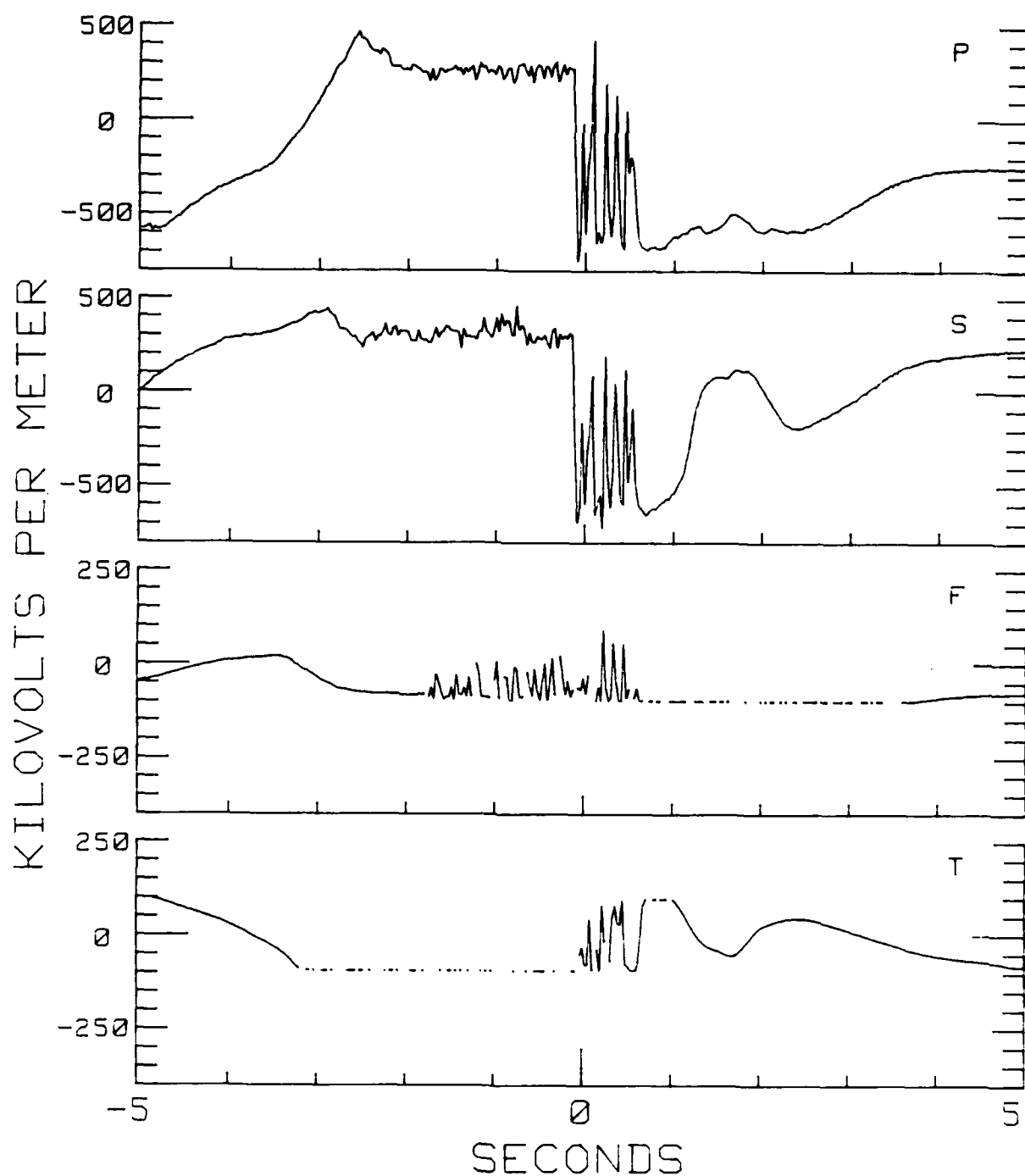


Fig. 5 — Field values at Port, Starboard, Forward, and Tail meters



JUNE2185L3

2109:02.37

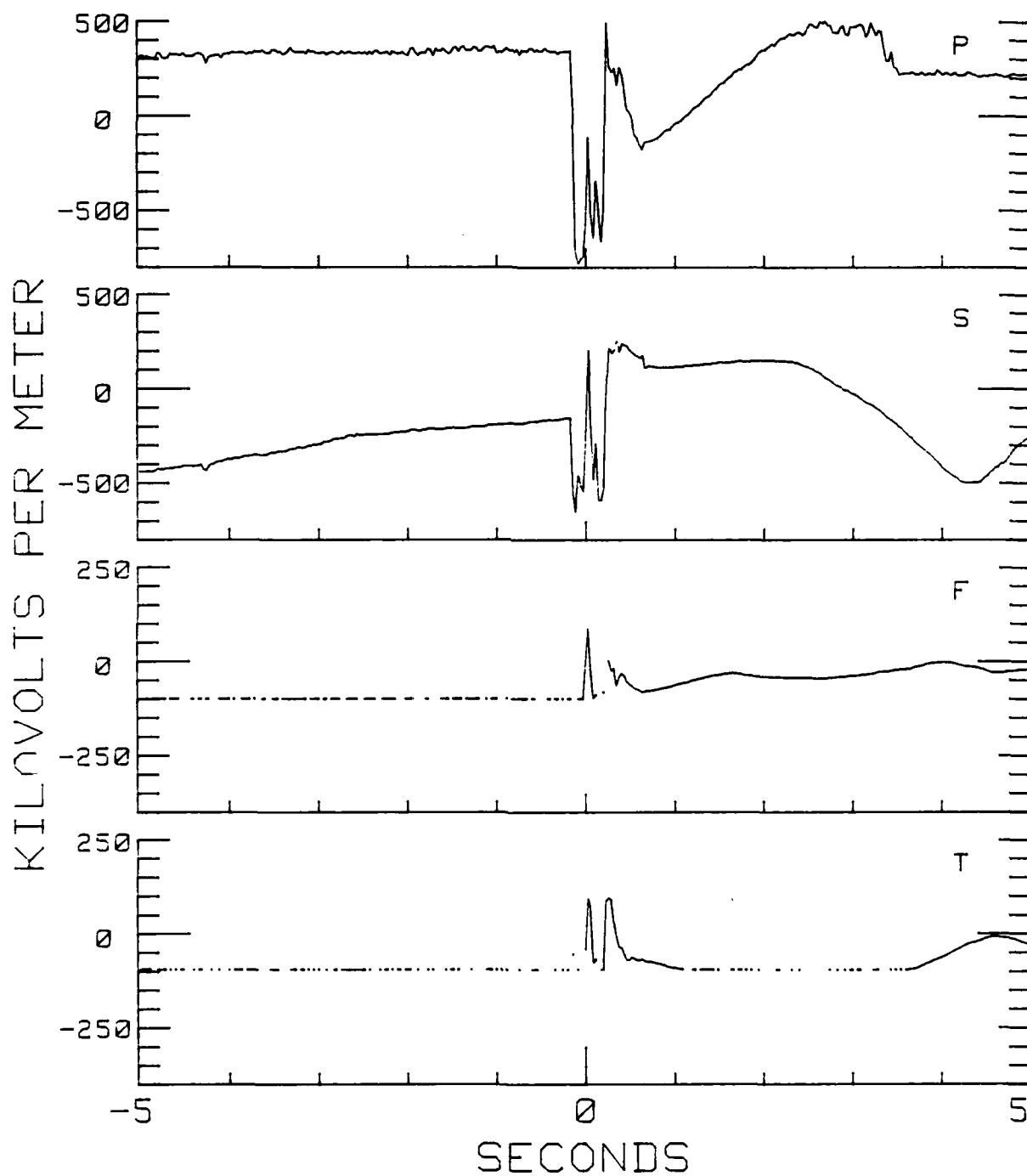


Fig. 6 — Field values at Port, Starboard, Forward, and Tail meters

JUNE2185L3

2118:02.97

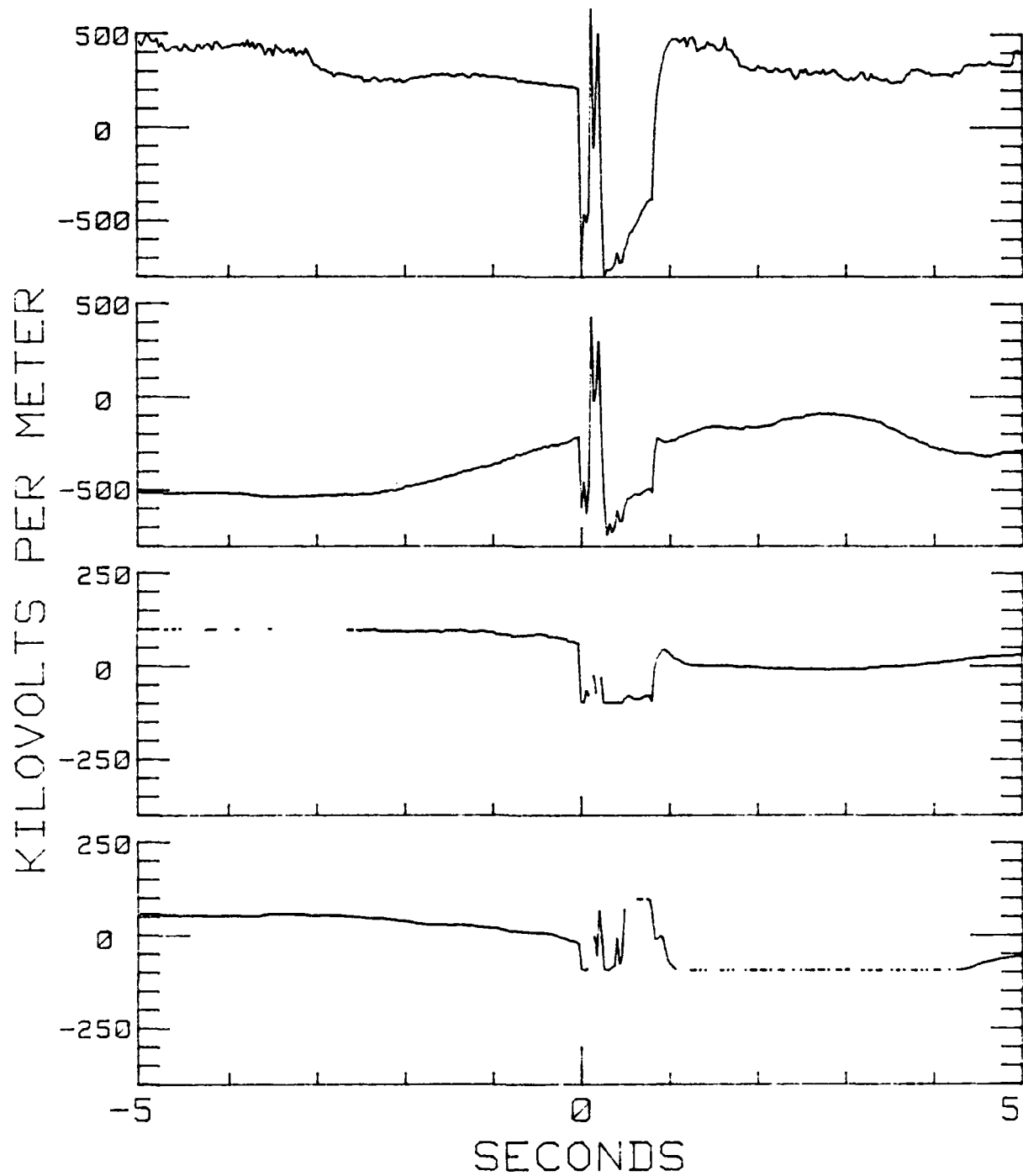


Fig. 7 — Field values at Port, Starboard, Forward, and Tail meters

JUNE2685L3

2040:29.71

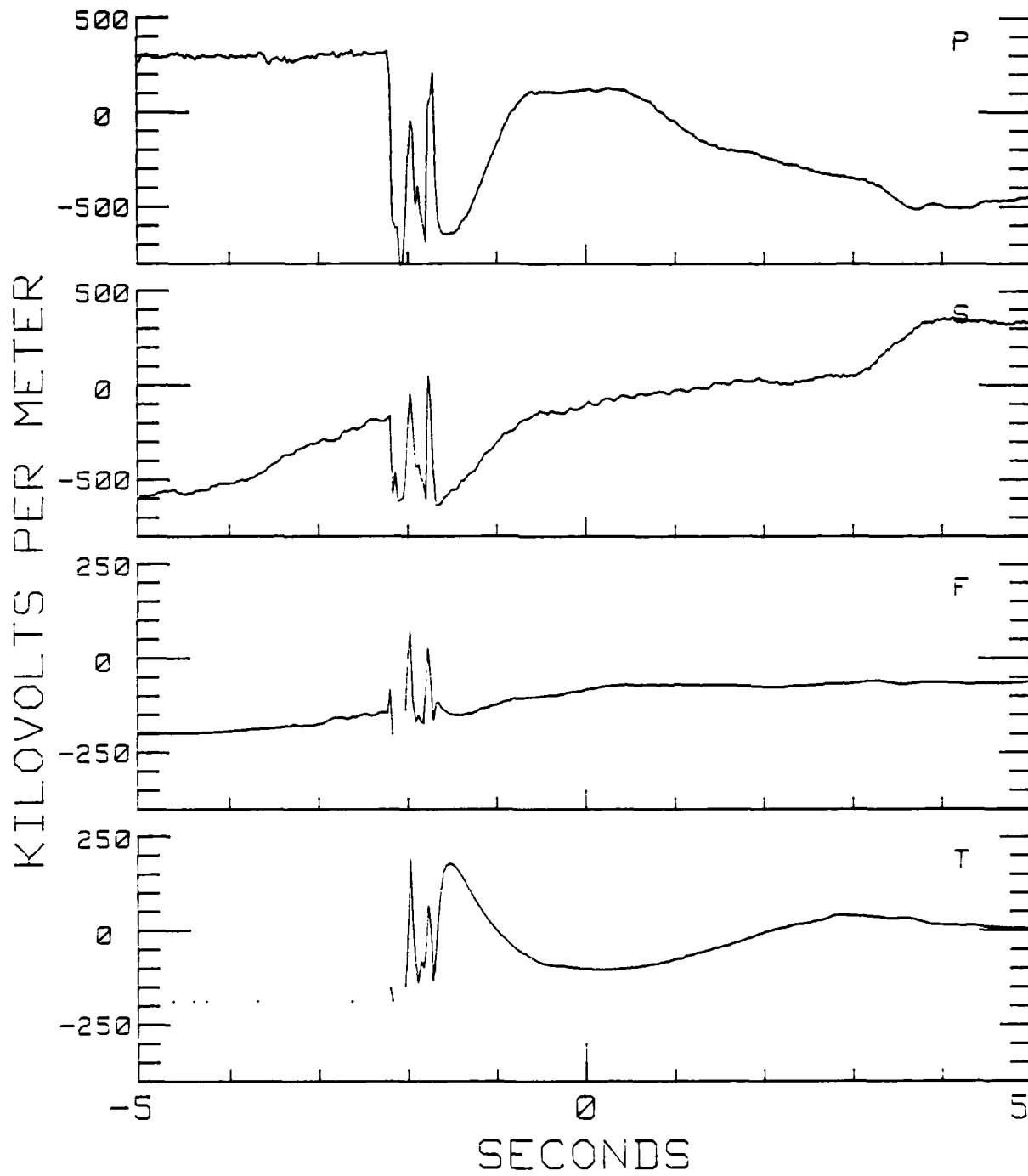


Fig. 8 — Field values at Port, Starboard, Forward, and Tail meters

JUNE2685L3

2055:24.46

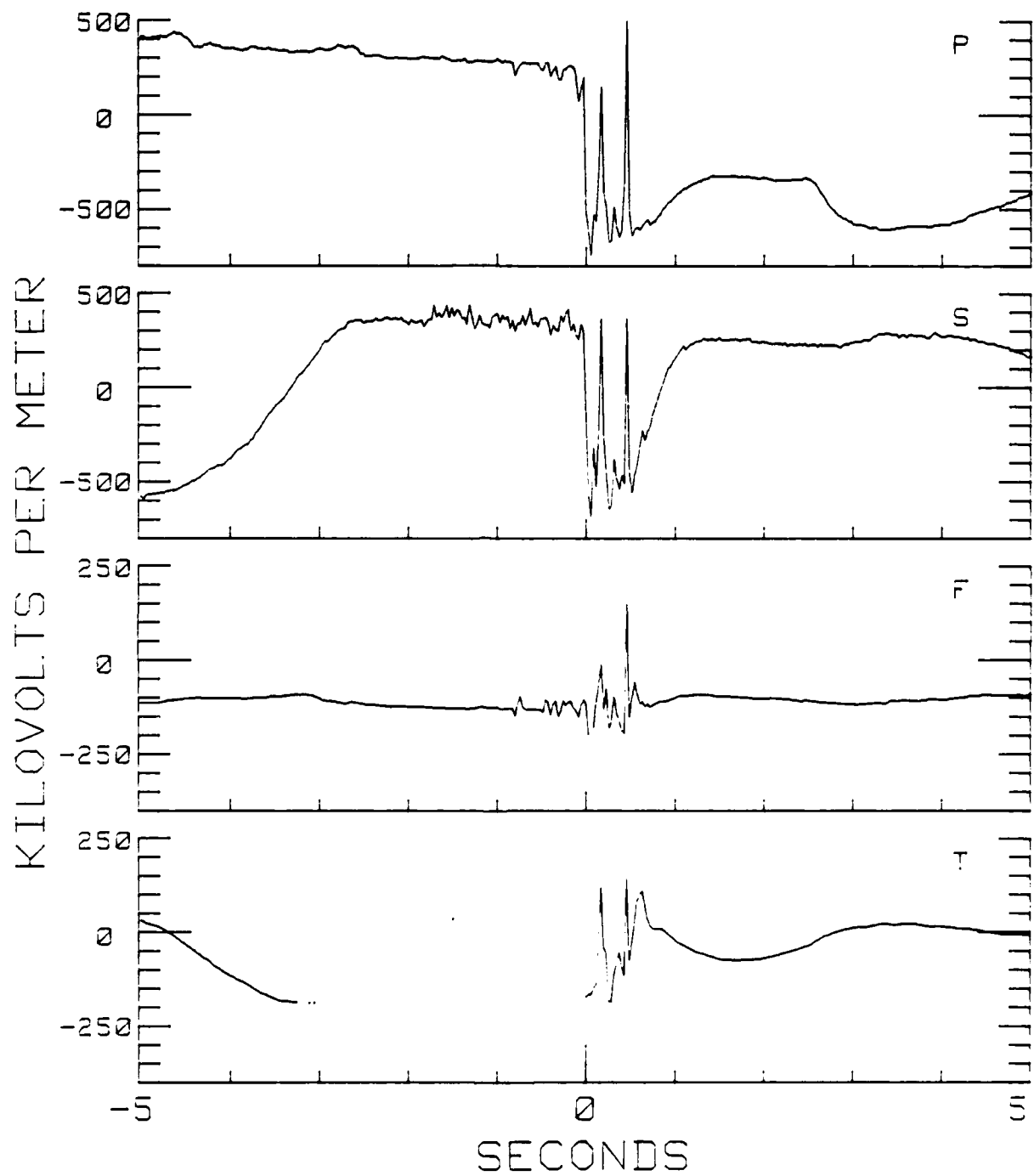


Fig. 9 — Field values at Port, Starboard, Forward, and Tail meters

JUNE2685L3

2100:15.94

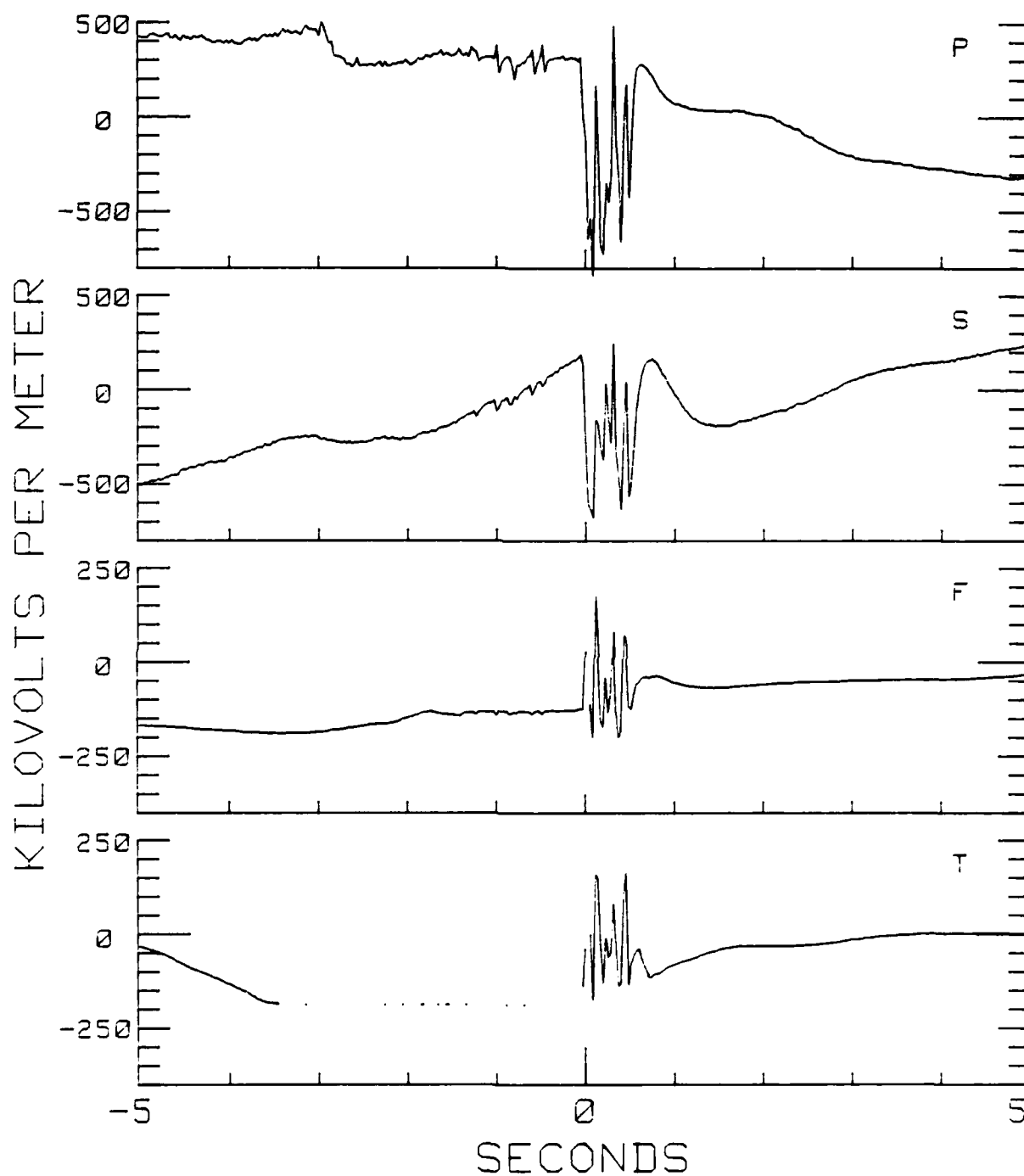


Fig. 10 — Field values at Port, Starboard, Forward, and Tail meters

JUNE 27 85L2

1940:18.17

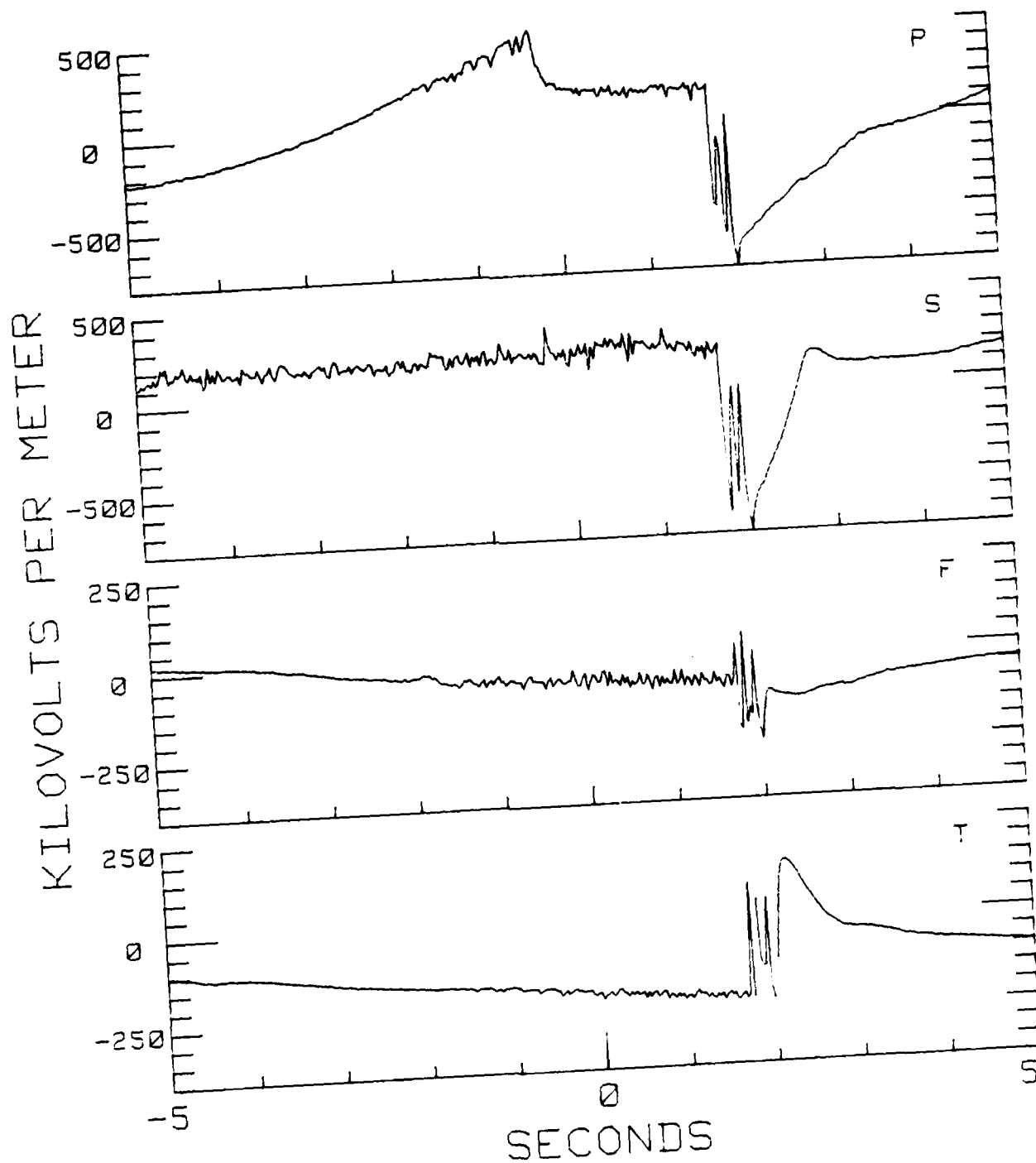


Fig. 11 — Field values at Port, Starboard, Forward, and Tail meters

JUNE2785L2

2032:43.6

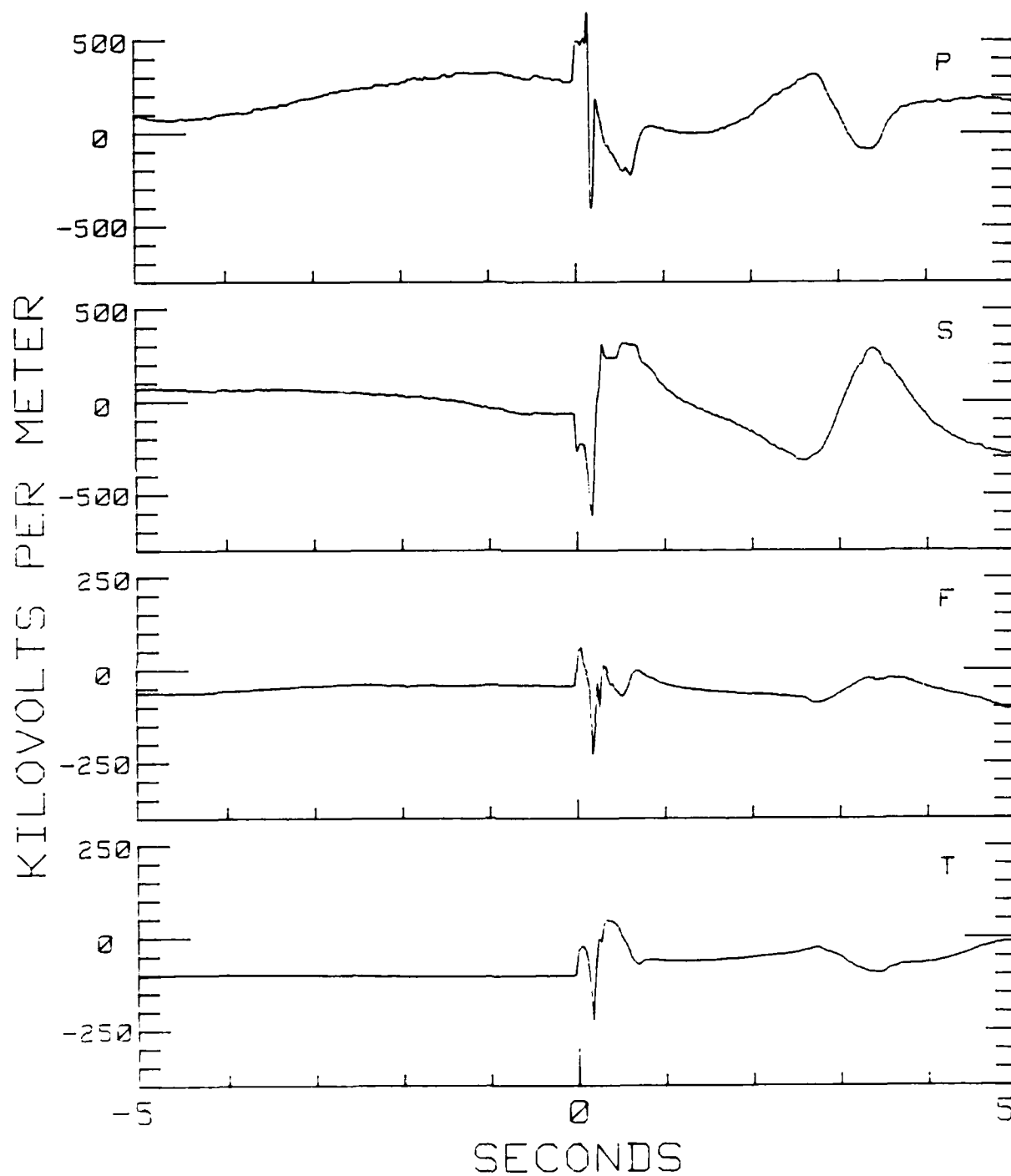


Fig. 12 — Field values at Port, Starboard, Forward, and Tail meters

JUNE2985L2

1748:59

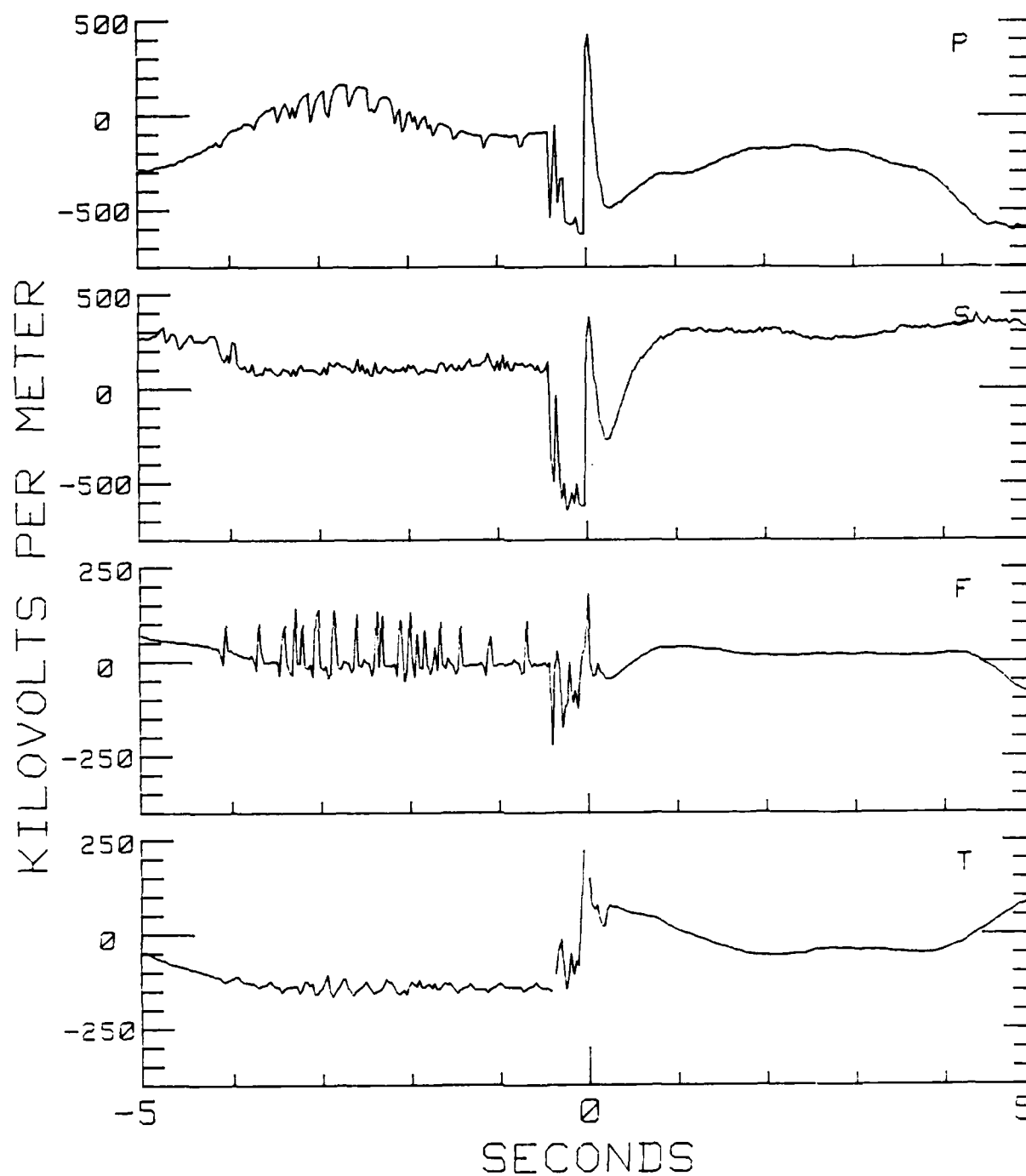


Fig. 13 — Field values at Port, Starboard, Forward, and Tail meters



JUNE2985L2

1849:49.6

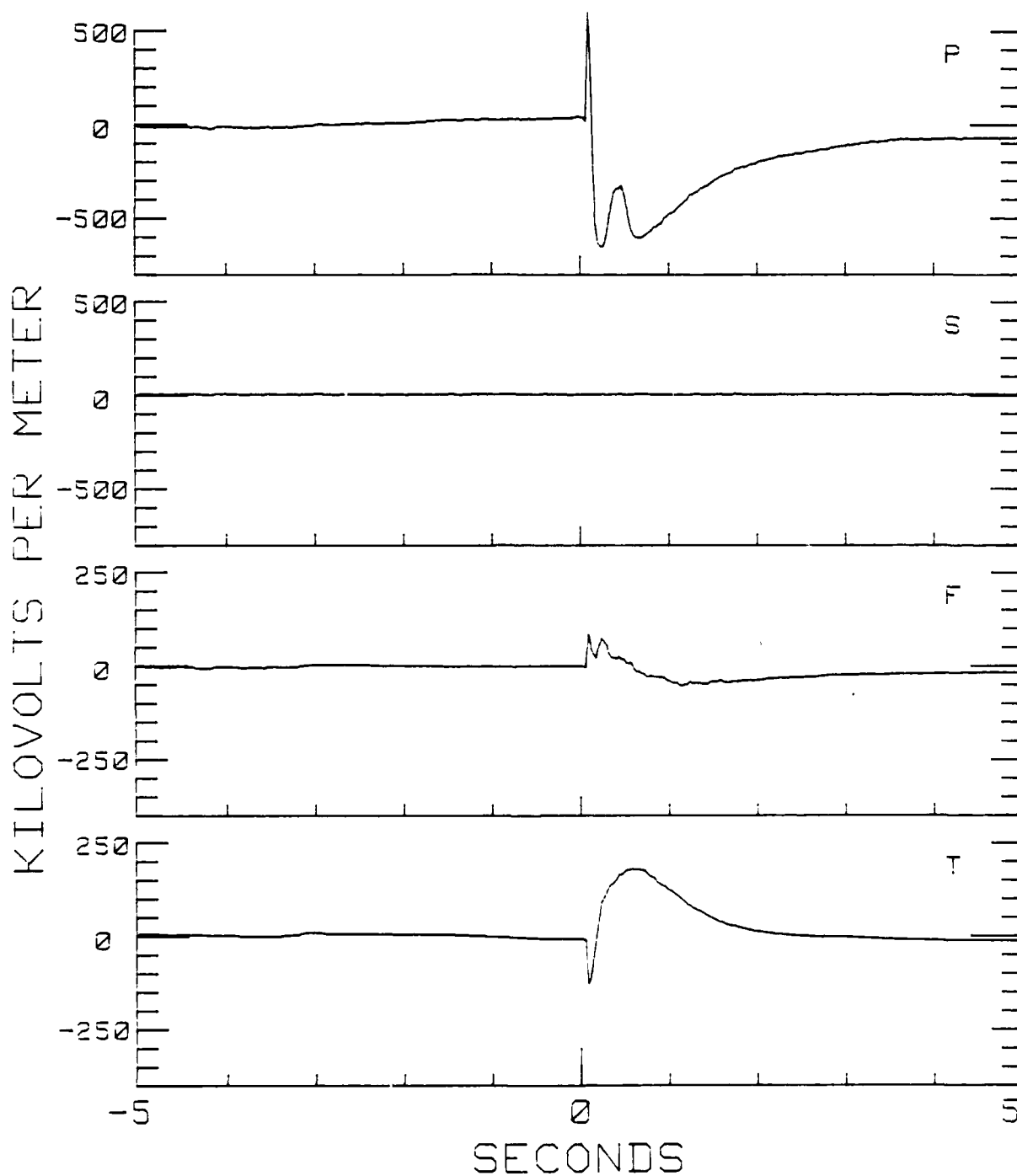


Fig. 14 — Field values at Port, Starboard, Forward, and Tail meters

JULY0685L1

1940:10.03

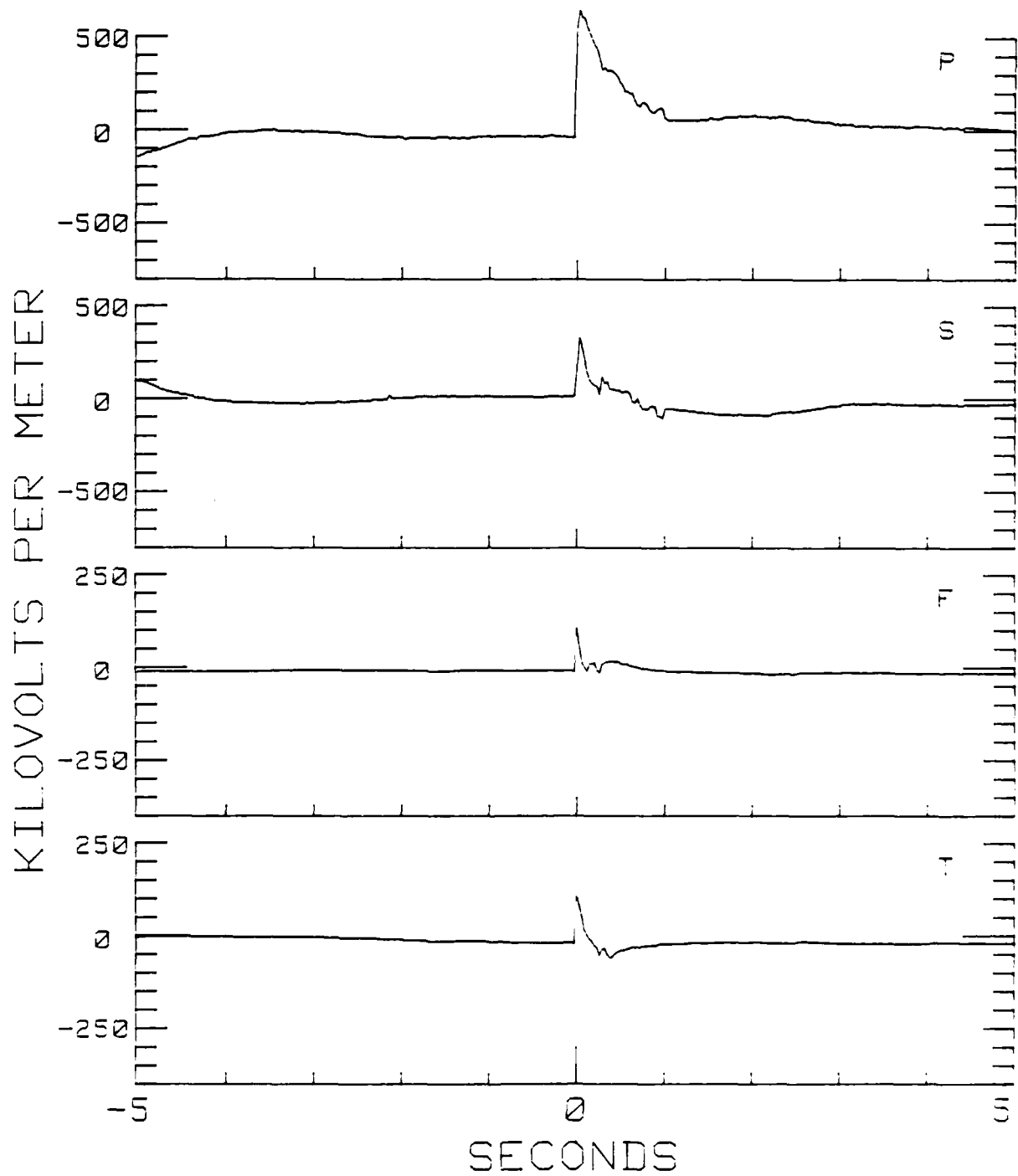


Fig. 15 — Field values at Port, Starboard, Forward, and Tail meters

JULY 15 85 L7

1738:44.06

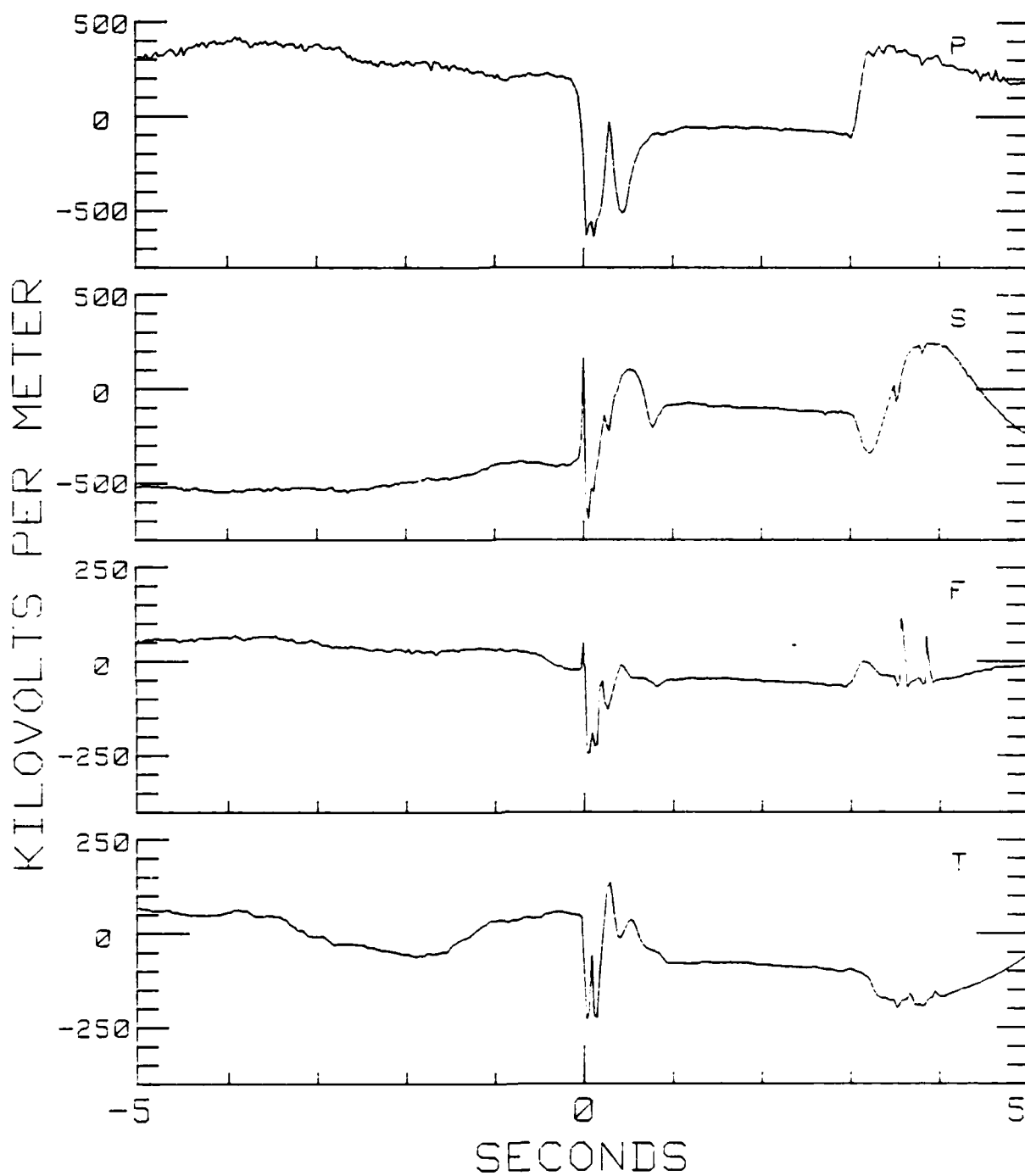


Fig. 16 — Field values at Port, Starboard, Forward, and Tail meters

JULY 15 85L7

1742:24.29

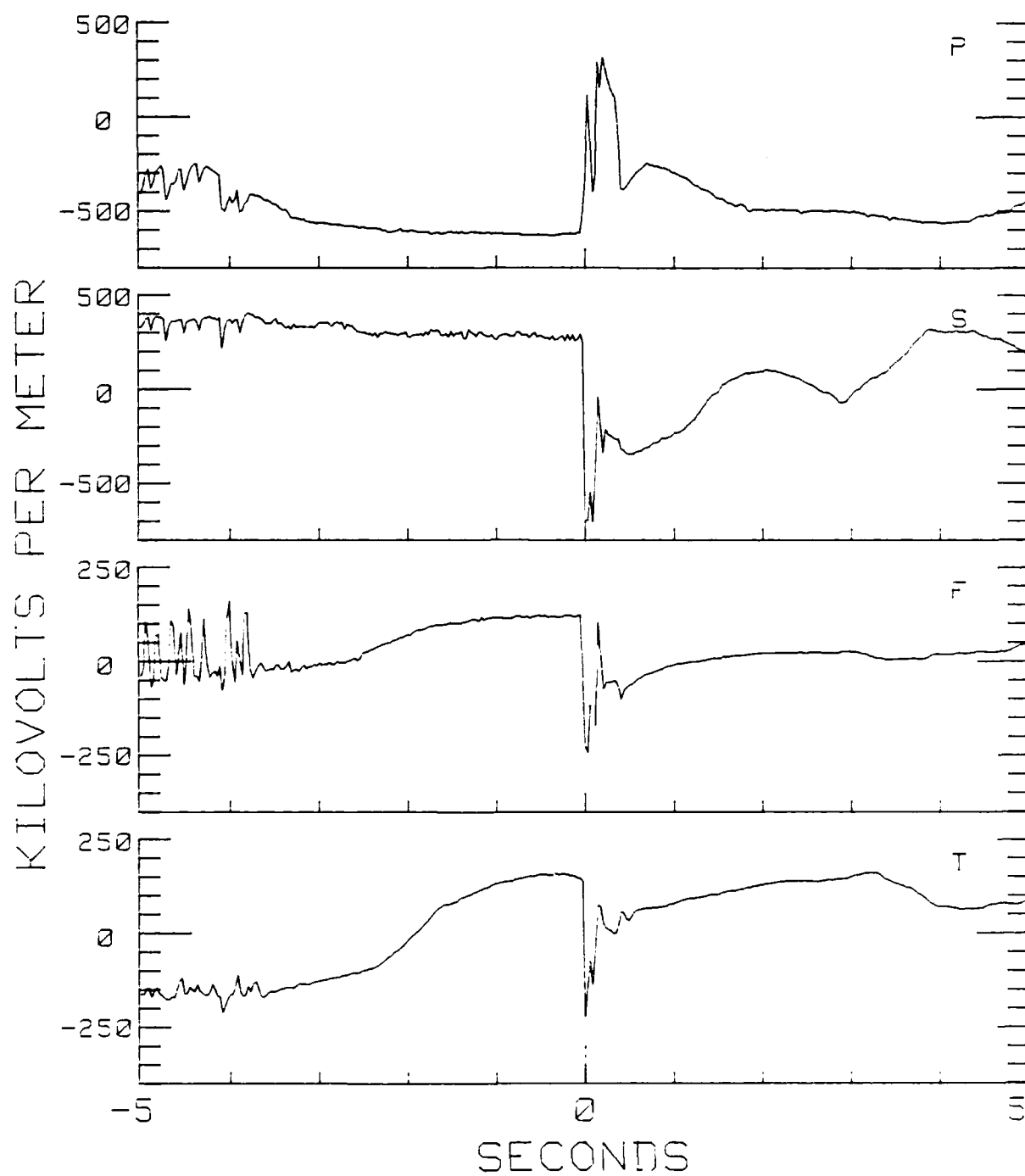


Fig. 17 — Field values at Port, Starboard, Forward, and Tail meters

JULY 15 85L7

1824:18.23

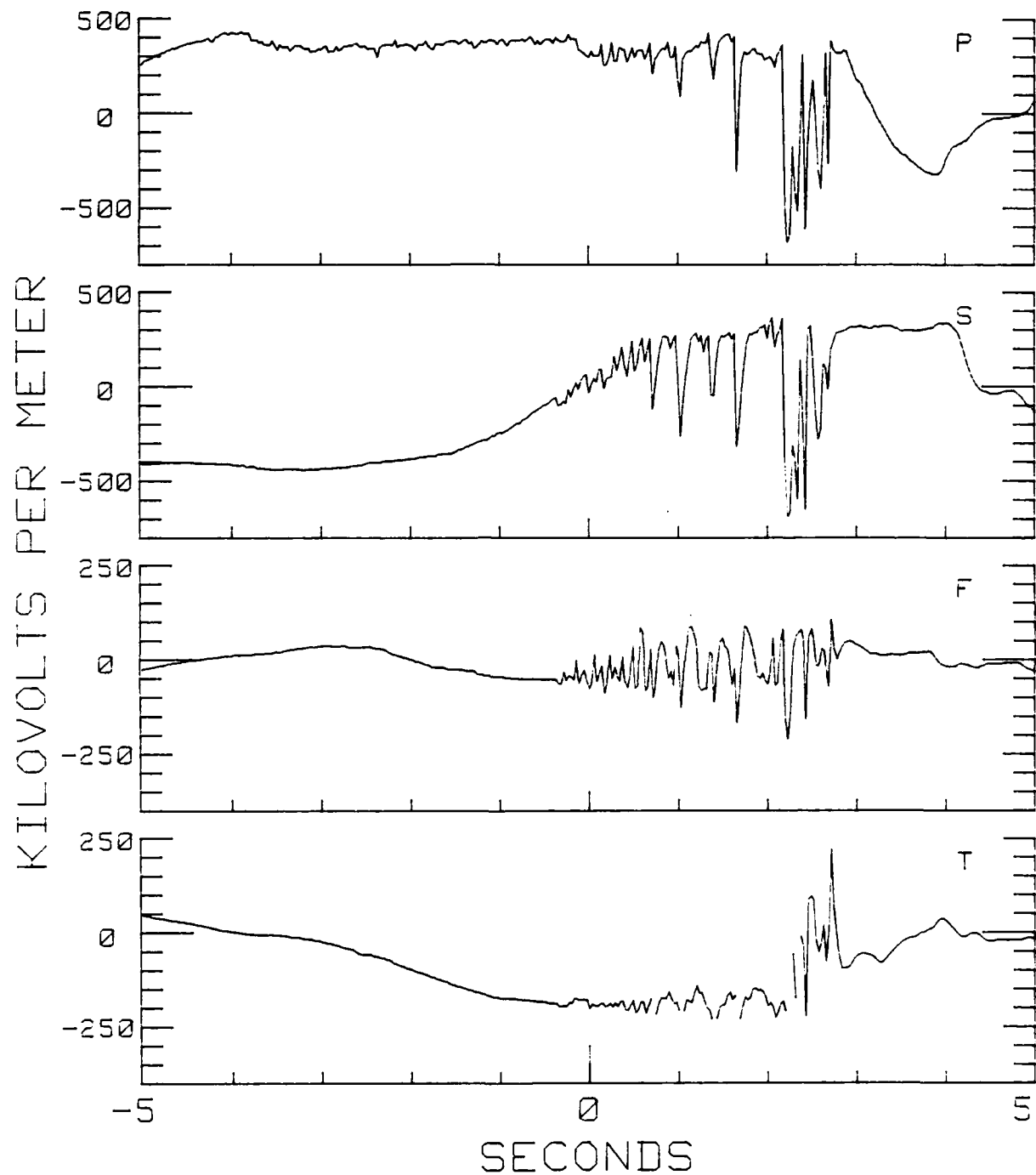


Fig. 18 — Field values at Port, Starboard, Forward, and Tail meters

JULY 15 85 L7

1854:39.89

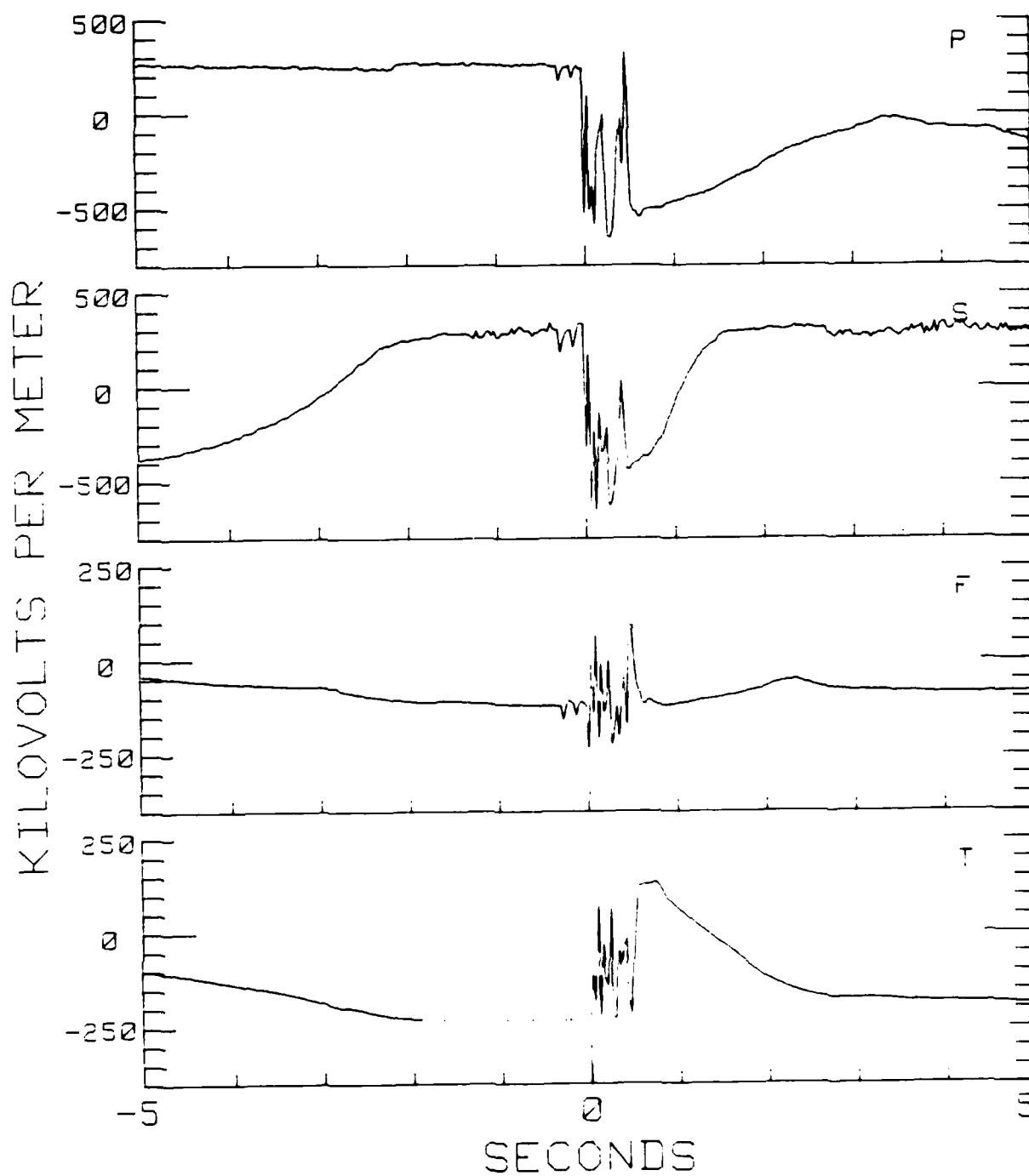


Fig. 19 — Field values at Port, Starboard, Forward, and Tail meters

JULY 15 85L7

1940:56.51

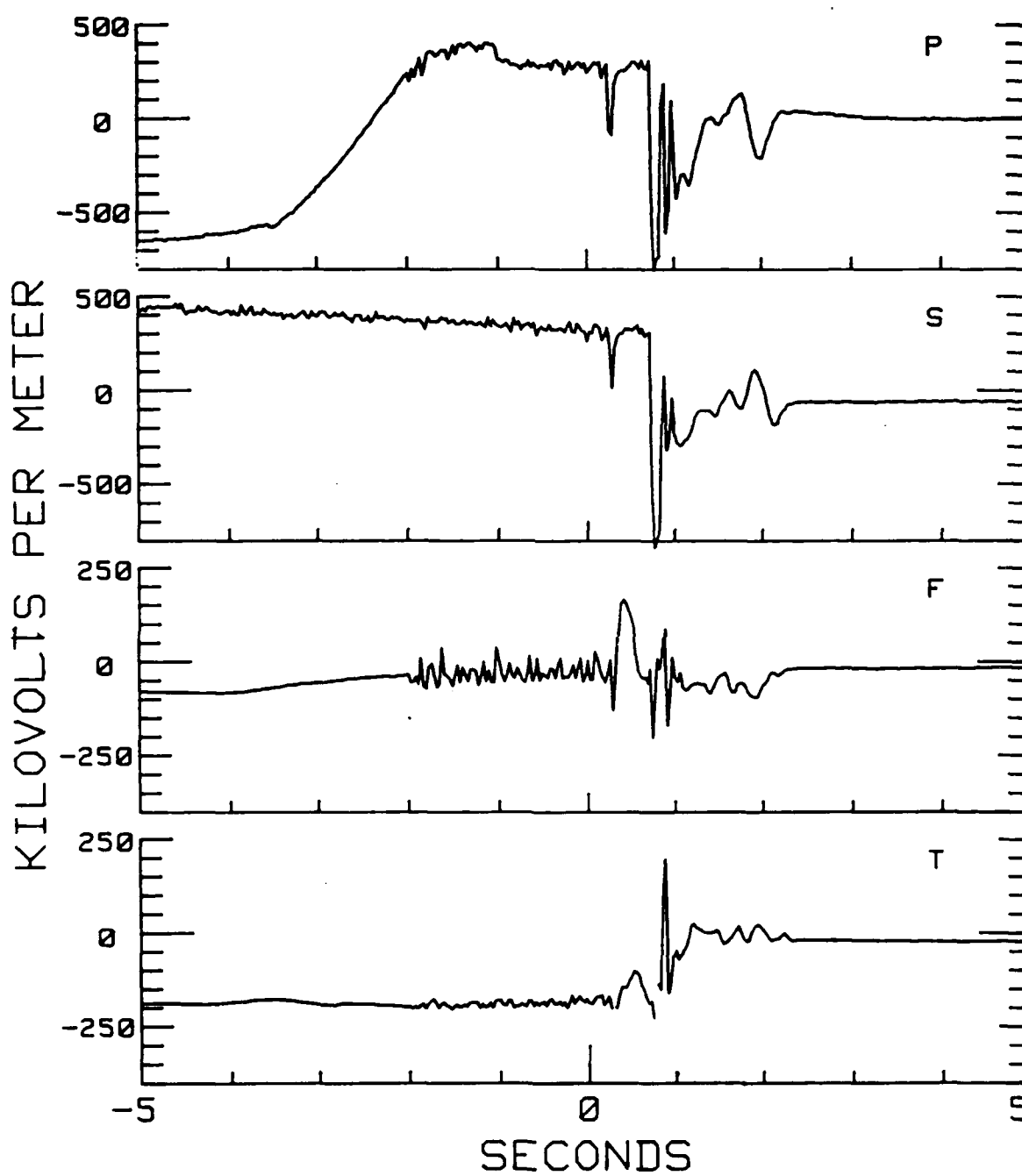


Fig. 20 — Field values at Port, Starboard, Forward, and Tail meters

JULY 15 85L7

1944:34.71

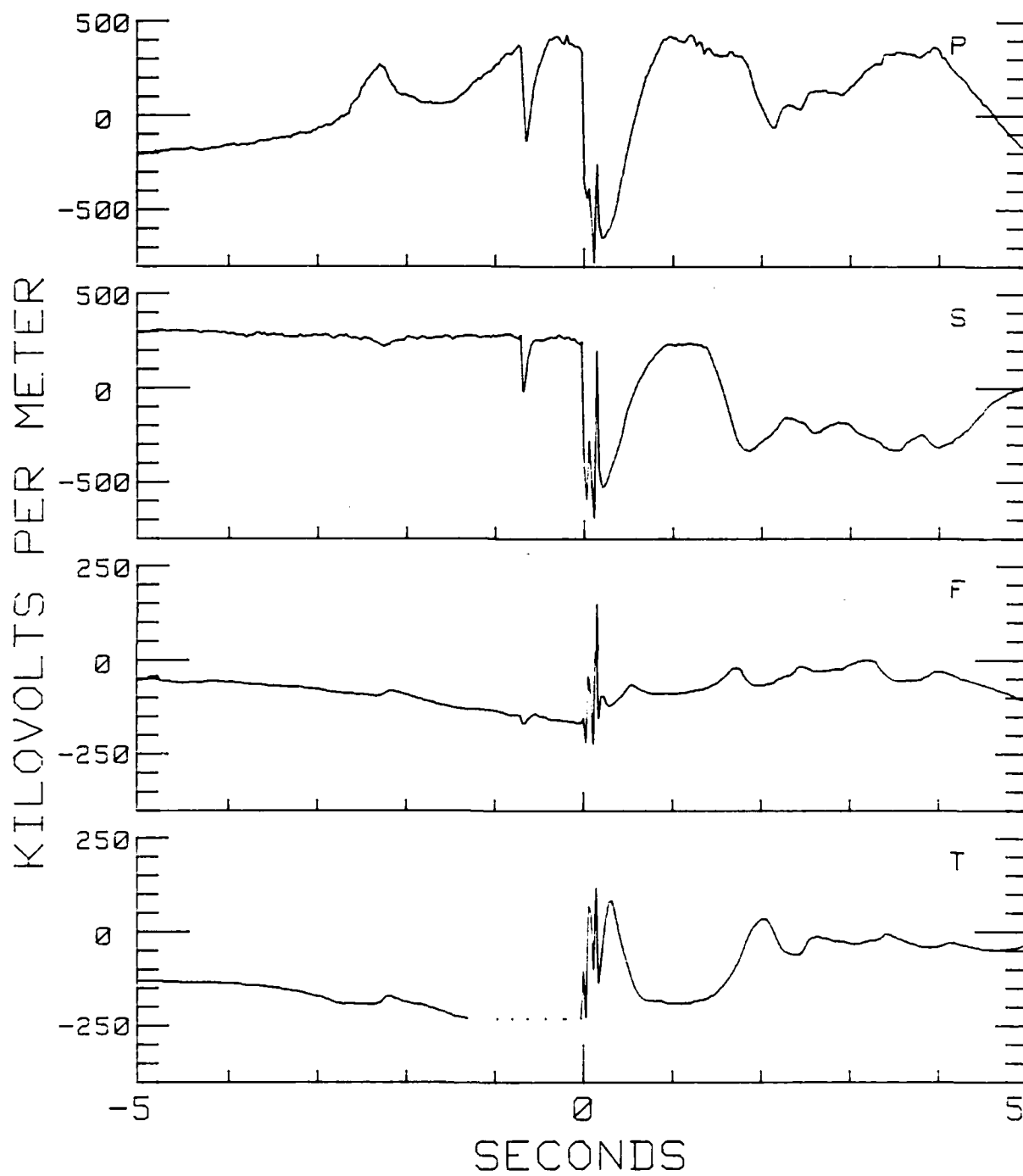


Fig. 21 — Field values at Port, Starboard, Forward, and Tail meters



JULY 15 85L7

1949:16.74

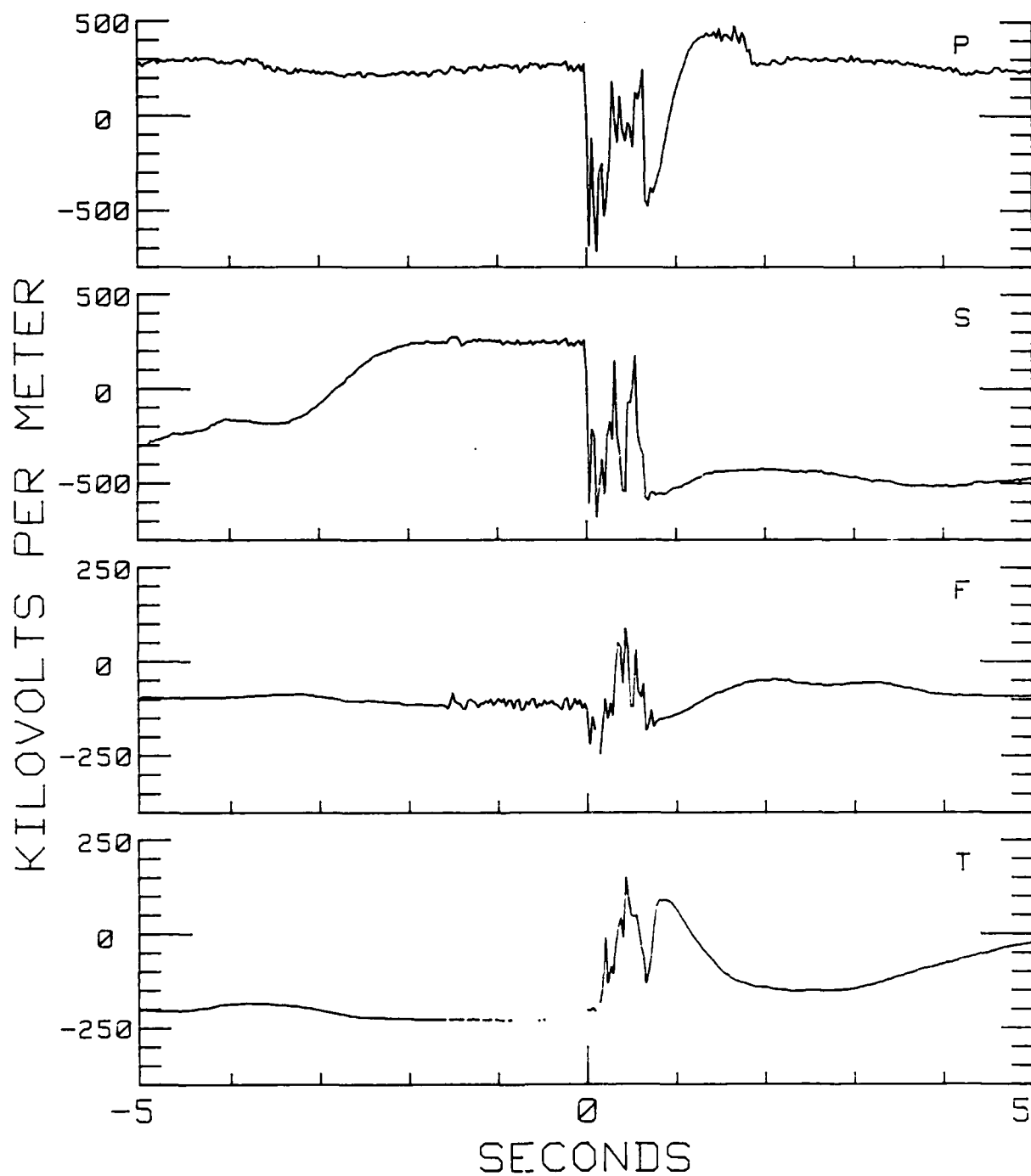


Fig. 22 — Field values at Port, Starboard, Forward, and Tail meters

JUL 15 85 L 1

2056:26.94

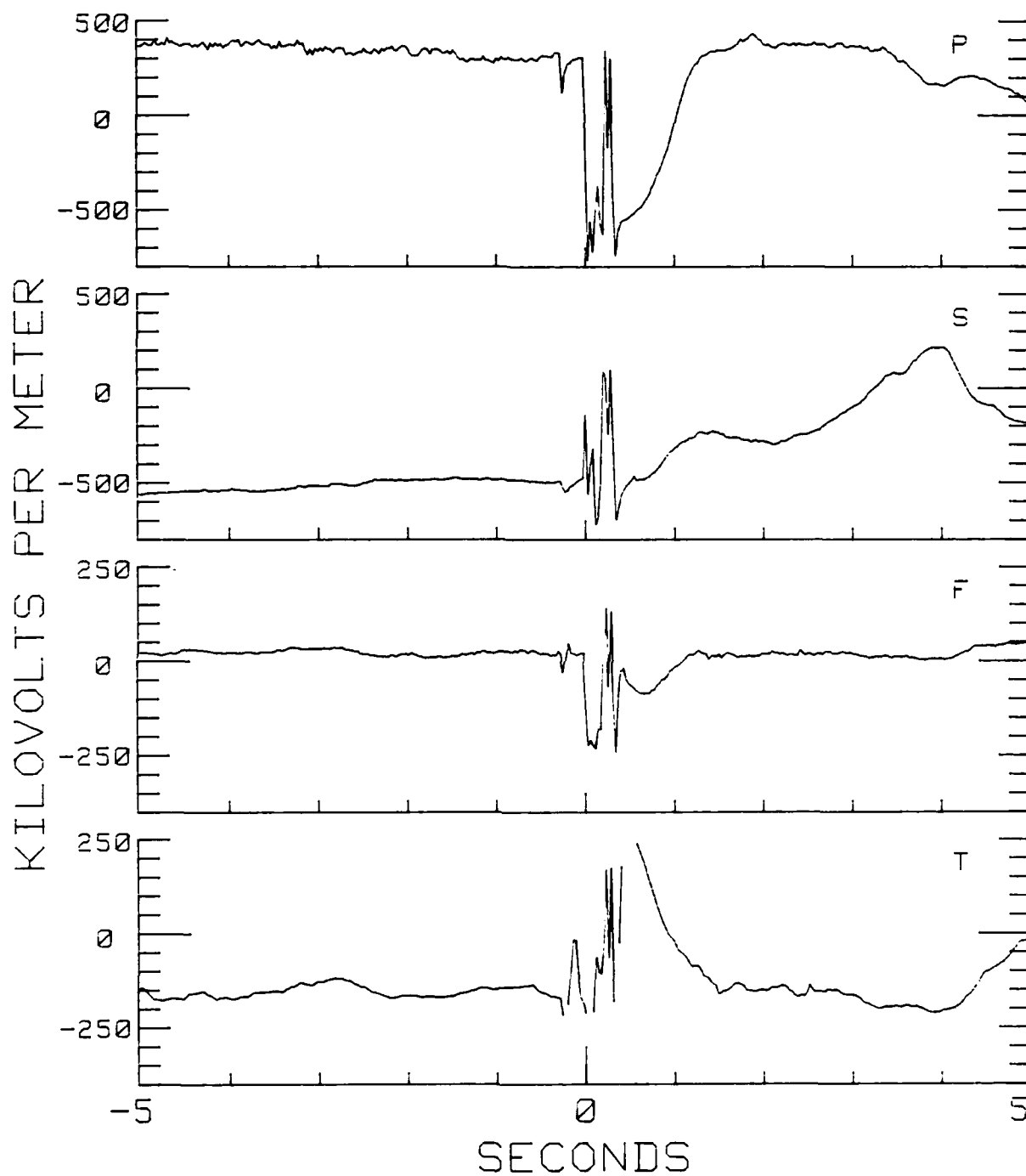


Fig. 23 — Field values at Port, Starboard, Forward, and Tail meters

JULY2685L5

2321:20.91

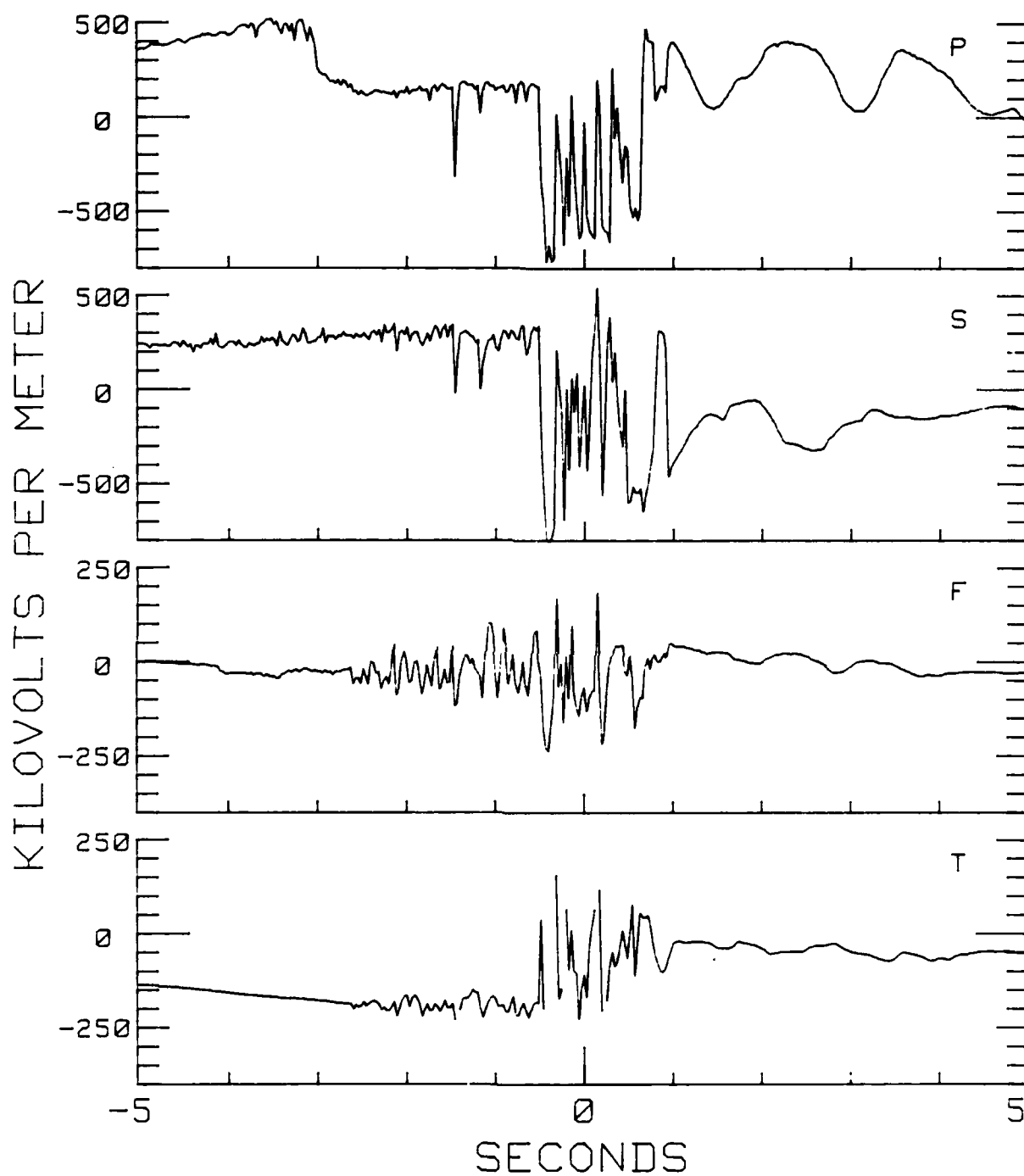


Fig. 24 — Field values at Port, Starboard, Forward, and Tail meters

JULY2685L5

2333:23.34

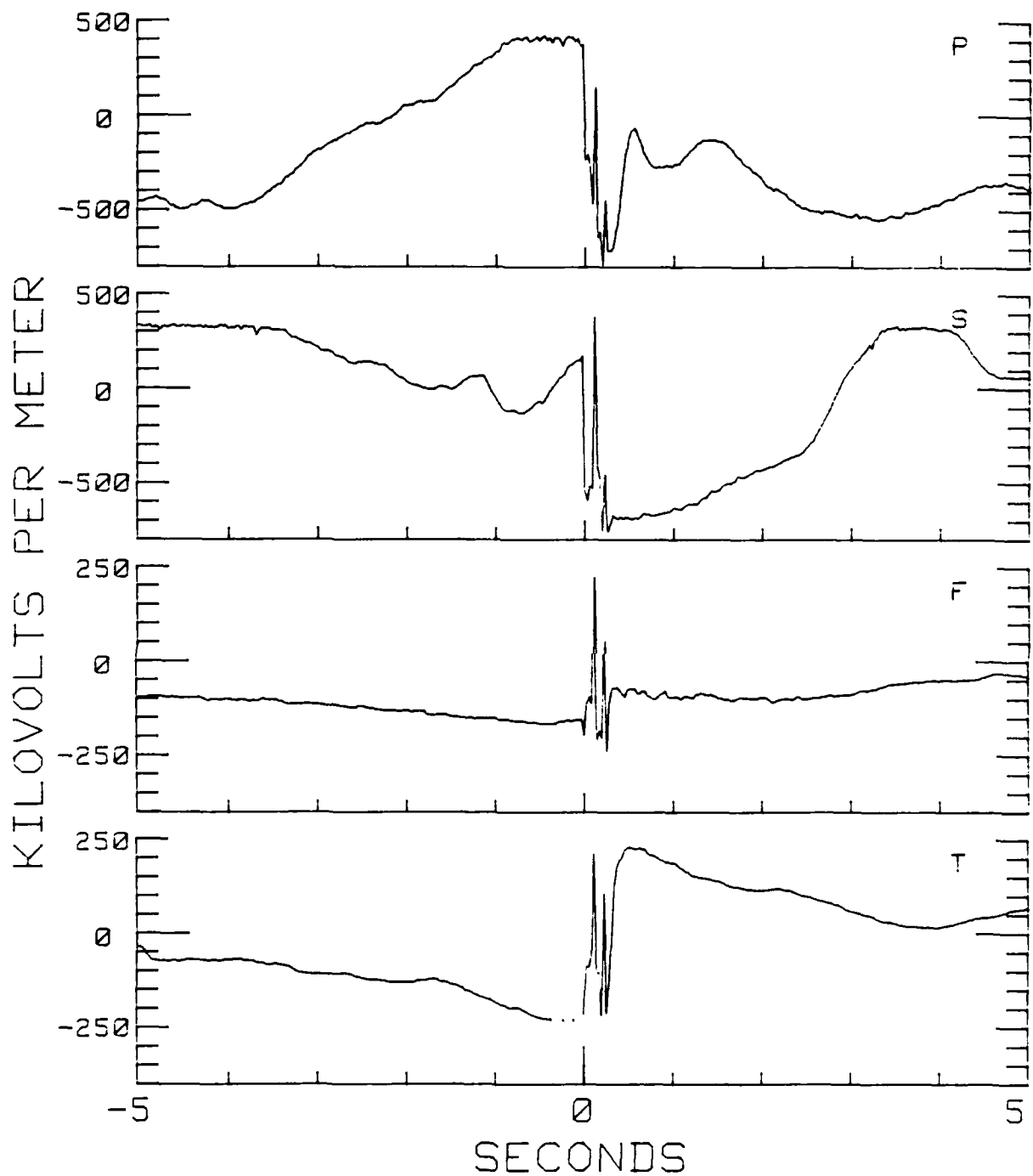


Fig. 25 — Field values at Port, Starboard, Forward, and Tail meters

JULY2685L5

2351:58.13

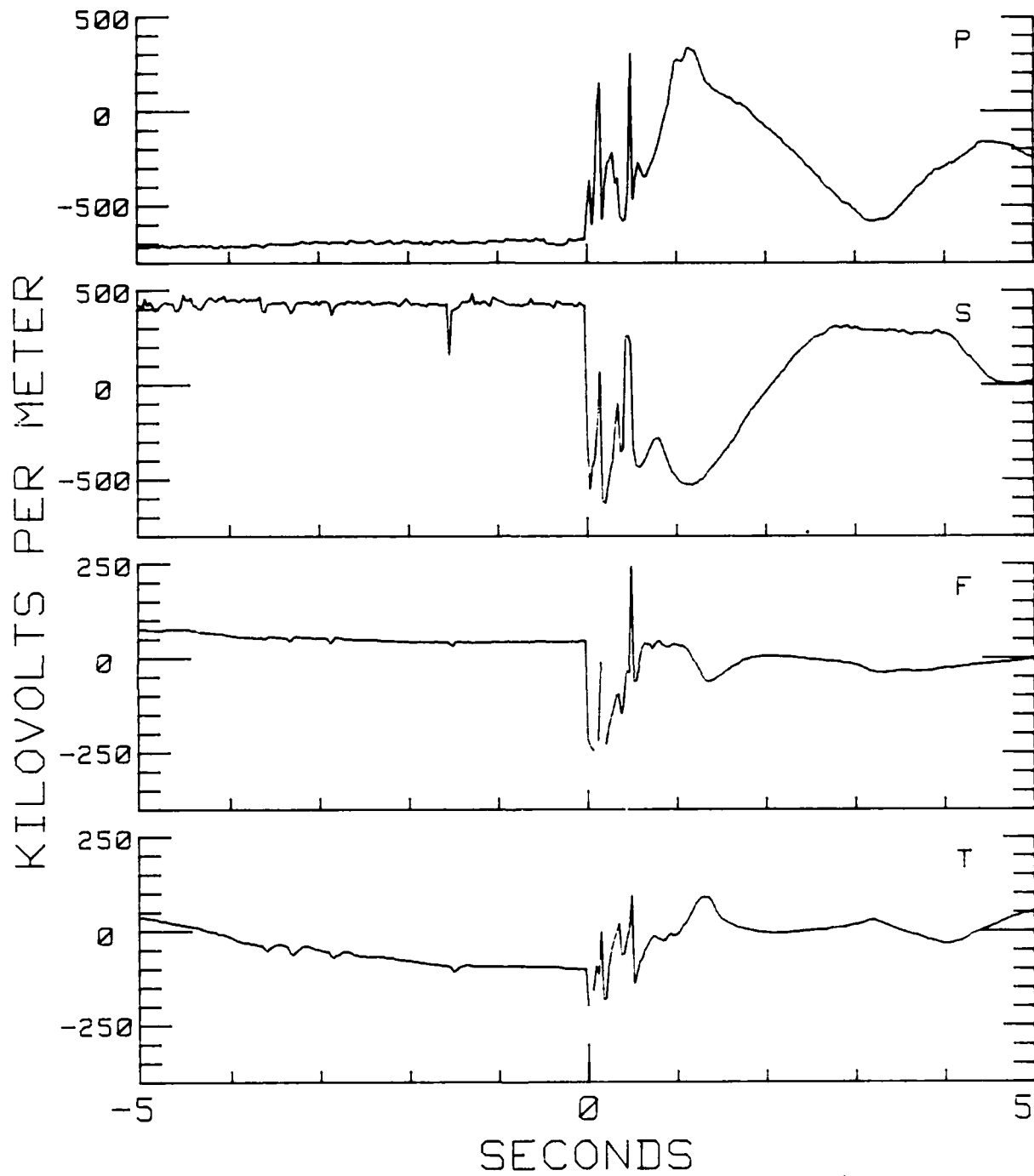


Fig. 26 — Field values at Port, Starboard, Forward, and Tail meters

JULY2785L5

0004:19.72

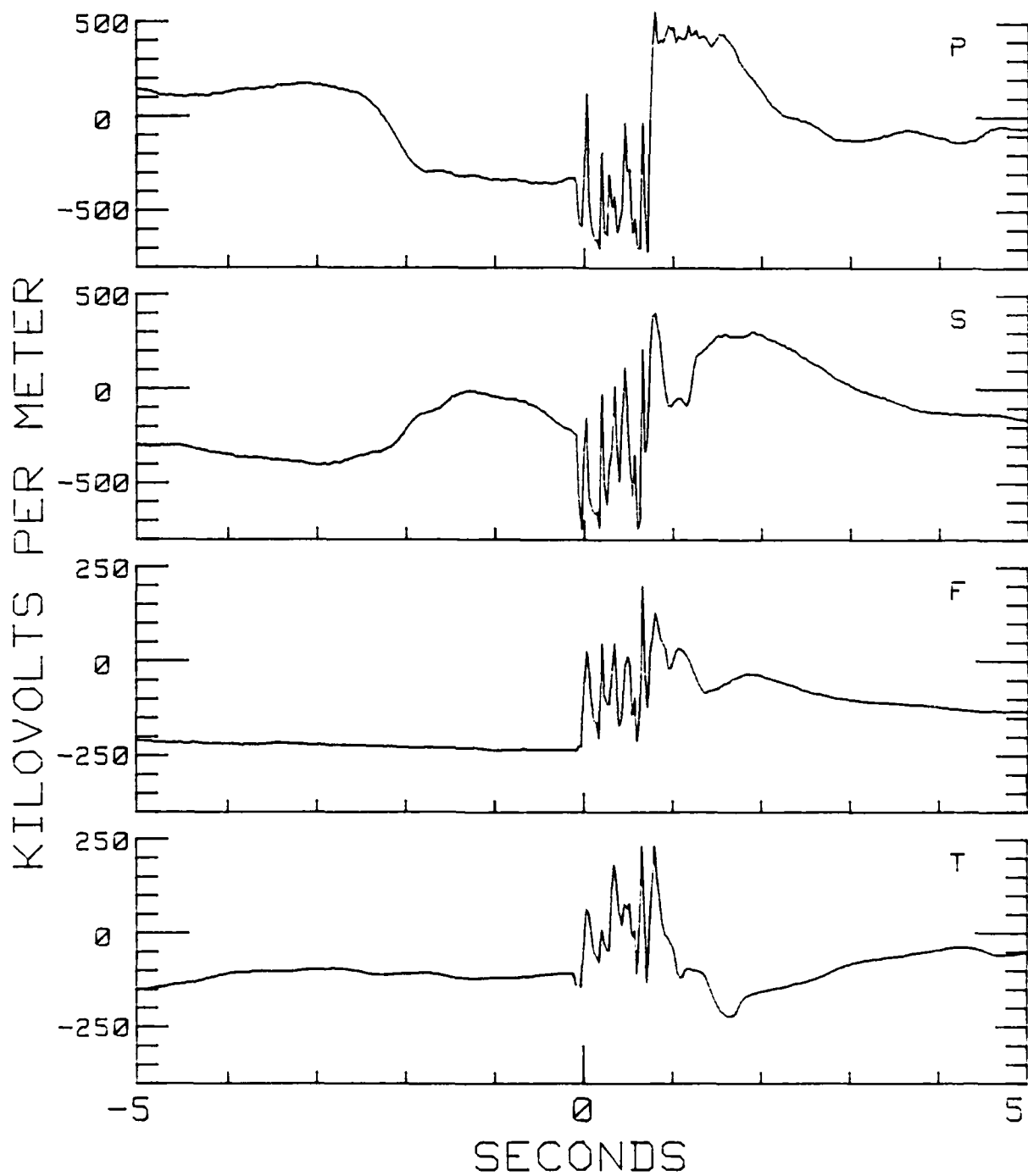


Fig. 27 — Field values at Port, Starboard, Forward, and Tail meters

JULY2785L5

0014:55.0

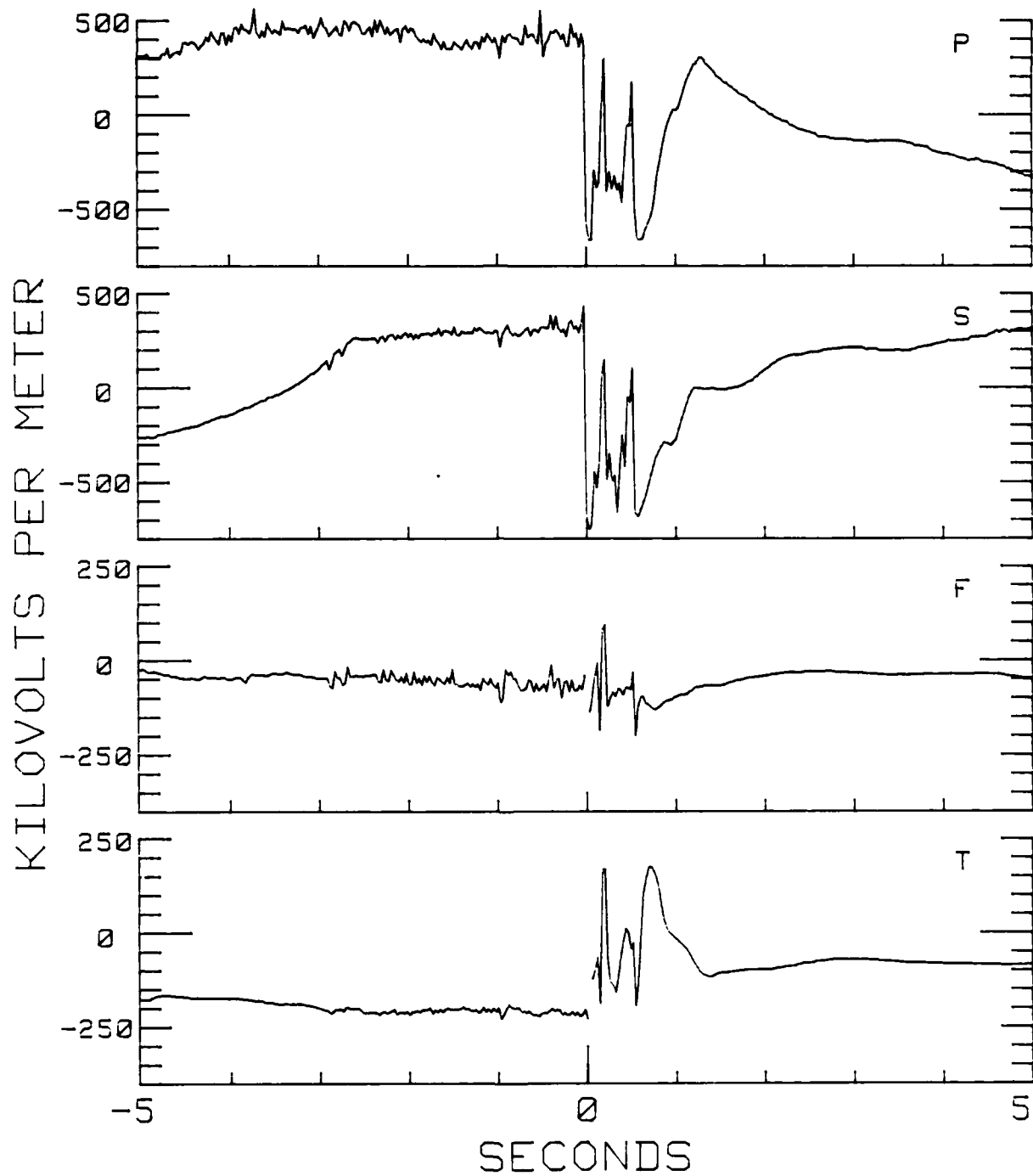


Fig. 28 — Field values at Port, Starboard, Forward, and Tail meters

JULY3085L2

2028:18.51

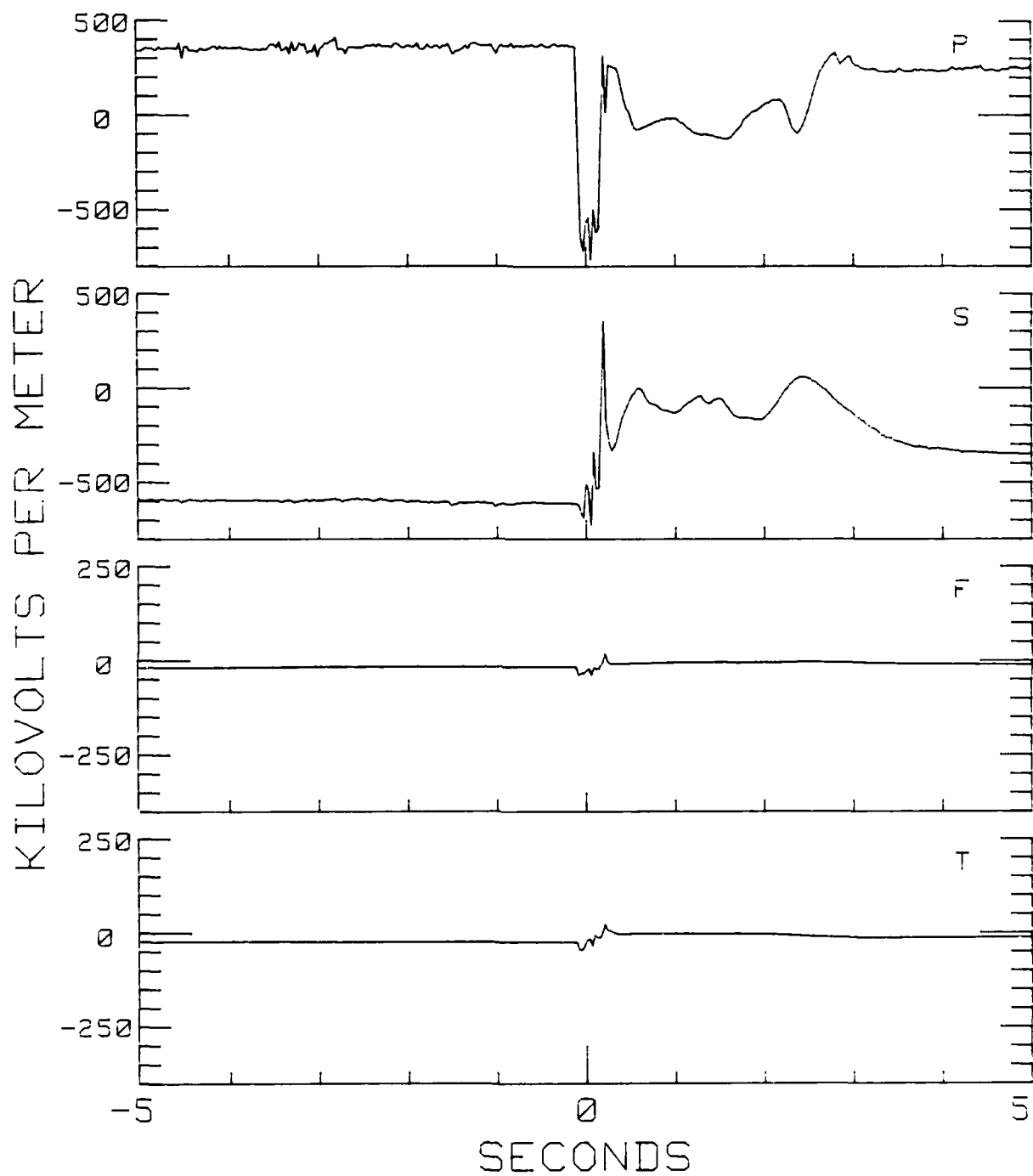


Fig. 29 — Field values at Port, Starboard, Forward, and Tail meters



JULY3085L2

2118:33.37

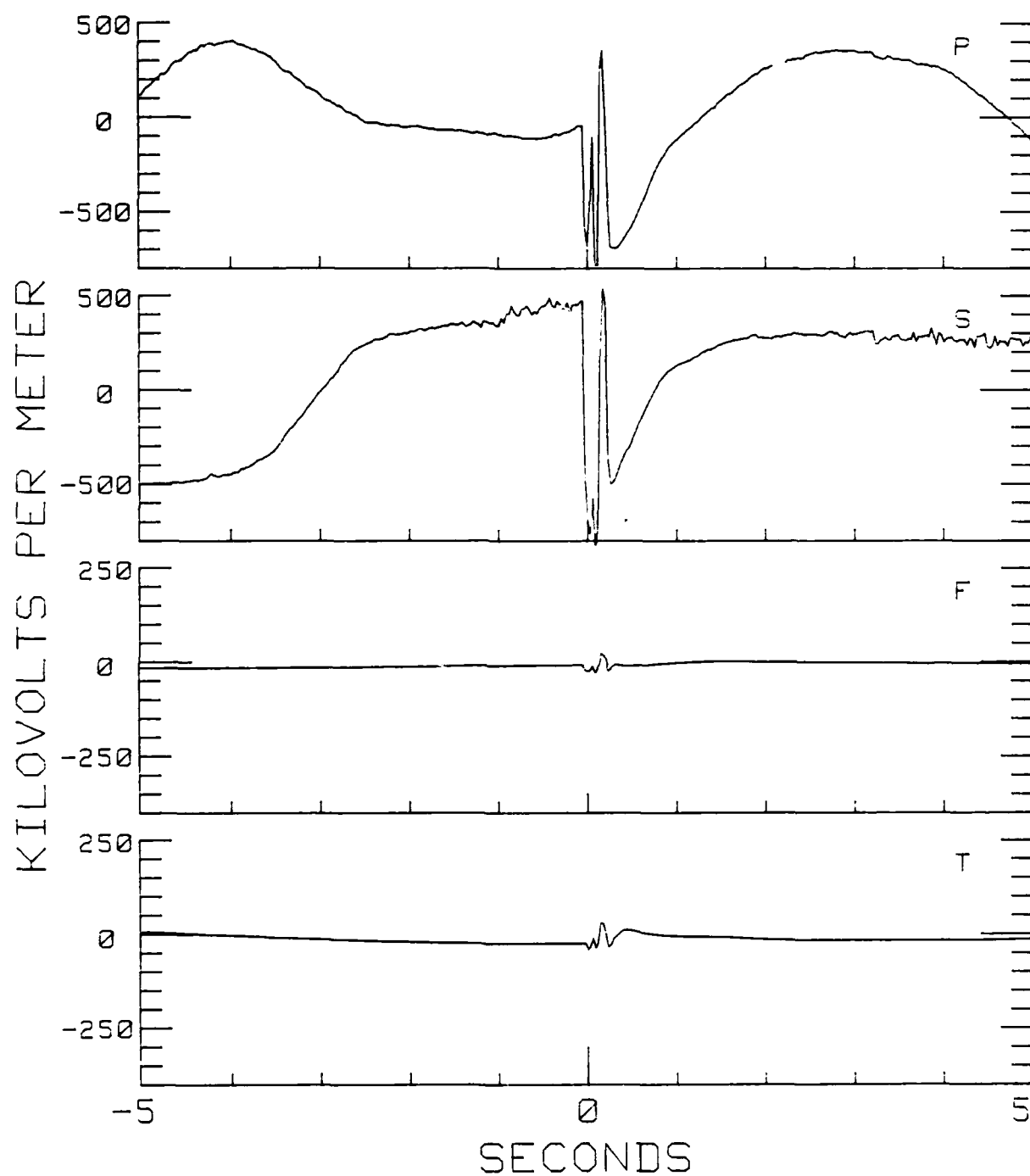


Fig. 30 — Field values at Port, Starboard, Forward, and Tail meters

AUG0385L1

1946:08.31

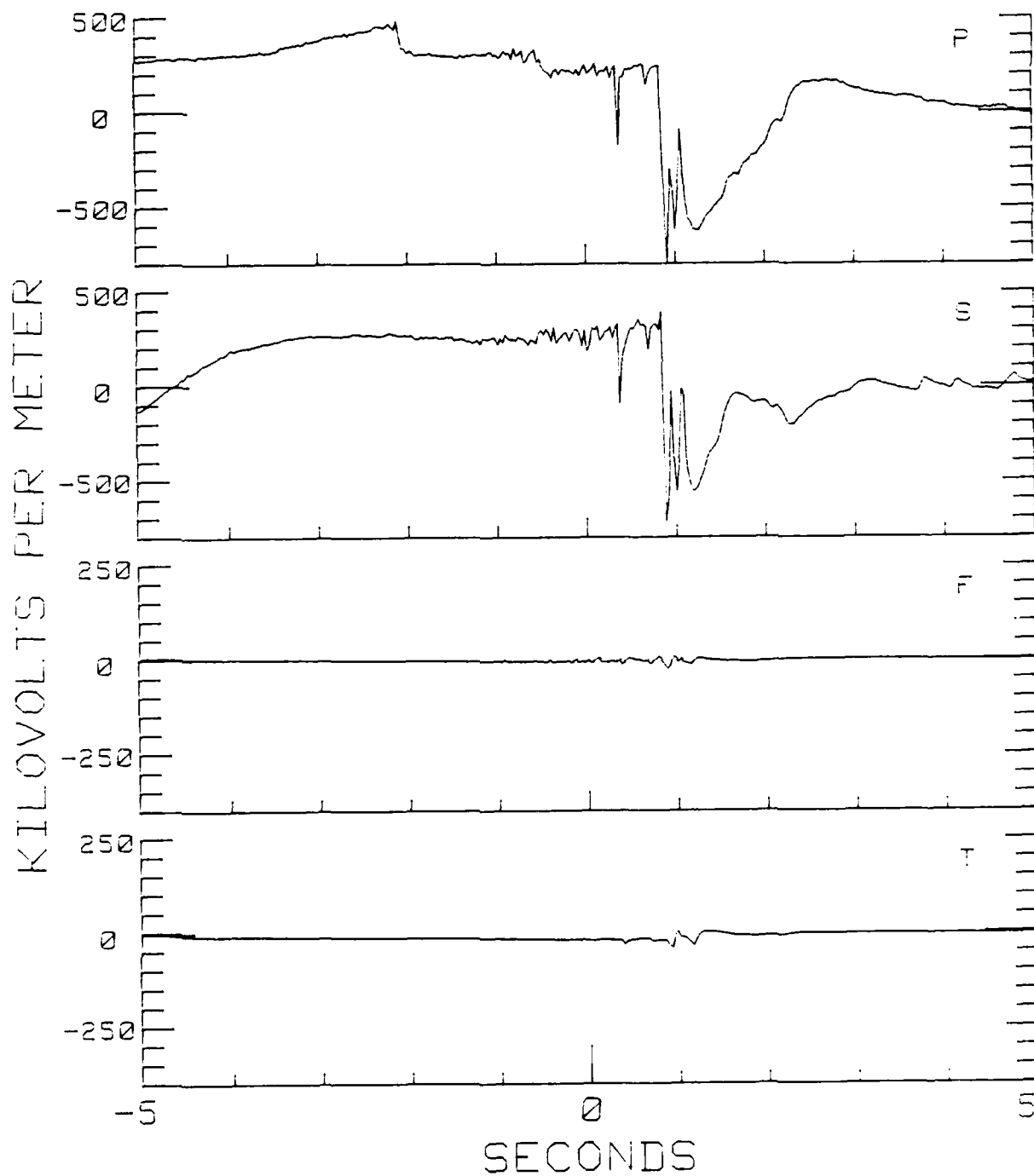


Fig. 31 — Field values at Port, Starboard, Forward, and Tail meters

AUG0885L2

2033:32.77

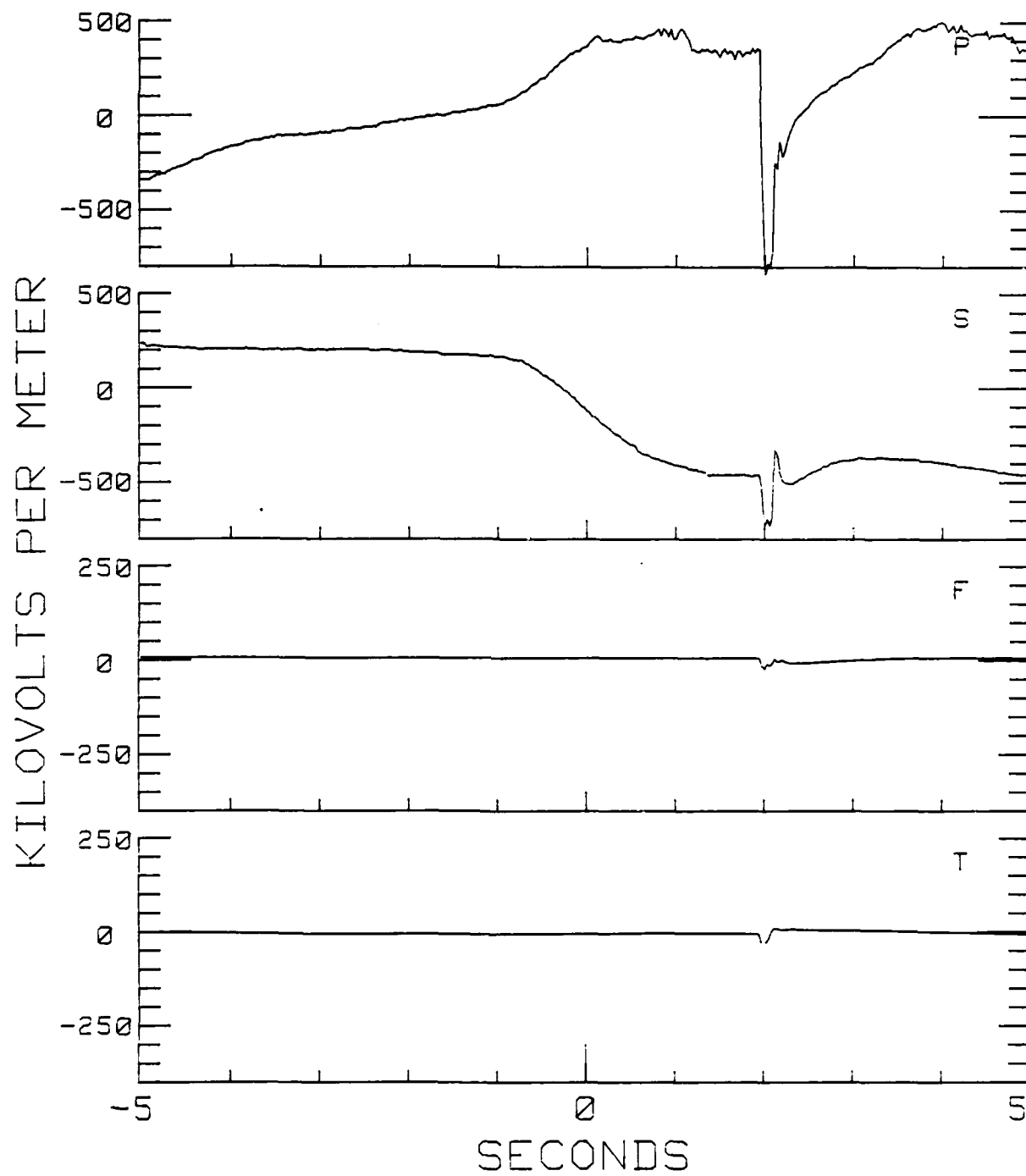


Fig. 32 — Field values at Port, Starboard, Forward, and Tail meters

AUG0885L2

2049:46.63

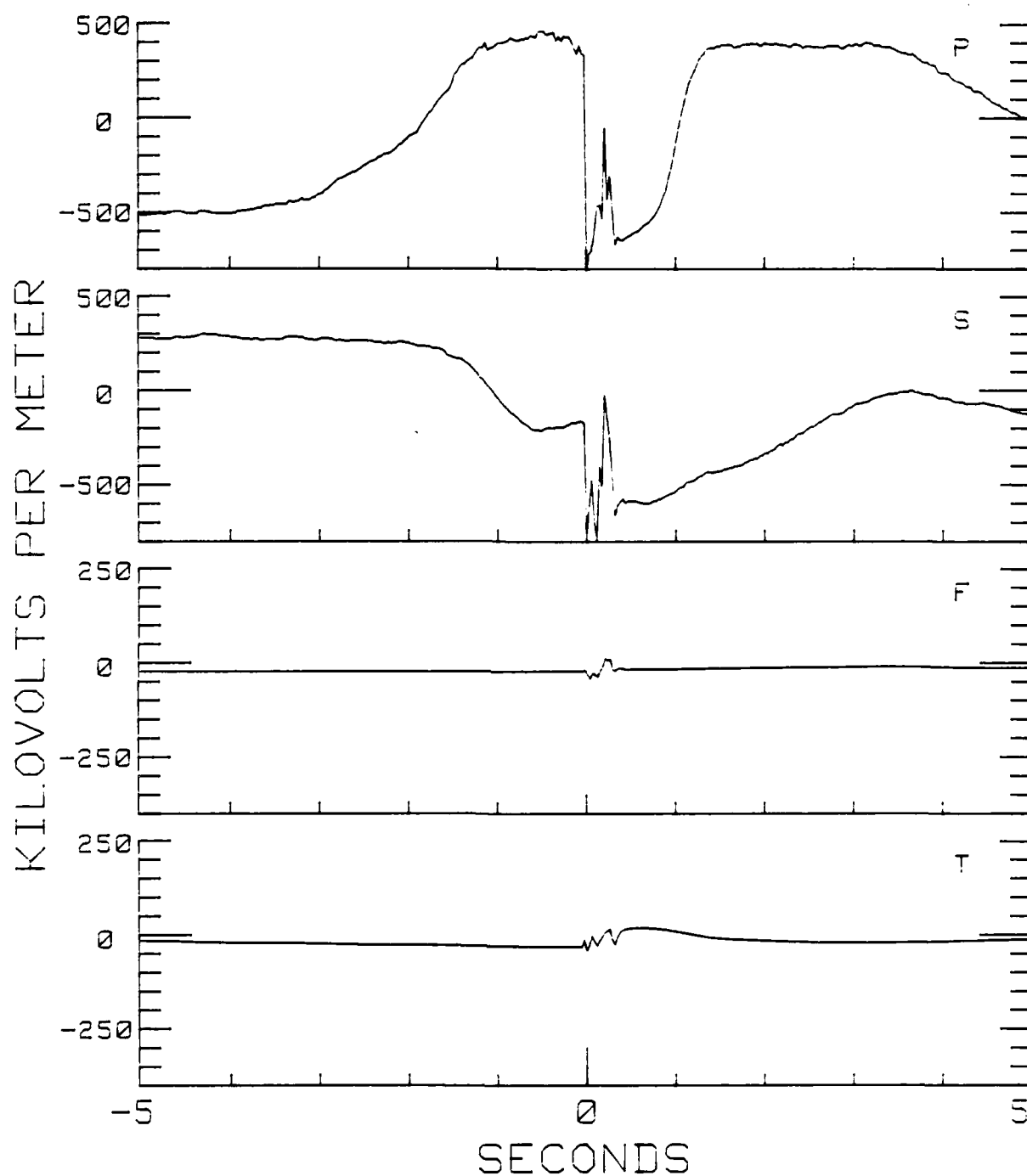


Fig. 33 — Field values at Port, Starboard, Forward, and Tail meters

AUG3085L2

2227:08.29

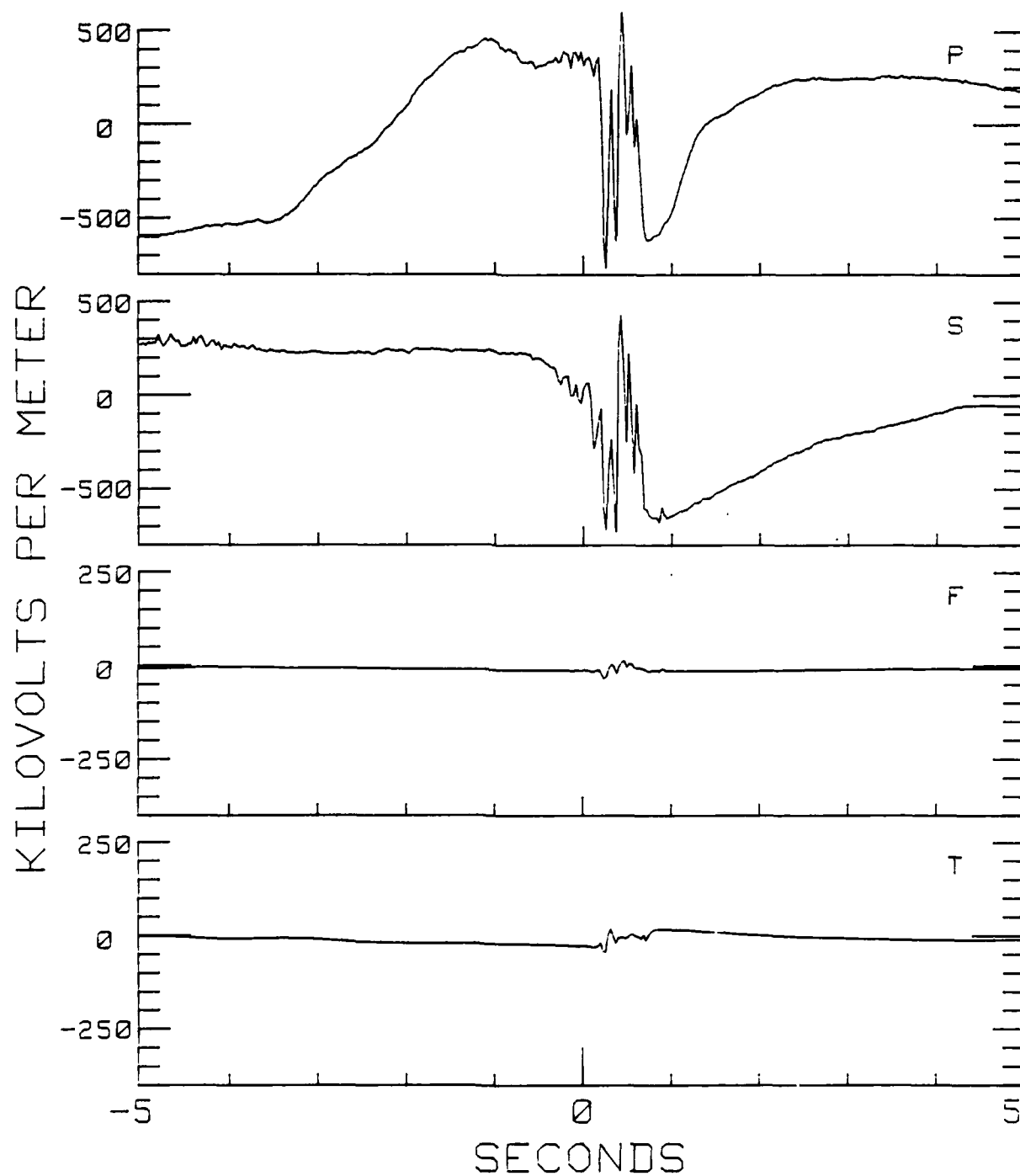


Fig. 34 — Field values at Port, Starboard, Forward, and Tail meters

AUG3085L2

2234:42.74

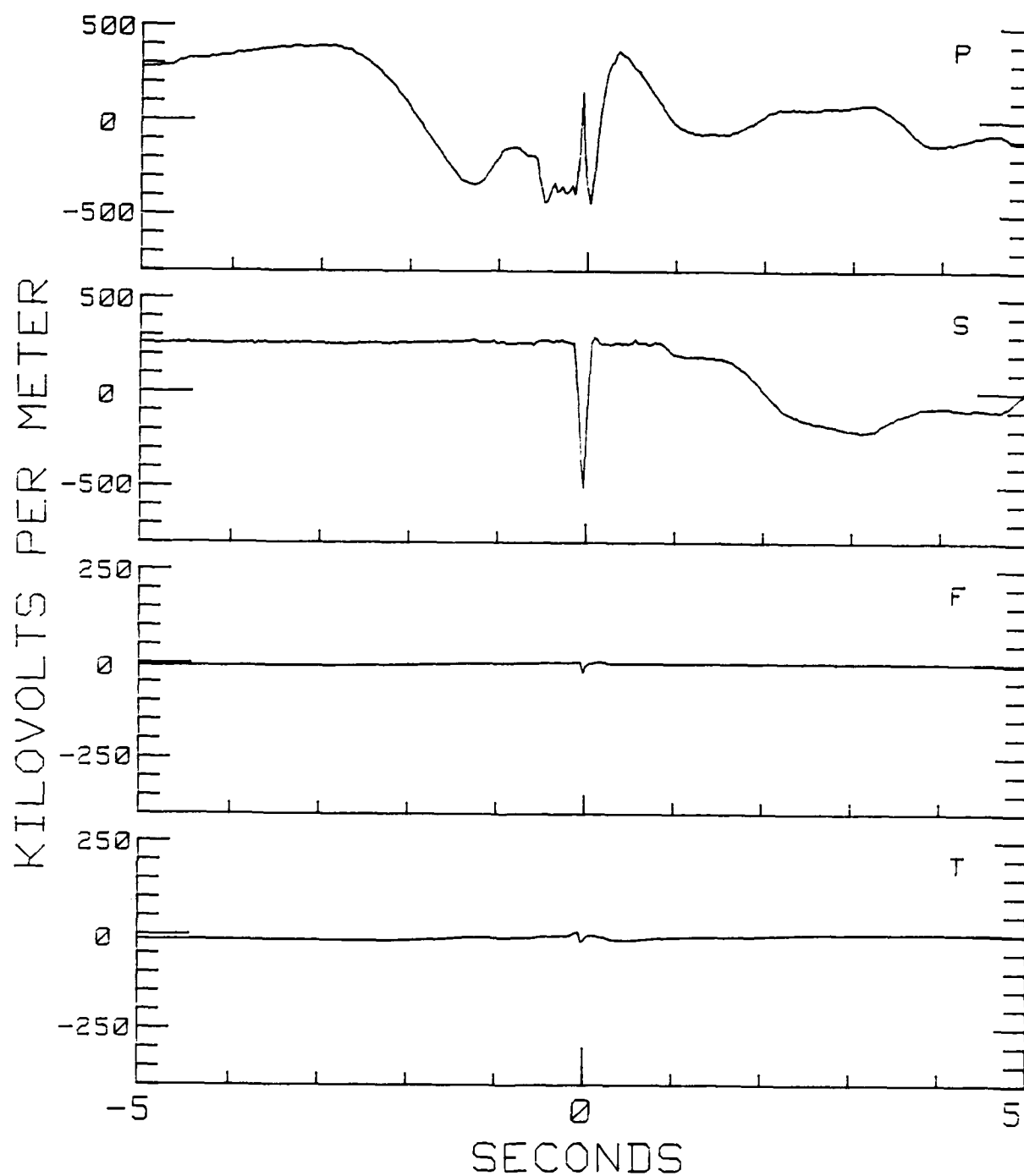


Fig. 35 — Field values at Port, Starboard, Forward and Tail meters

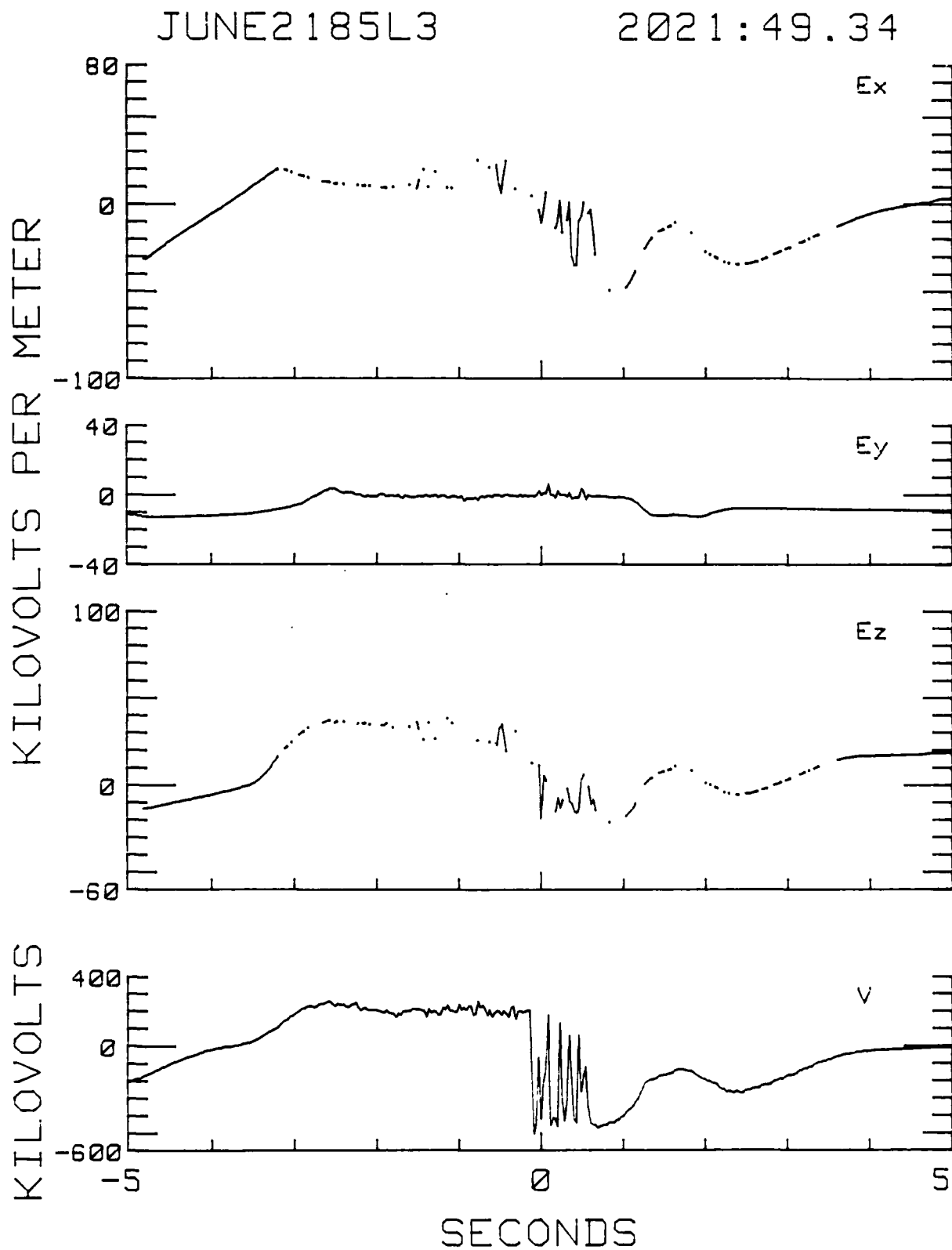


Fig. 36 — Cartesian vector field and aircraft potential

JUNE 21 85 L3

2109:02.37

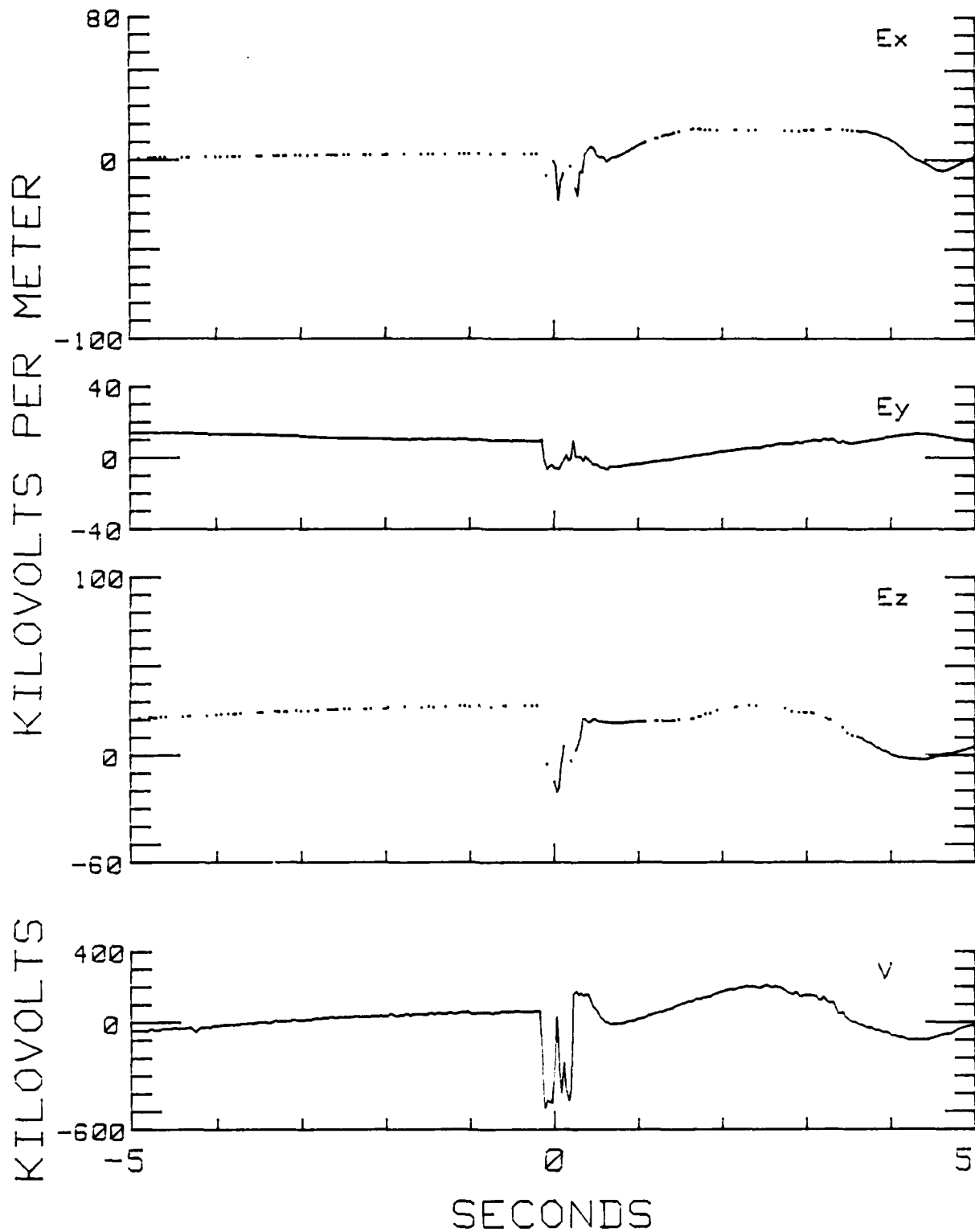


Fig. 37 — Cartesian vector field and aircraft potential



JUNE2185L3

2118:02.97

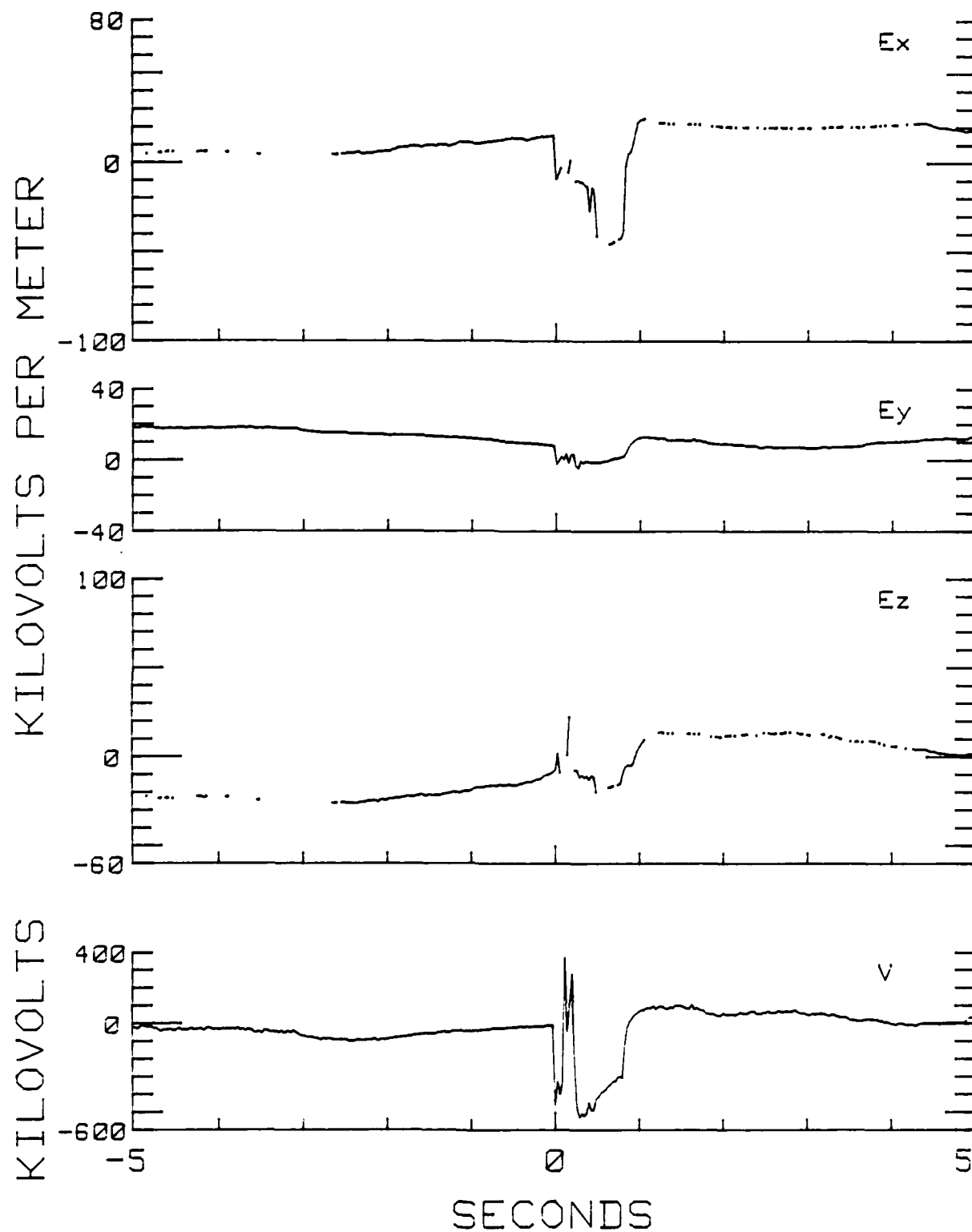


Fig. 38 — Cartesian vector field and aircraft potential

JUNE2685L3

2040:29.71

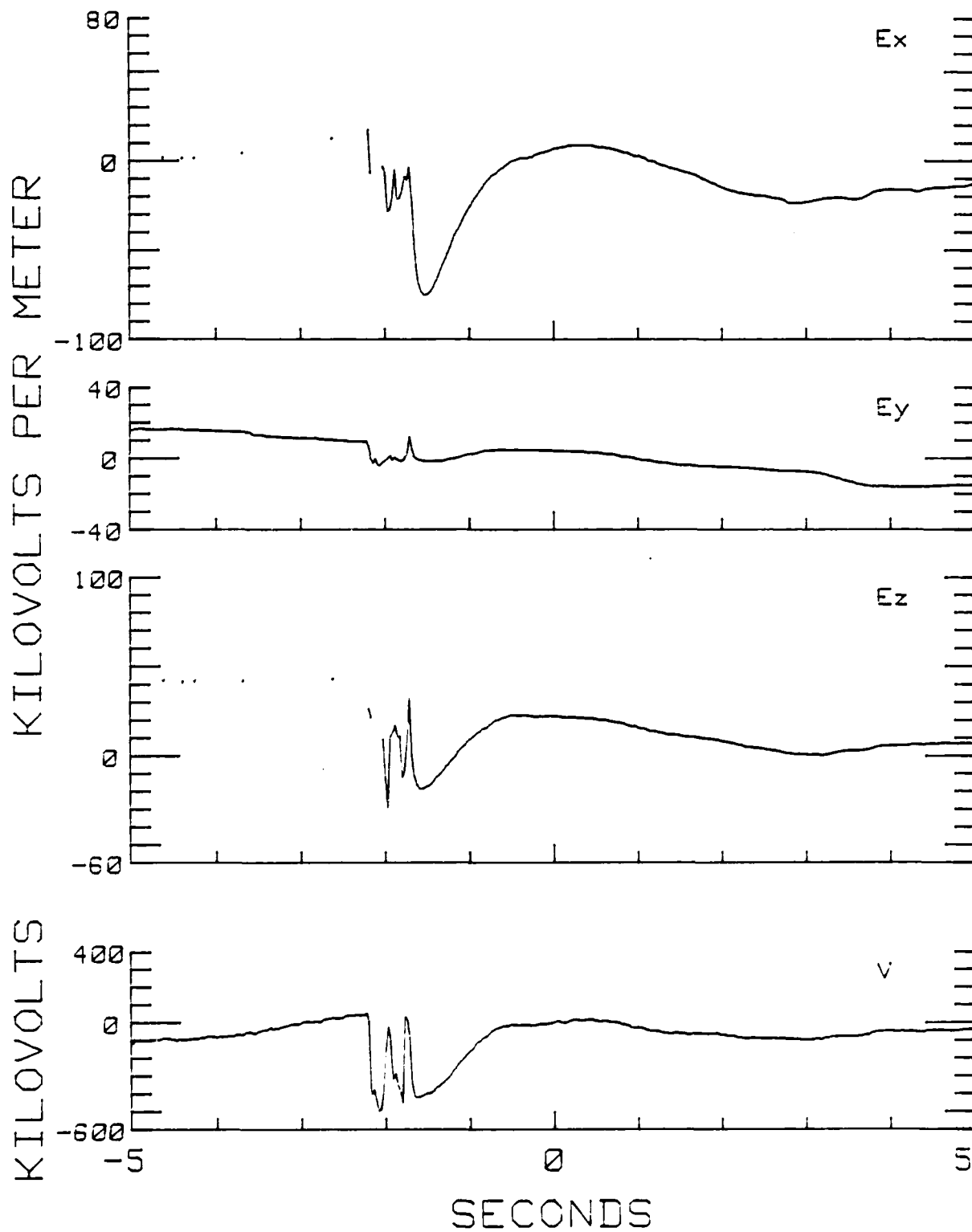


Fig. 39 — Cartesian vector field and aircraft potential

JUNE2685L3

2055:24.46

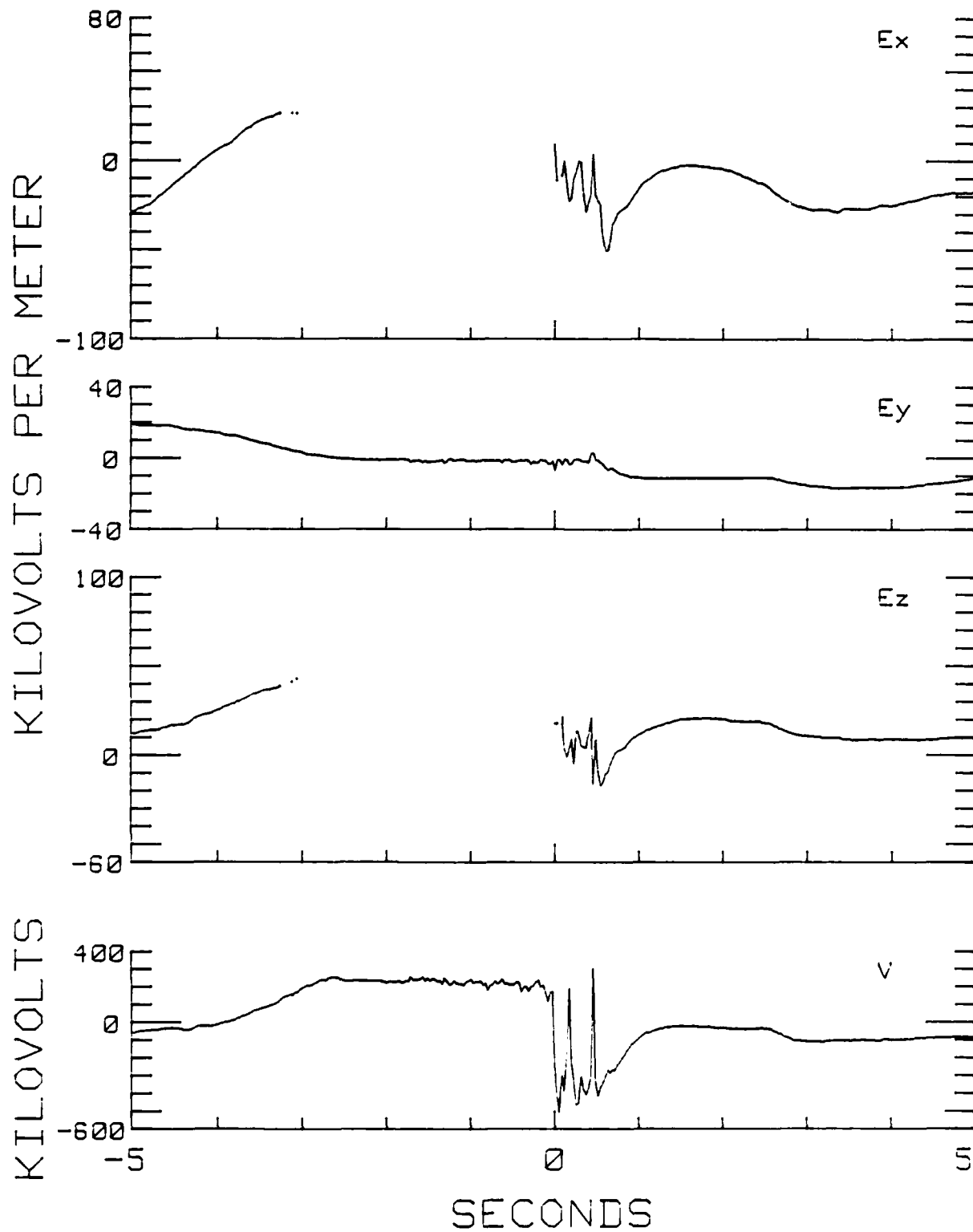


Fig. 40 — Cartesian vector field and aircraft potential

JUNE2685L3

2100:15.94

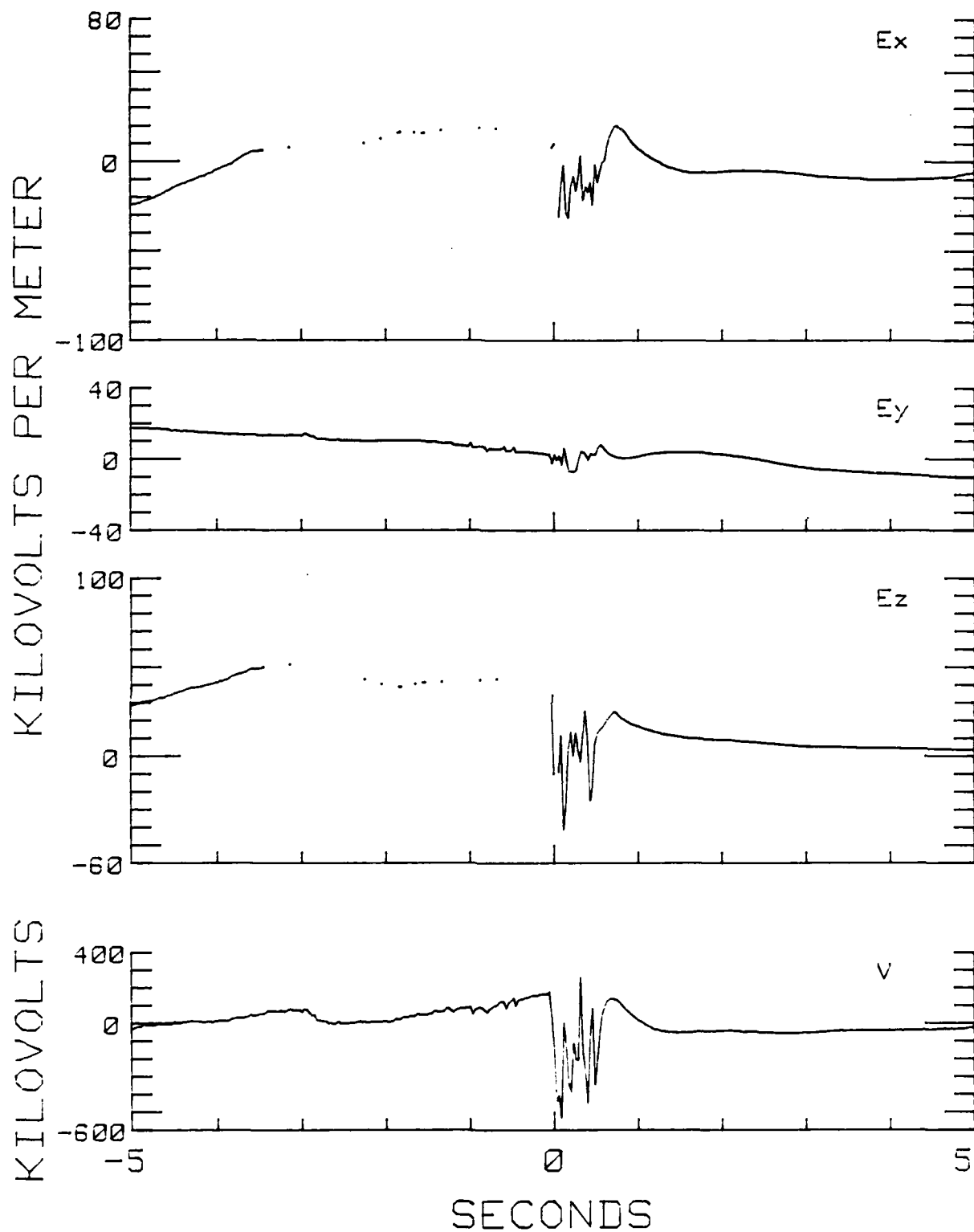


Fig. 41 — Cartesian vector field and aircraft potential

JUNE2785L2

1940:18.17

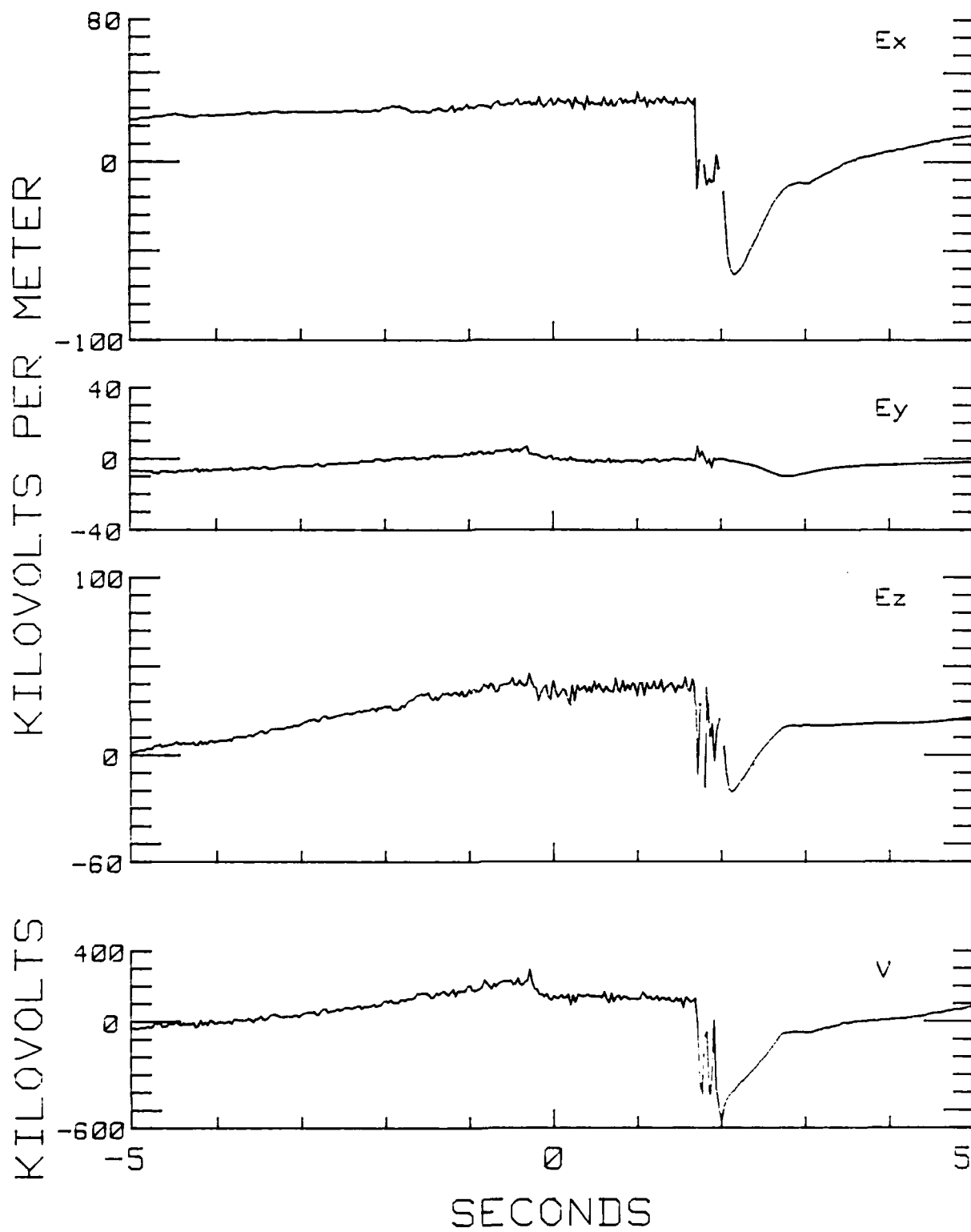


Fig. 42 — Cartesian vector field and aircraft potential

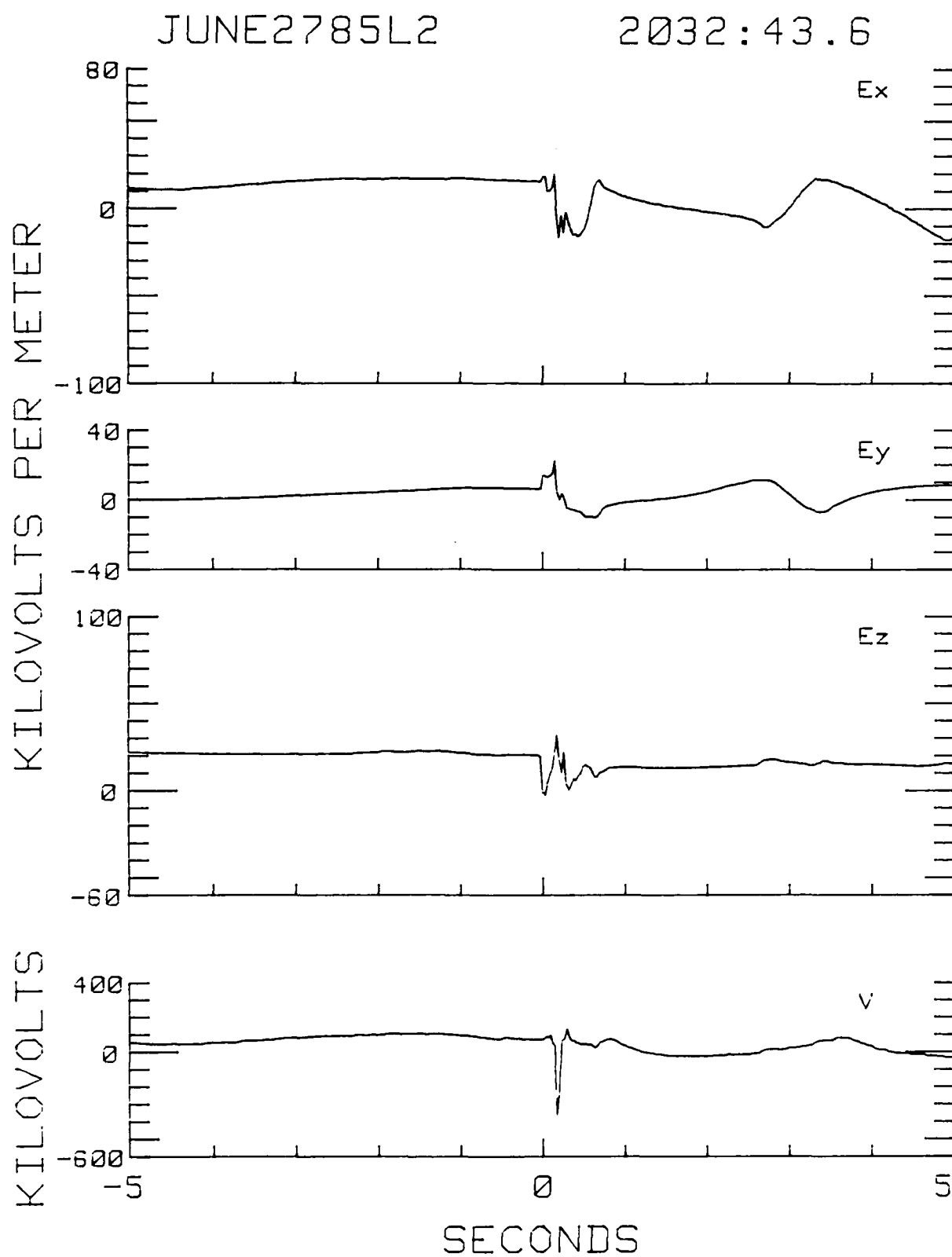


Fig. 43 — Cartesian vector field and aircraft potential

JUNE2985L2

1748:59

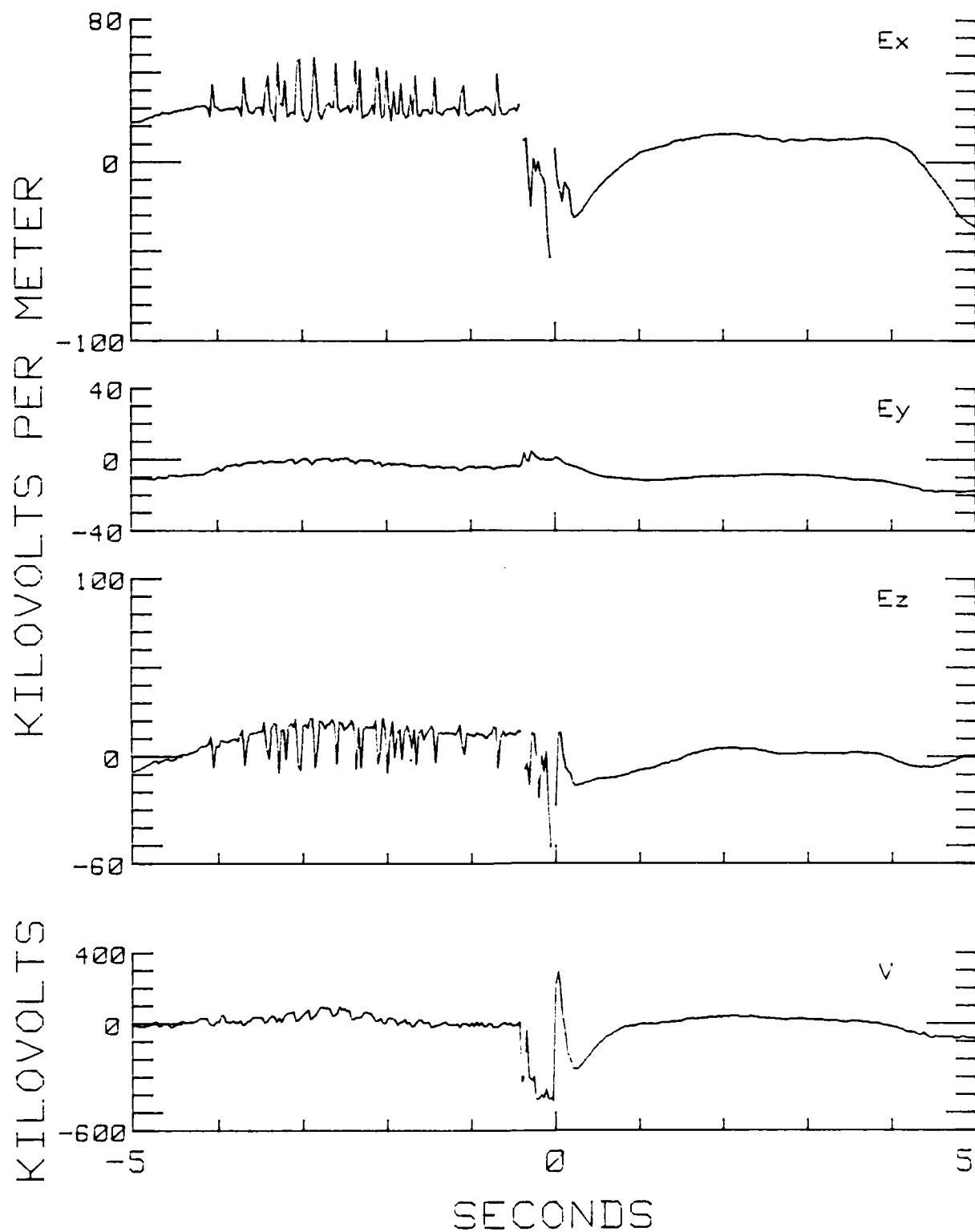


Fig. 44 — Cartesian vector field and aircraft potential

JULY0685L1

1940:10.03

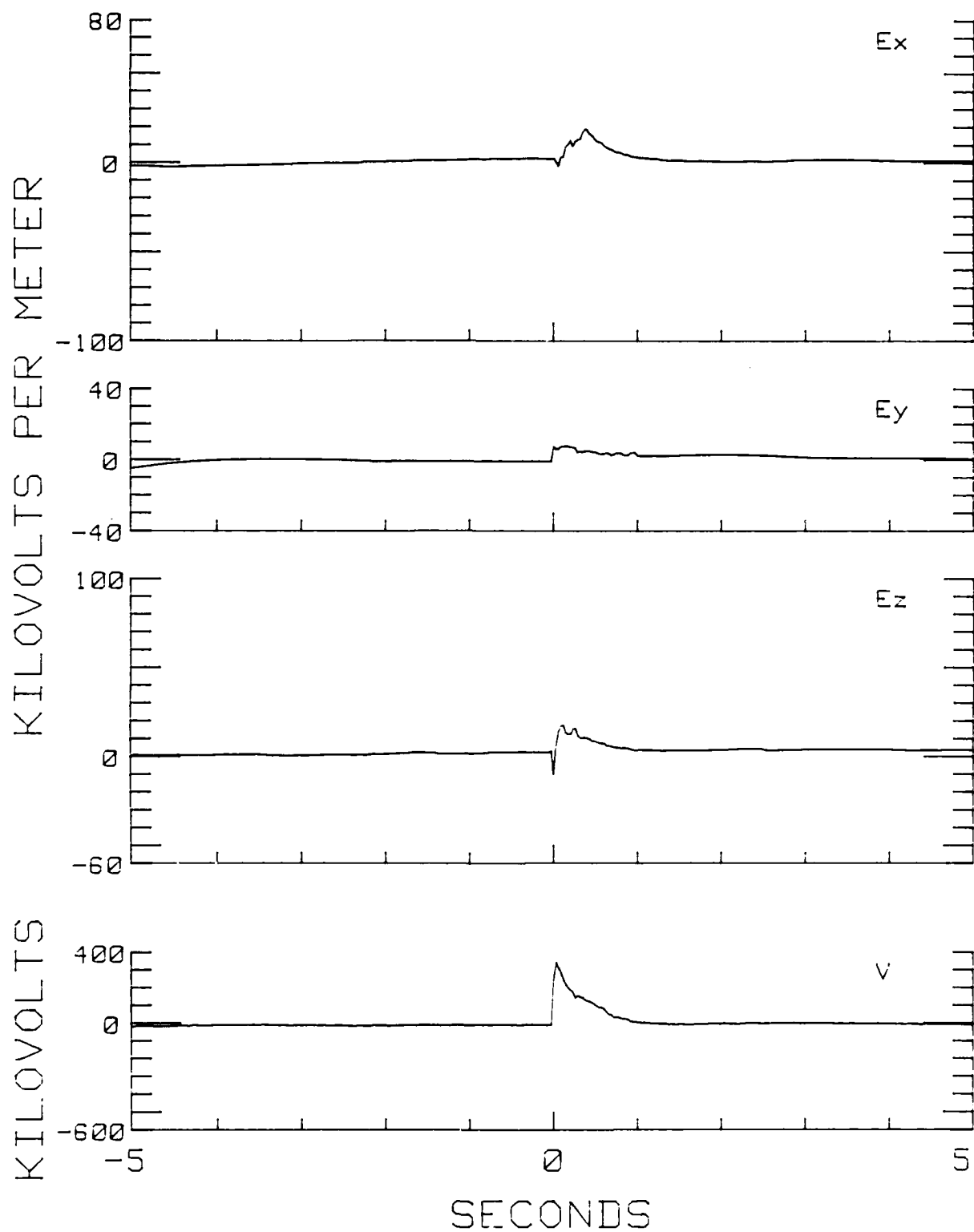


Fig. 45 — Cartesian vector field and aircraft potential



JULY 1585L7

1738:44.06

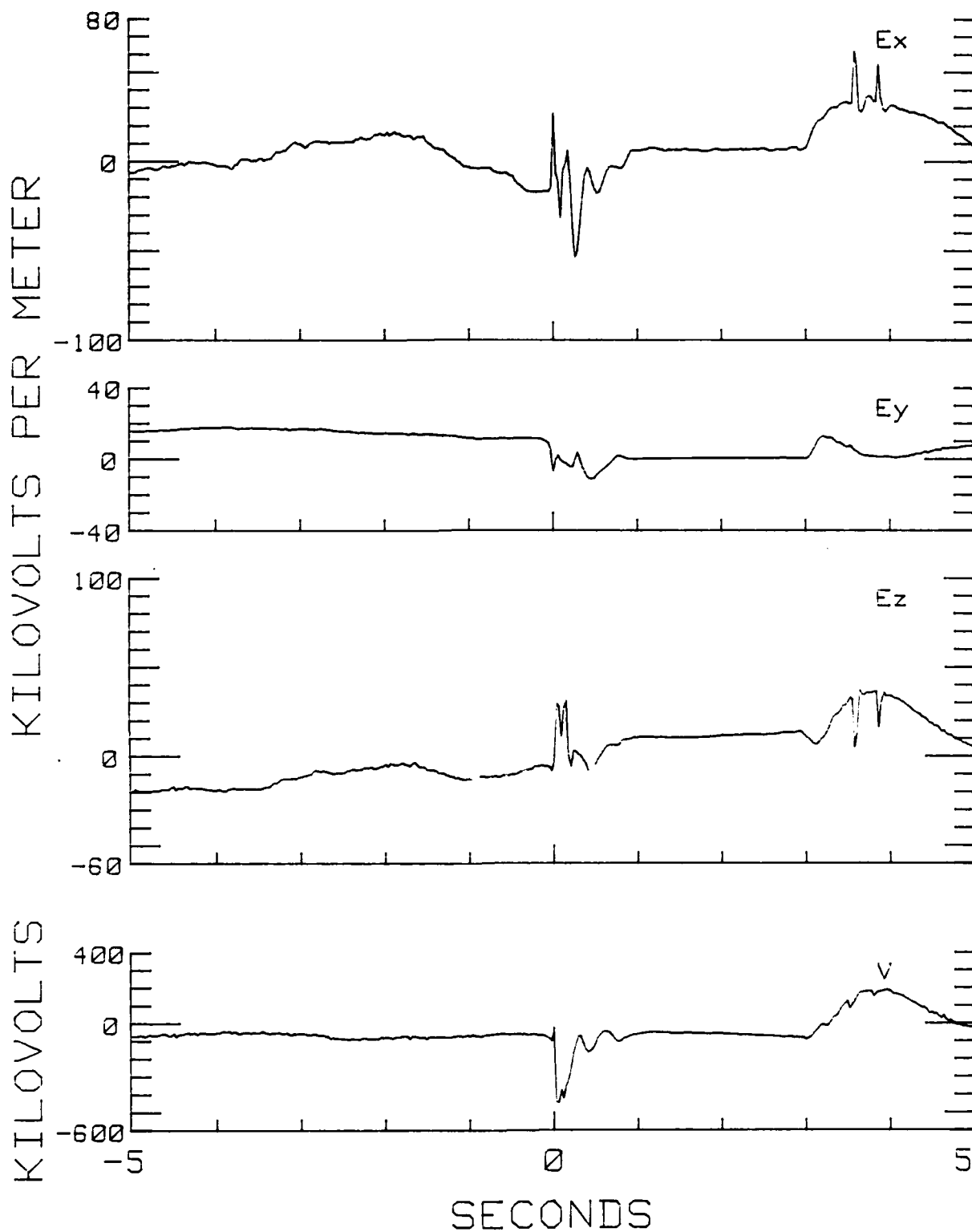


Fig. 46 — Cartesian vector field and aircraft potential

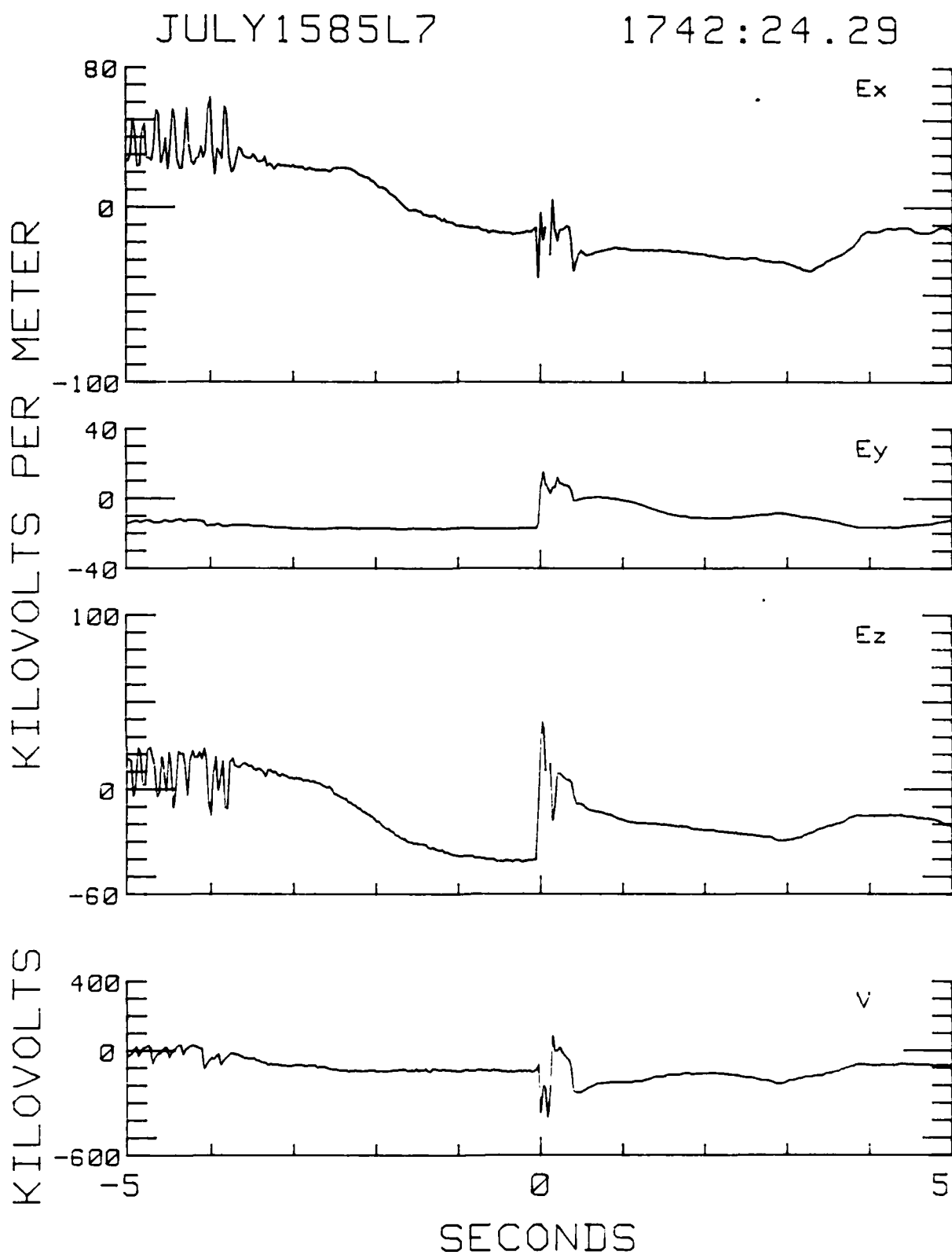


Fig. 47 — Cartesian vector field and aircraft potential

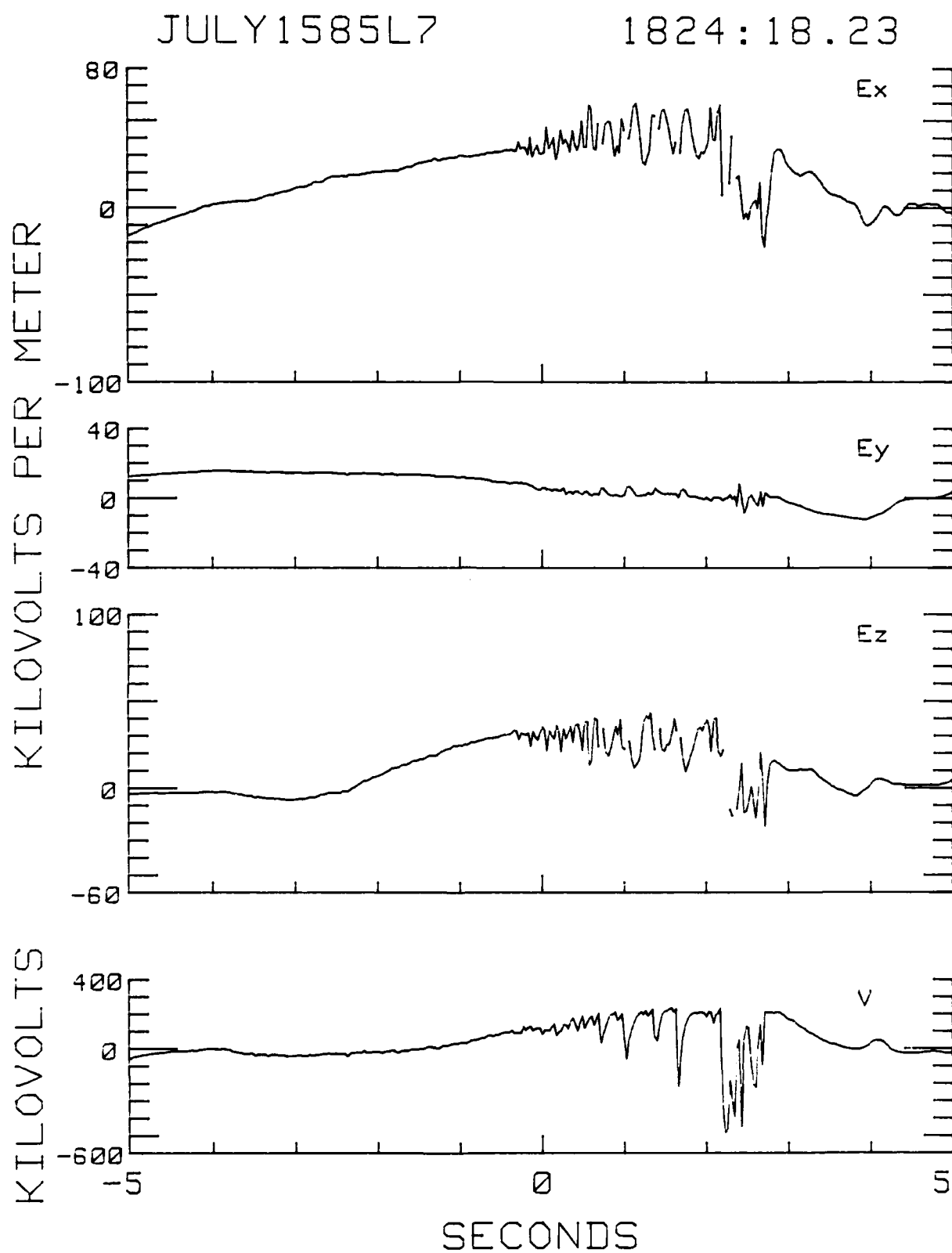


Fig. 48 — Cartesian vector field and aircraft potential

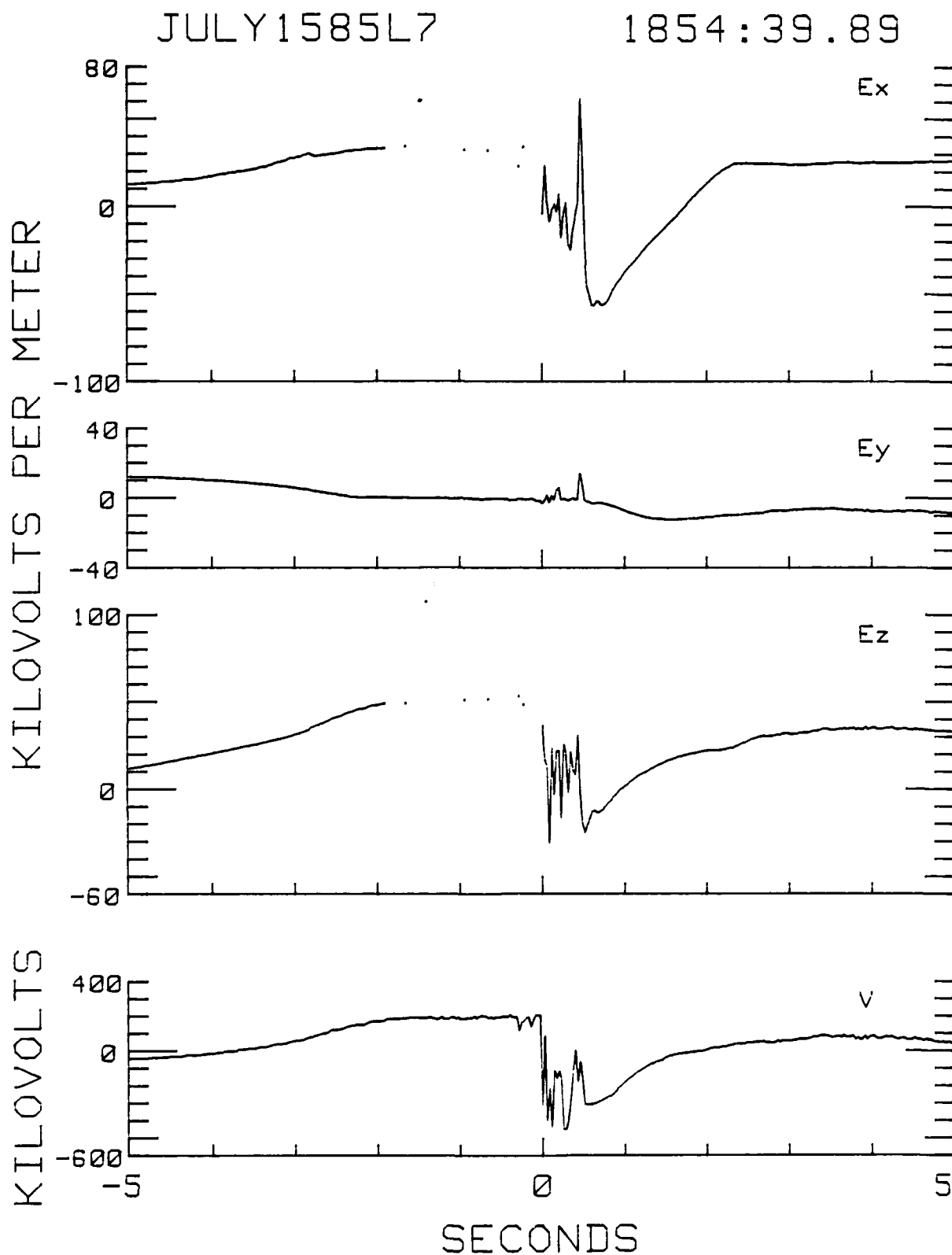


Fig. 49 — Cartesian vector field and aircraft potential

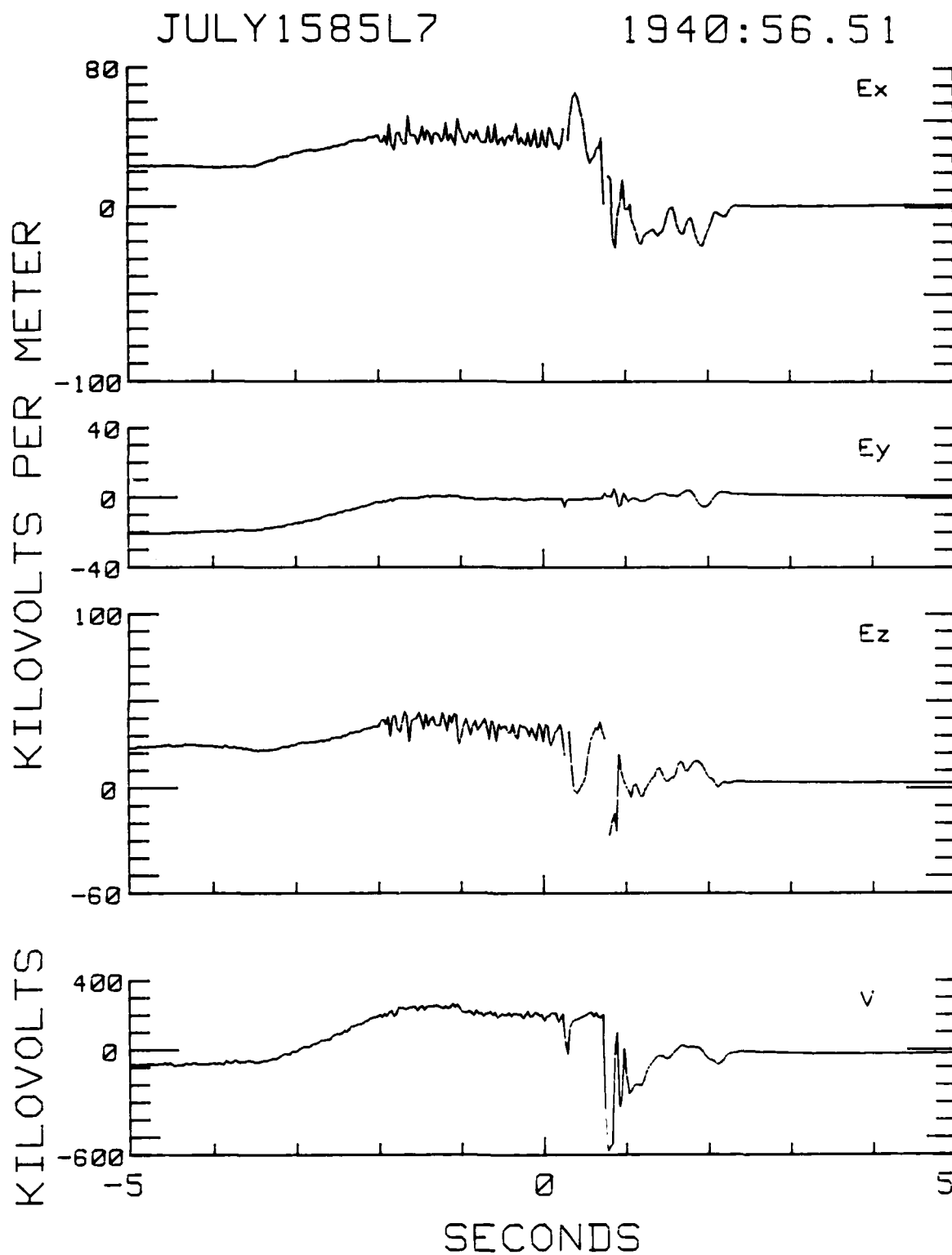


Fig. 50 — Cartesian vector field and aircraft potential

JULY 15 85L7

1944:34.71

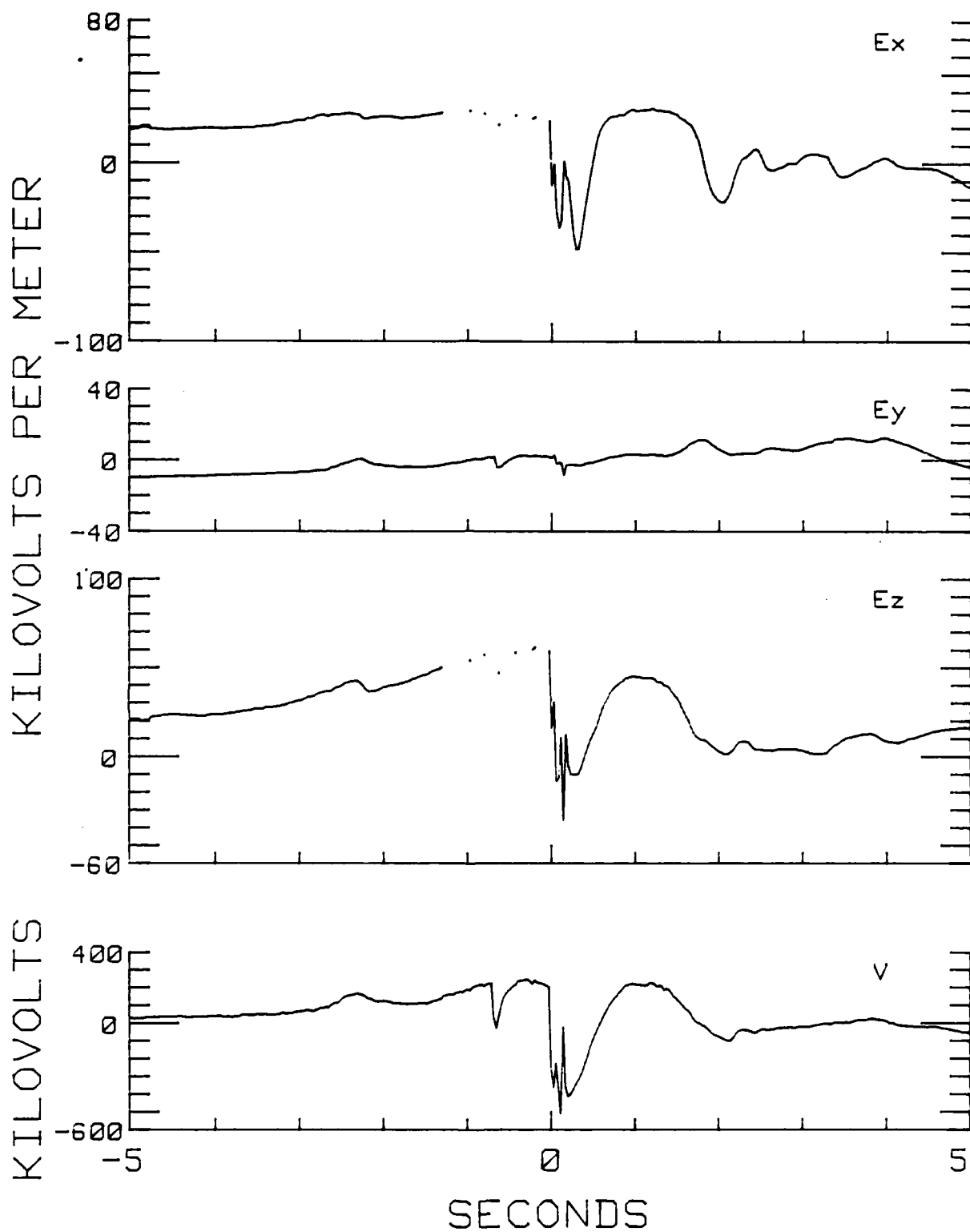


Fig. 51 — Cartesian vector field and aircraft potential

JULY 1585L7

1949:16.74

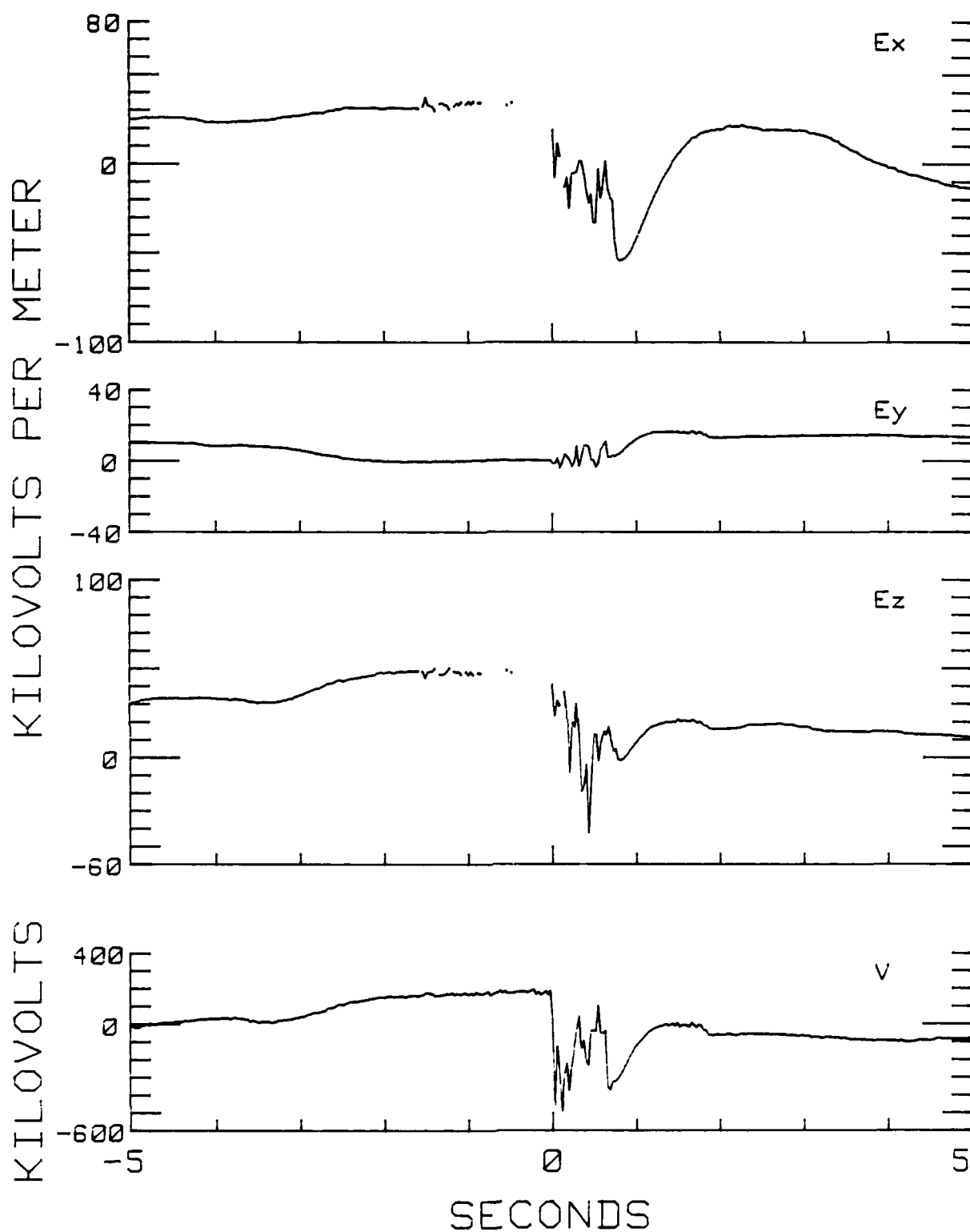


Fig. 52 — Cartesian vector field and aircraft potential

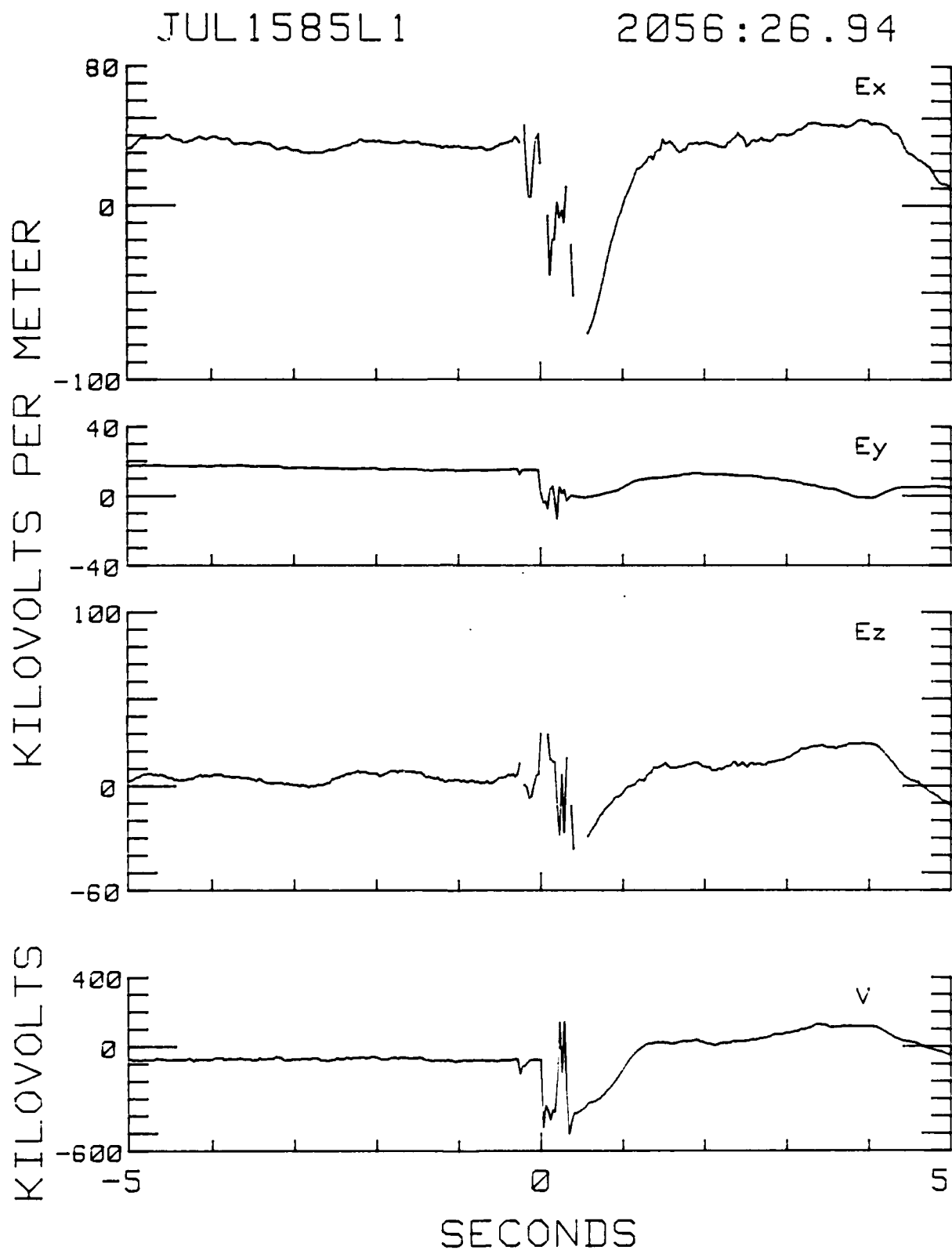


Fig. 53 — Cartesian vector field and aircraft potential



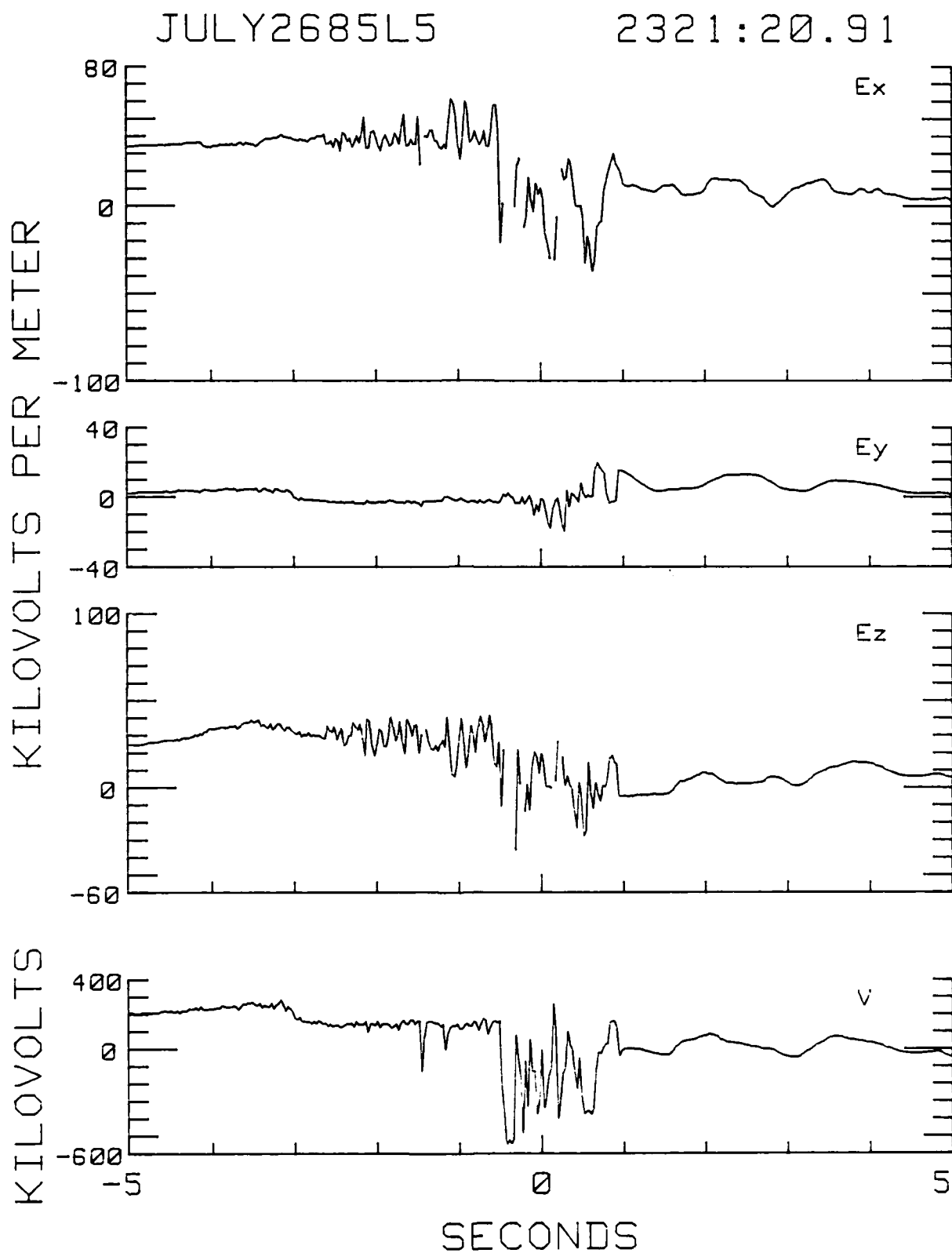


Fig. 54 — Cartesian vector field and aircraft potential

JULY2685L5

2333:23.34

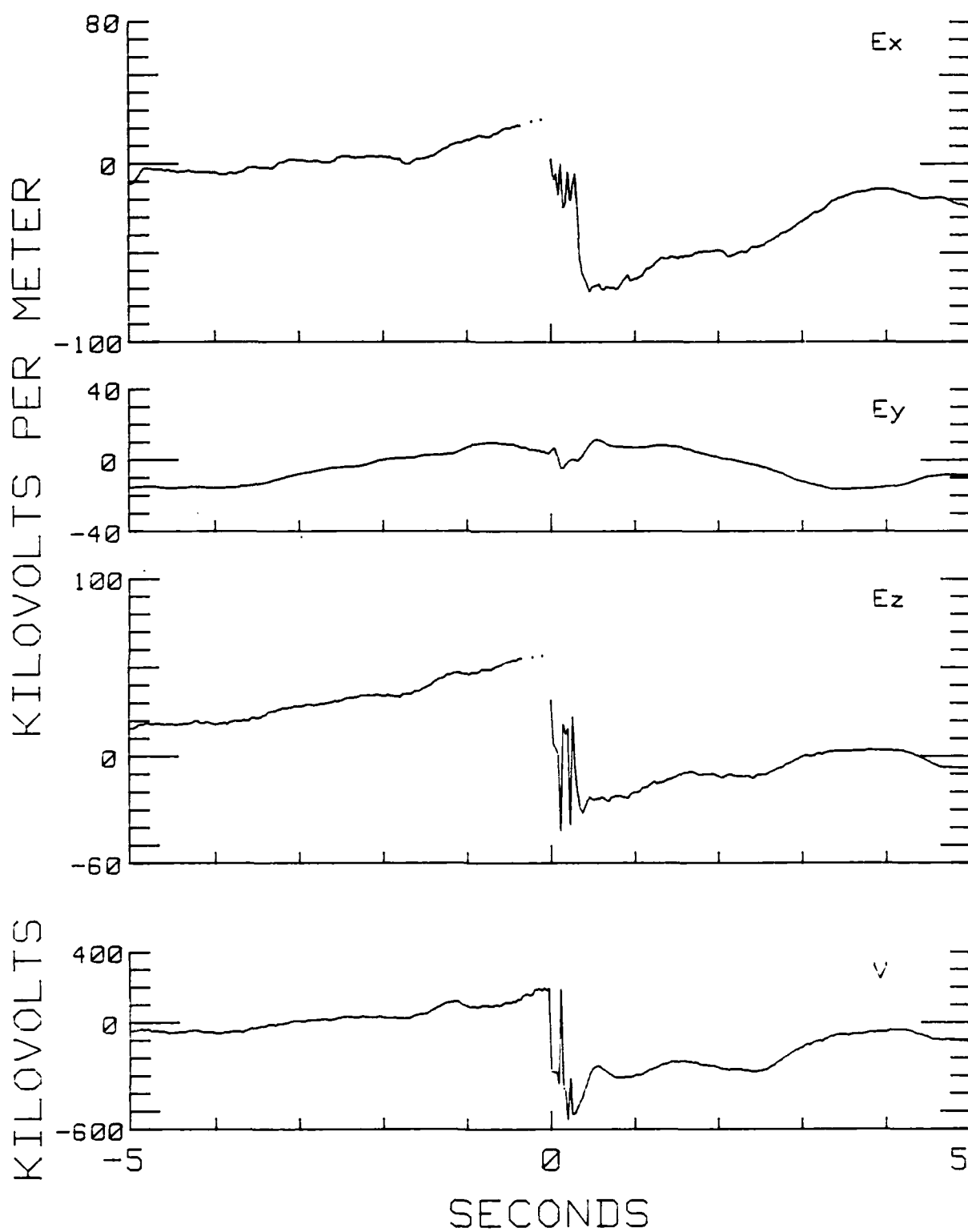


Fig. 55 — Cartesian vector field and aircraft potential

JULY2685L5

2351:58.13

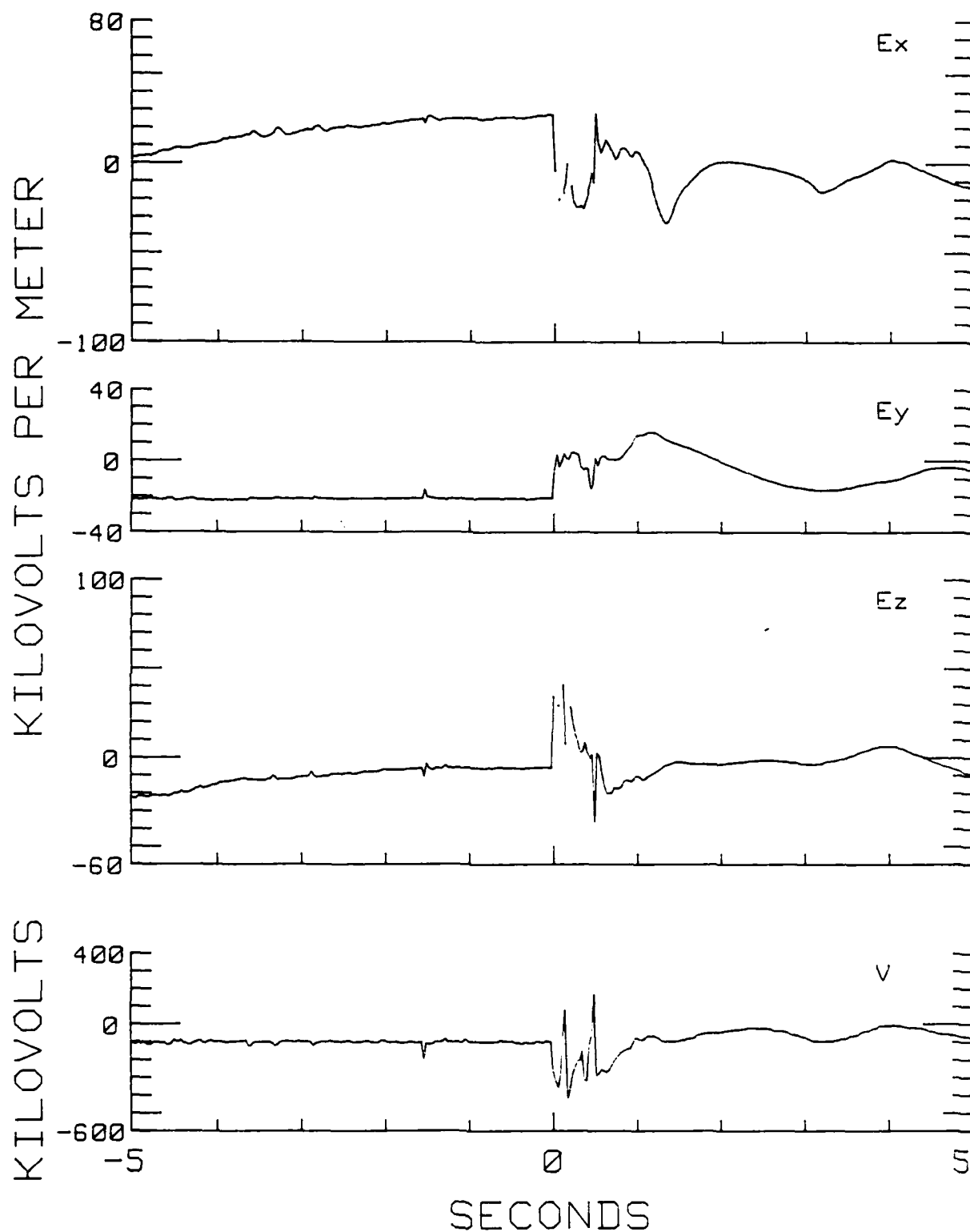


Fig. 56 — Cartesian vector field and aircraft potential

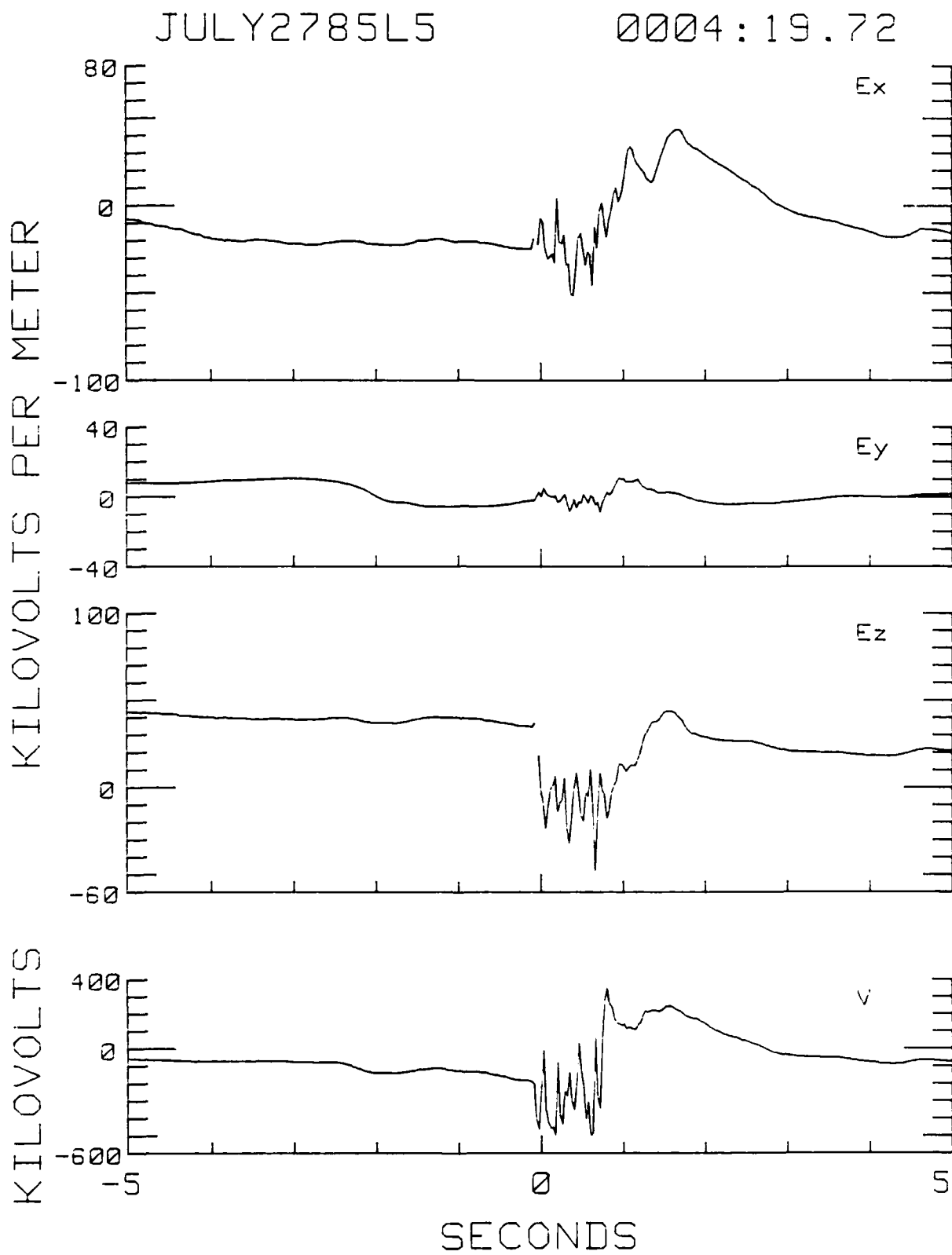


Fig. 57 — Cartesian vector field and aircraft potential

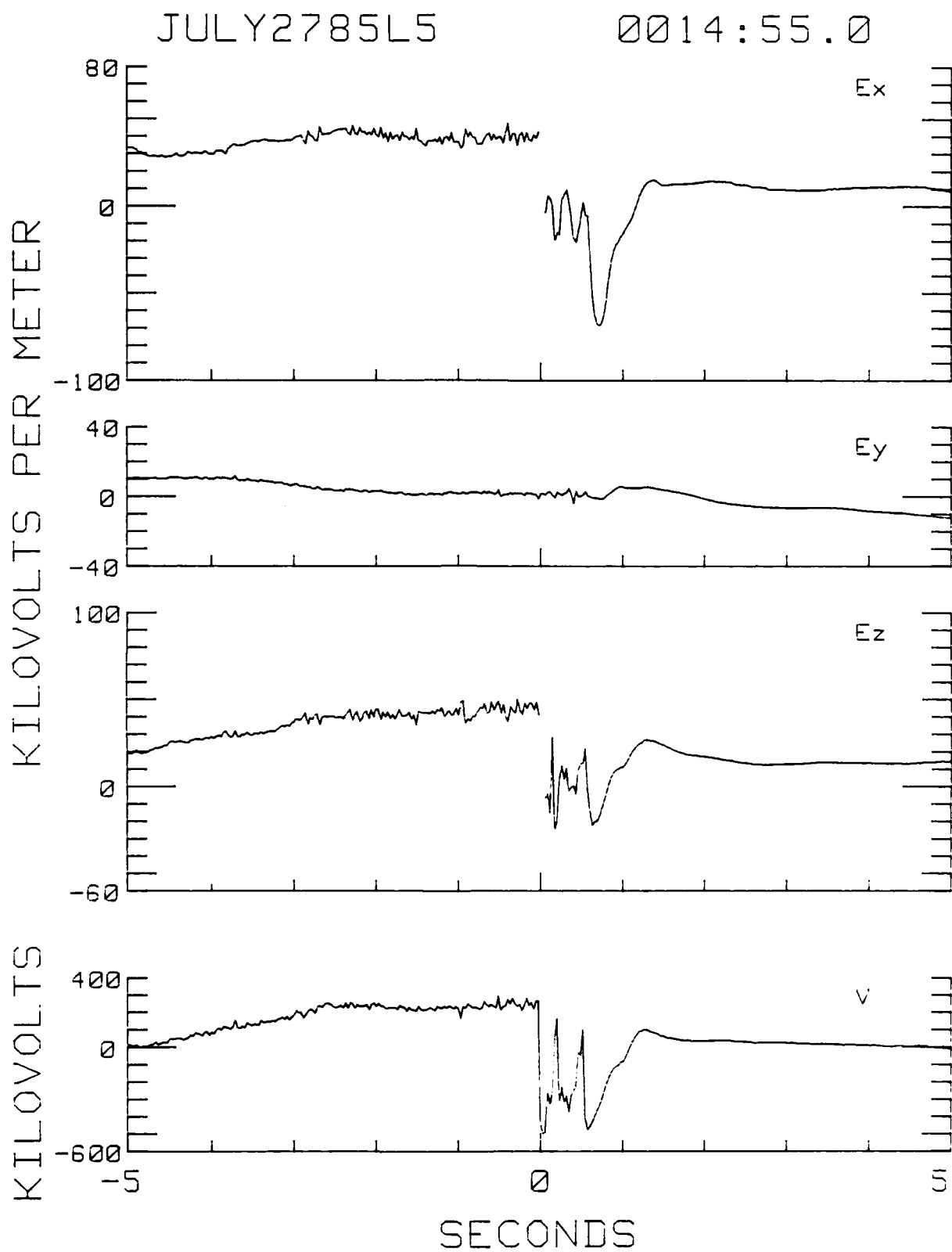


Fig. 58 — Cartesian vector field and aircraft potential

JULY3085L2

2028:18.51

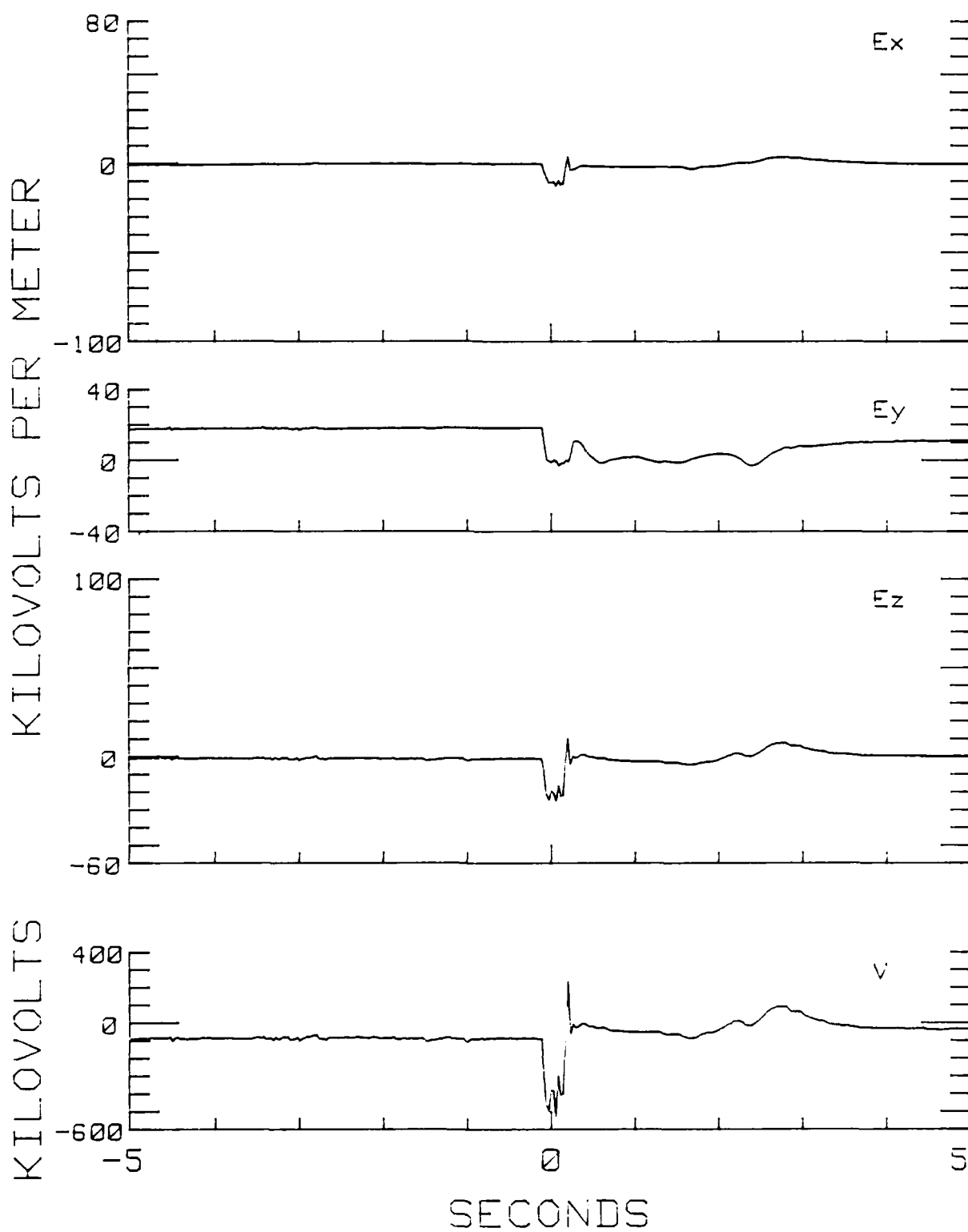


Fig. 59 — Cartesian vector field and aircraft potential

JULY3085L2

2118:33.37

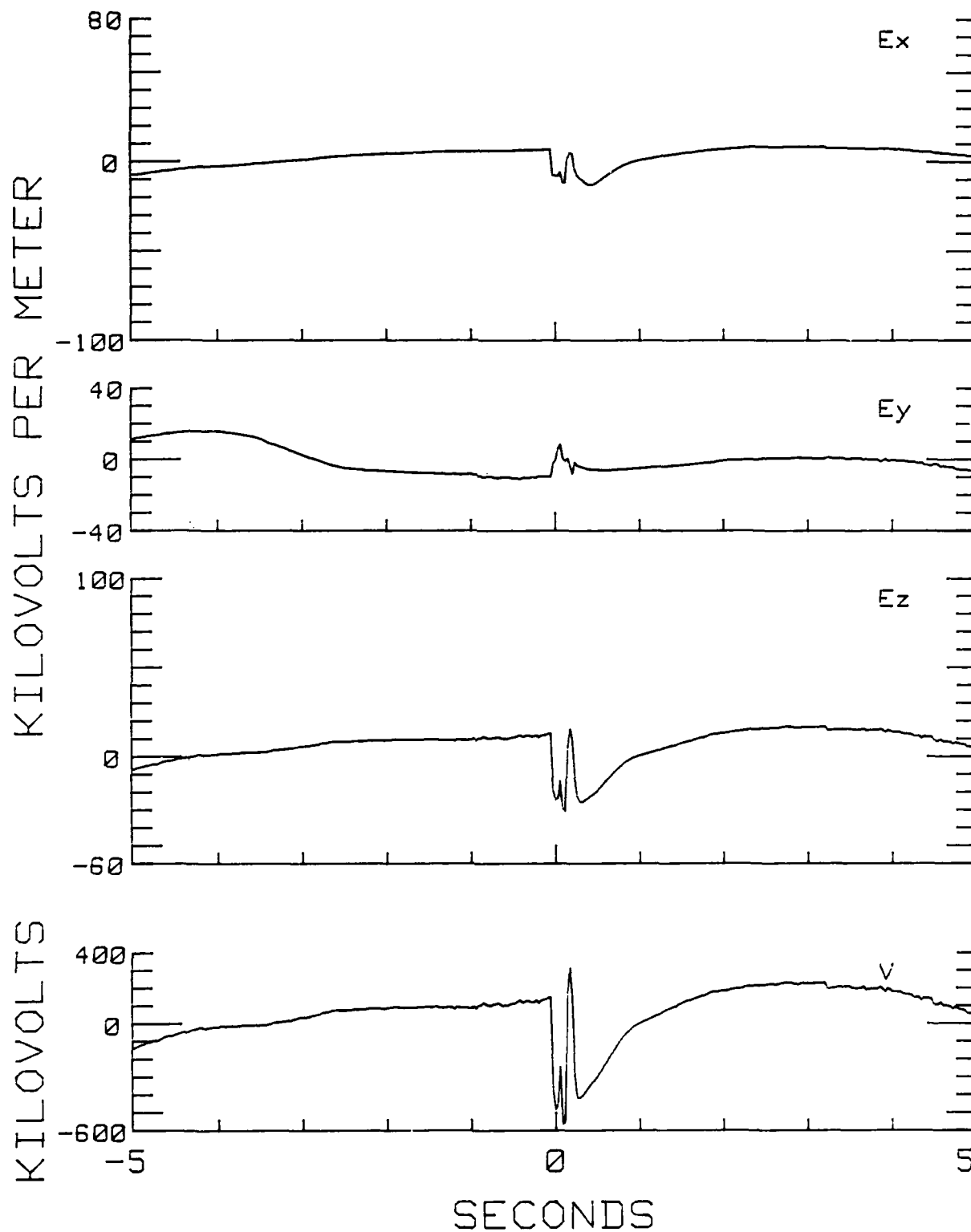


Fig. 60 — Cartesian vector field and aircraft potential

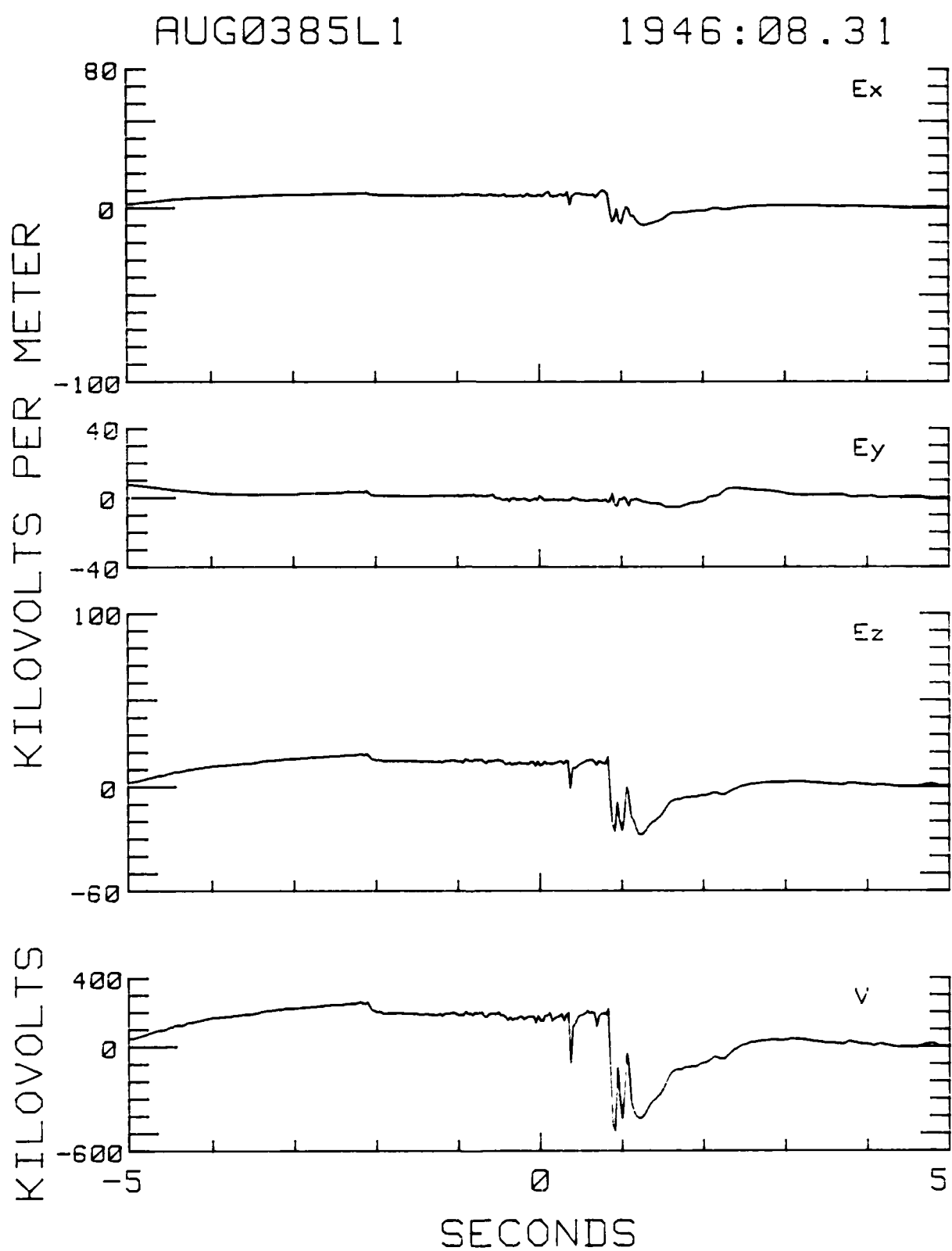


Fig. 61 — Cartesian vector field and aircraft potential



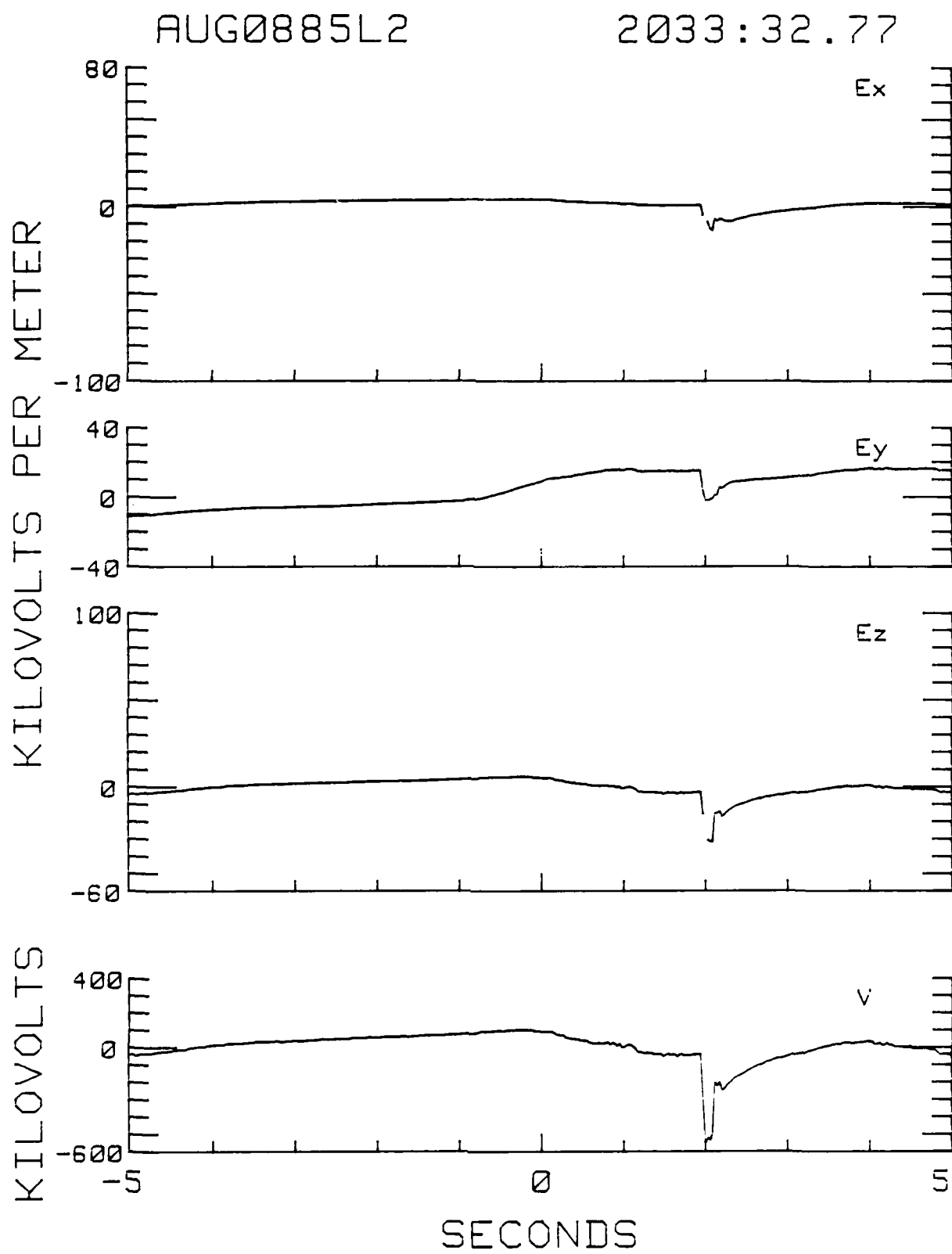


Fig. 62 — Cartesian vector field and aircraft potential

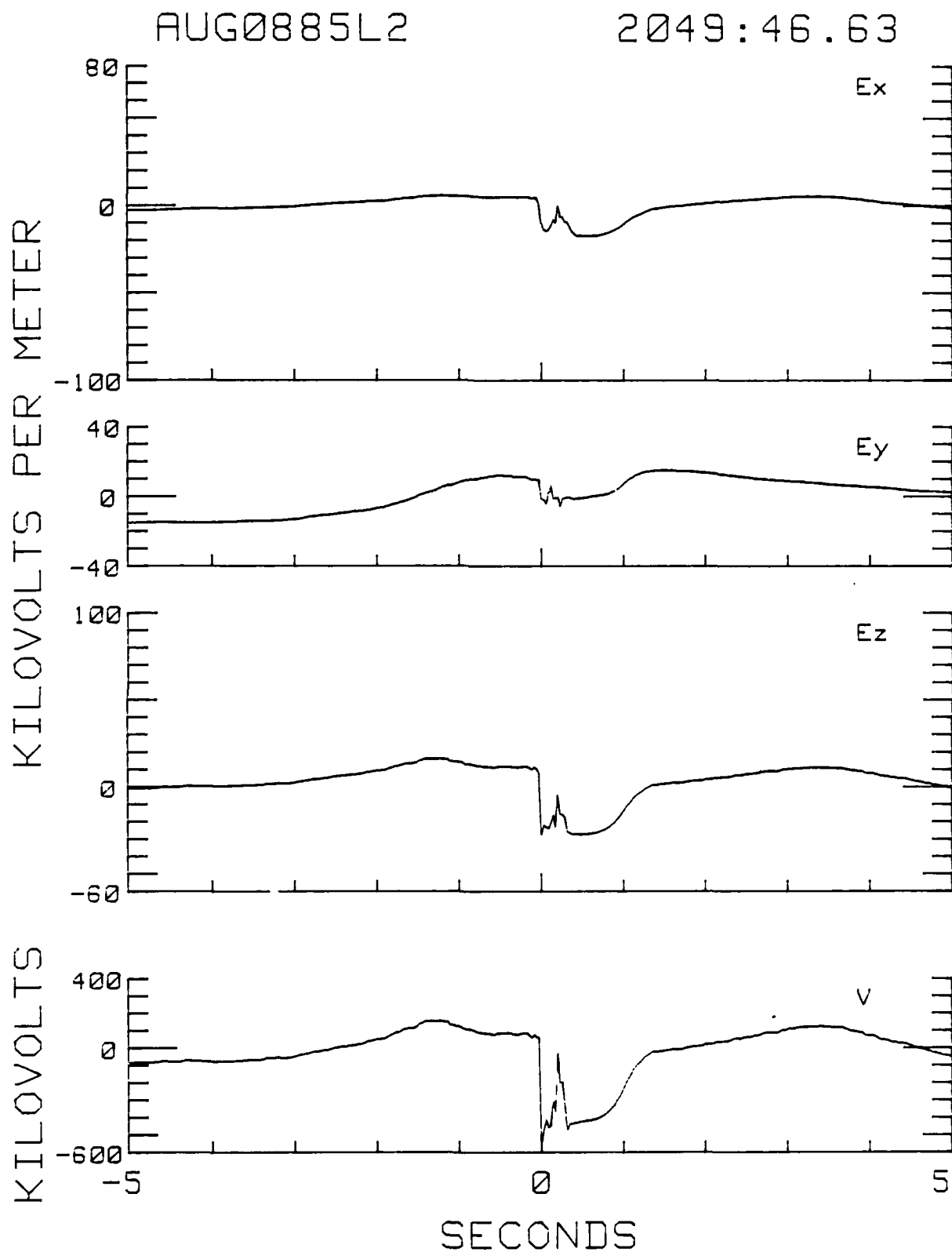


Fig. 63 — Cartesian vector field and aircraft potential

AUG3085L2

2227:08.29

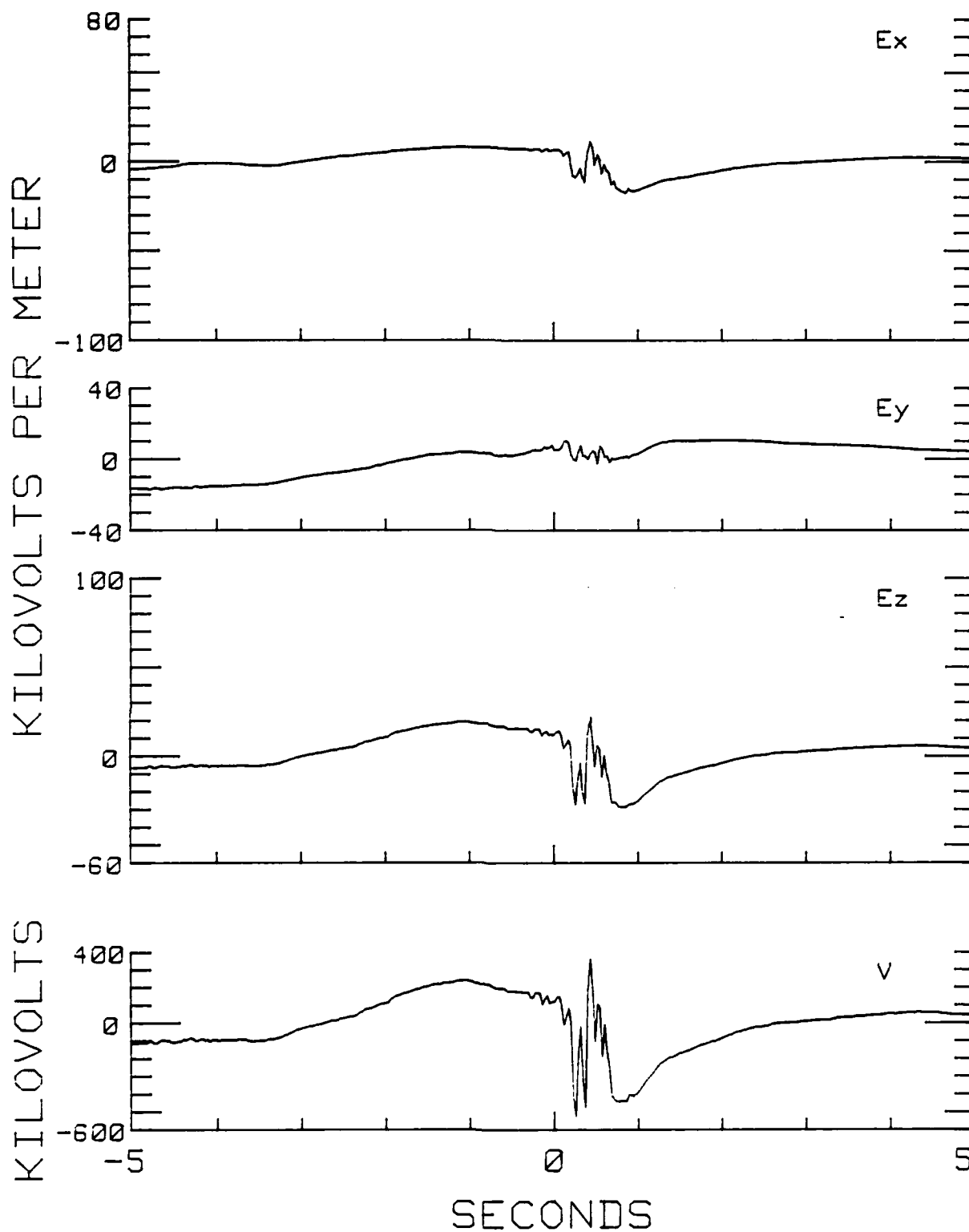


Fig. 64 — Cartesian vector field and aircraft potential

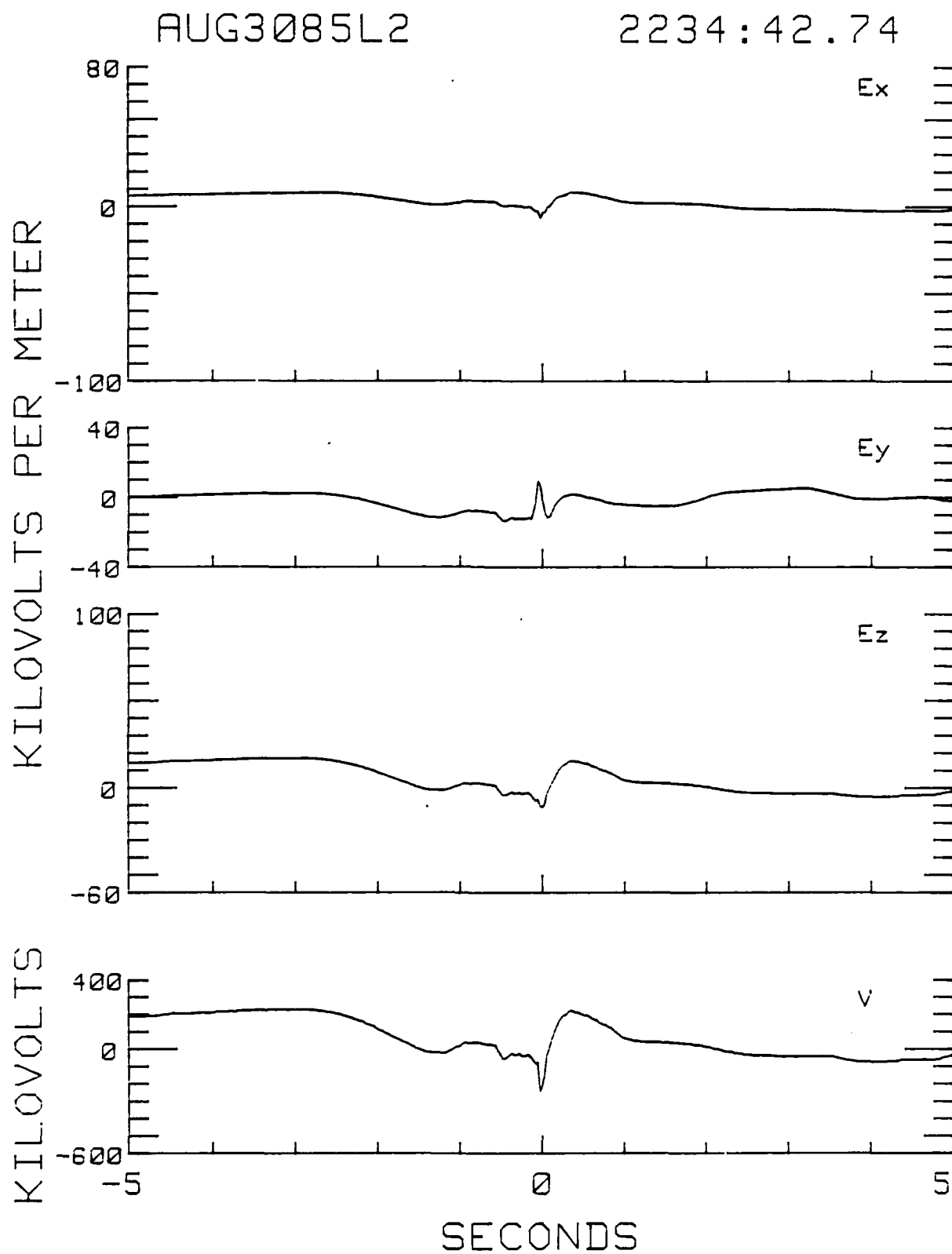


Fig. 65 — Cartesian vector field and aircraft potential

JUNE2185L3

2021:49.34

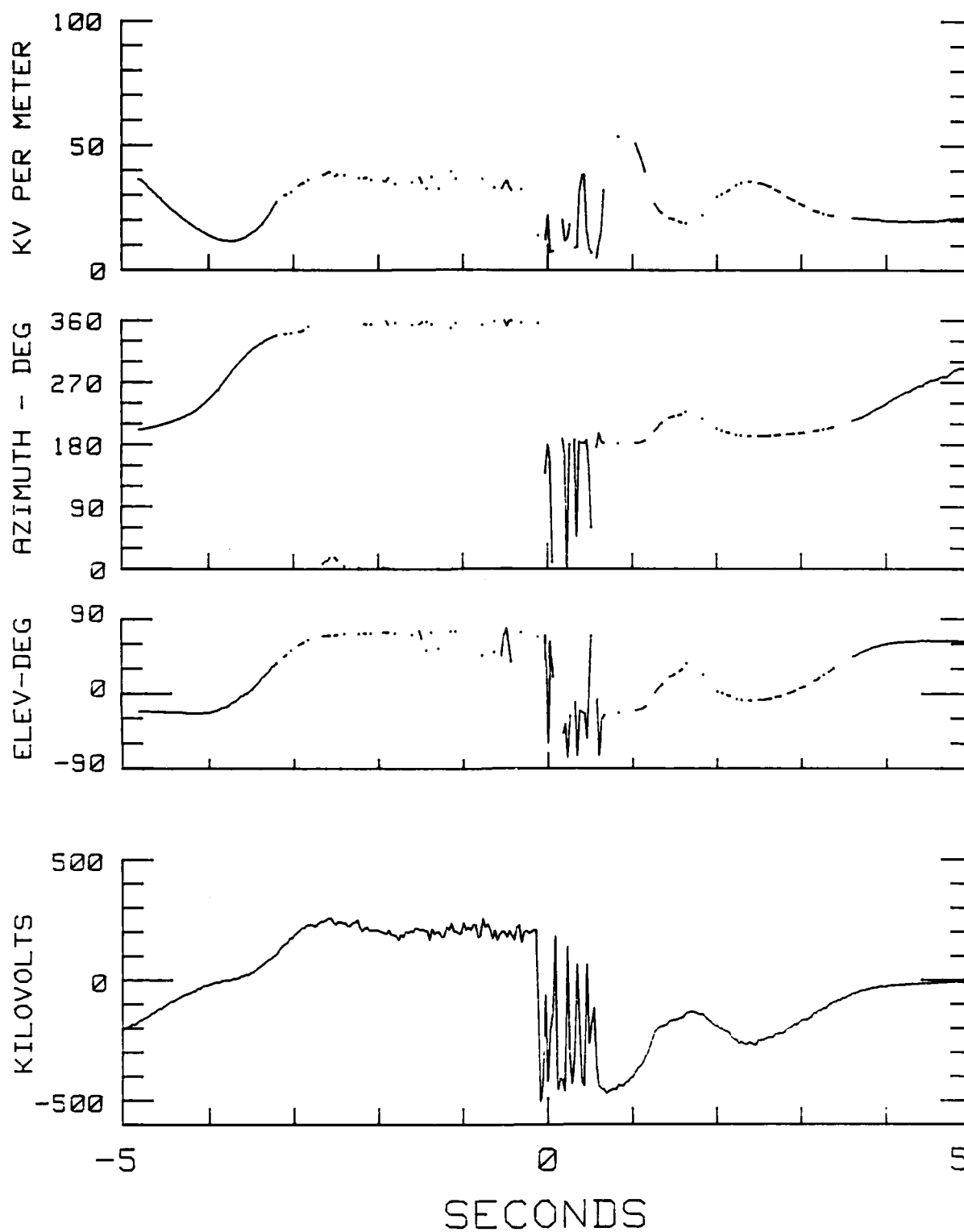


Fig. 66 — Vector field magnitude, azimuth, and elevation with aircraft potential

JUNE2185L3

2109:02.37

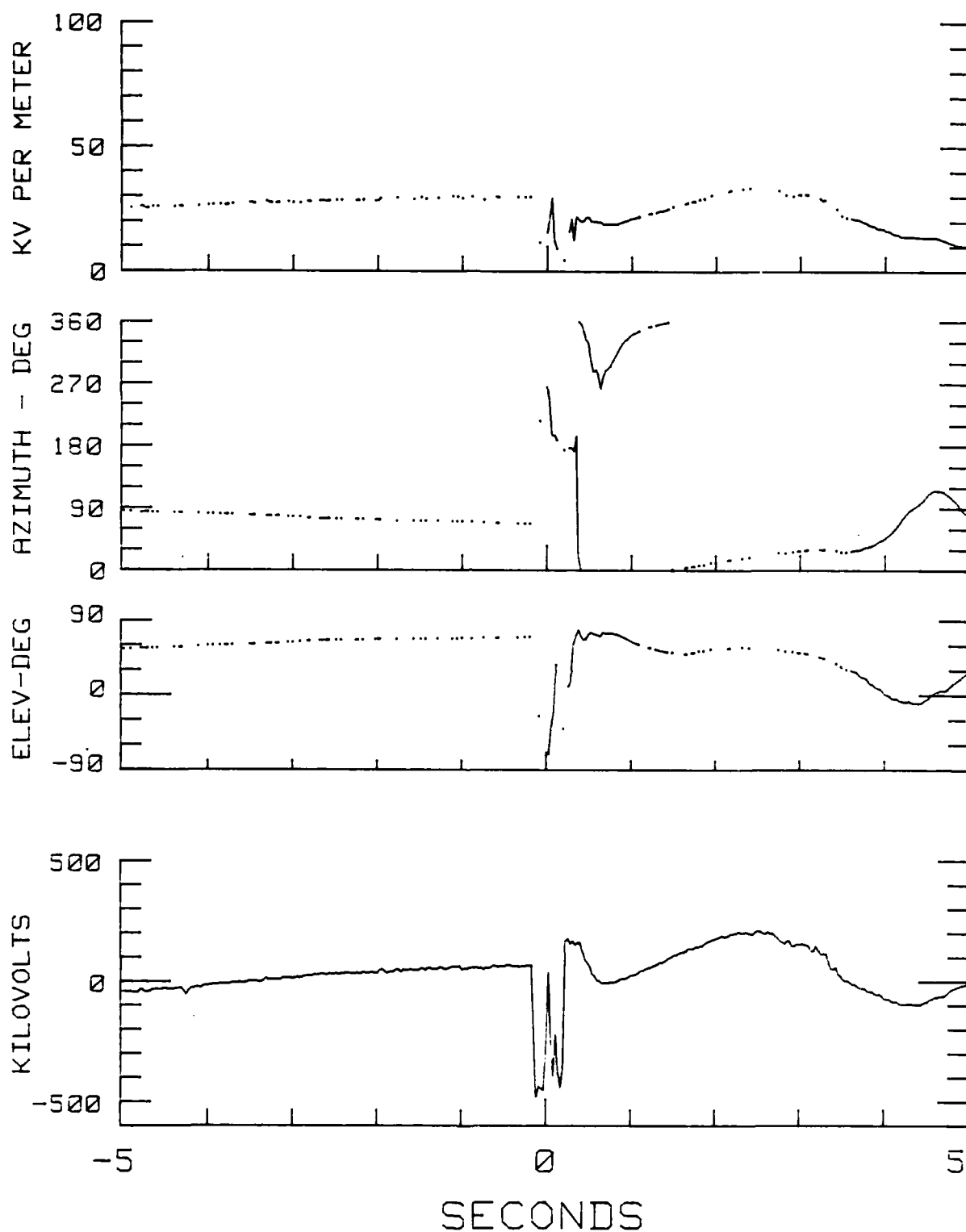


Fig. 67 — Vector field magnitude, azimuth, and elevation with aircraft potential

JUNE2185L3

2118:02.97

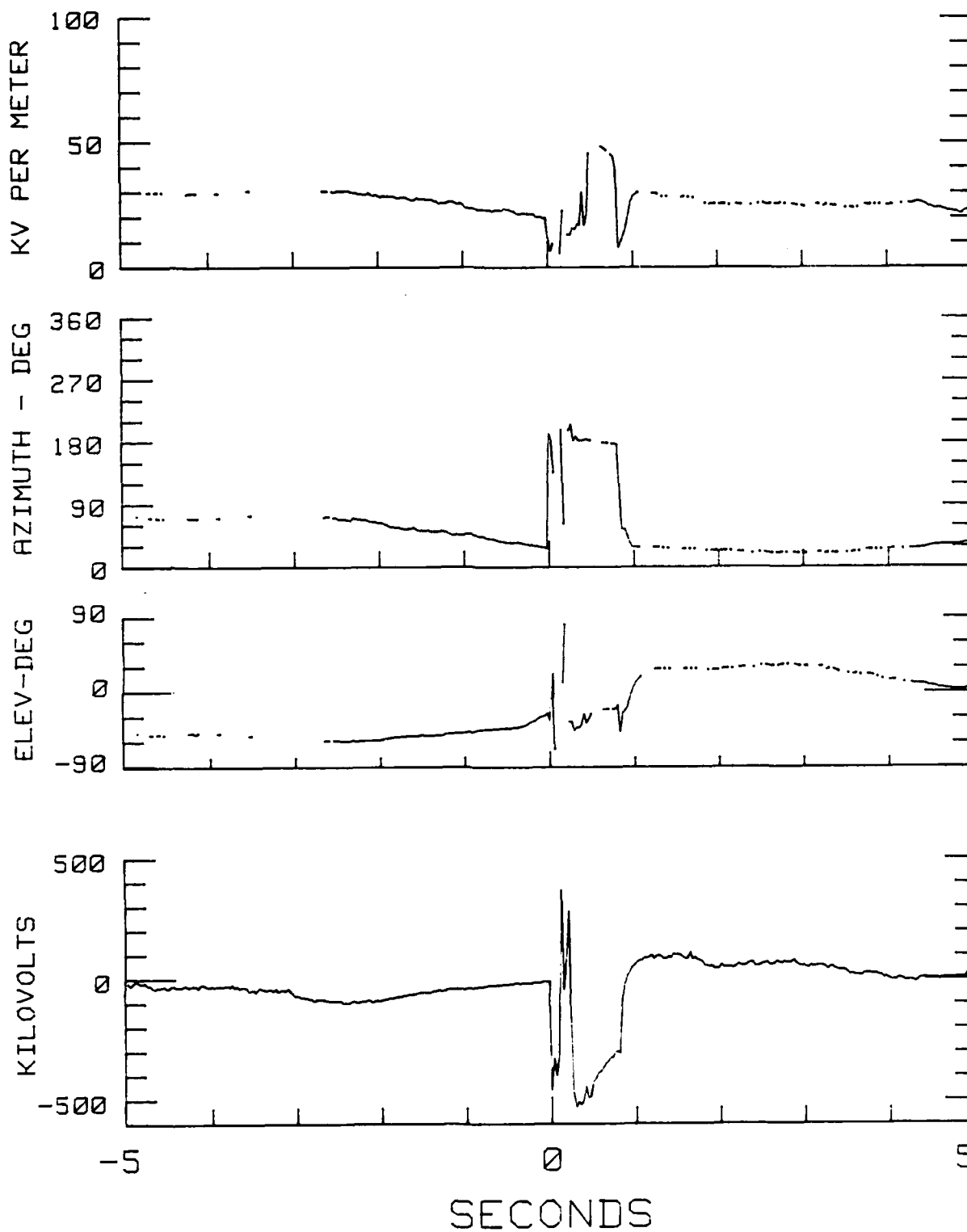


Fig. 68 — Vector field magnitude, azimuth, and elevation with aircraft potential

JUNE2685L3

2040:29.71

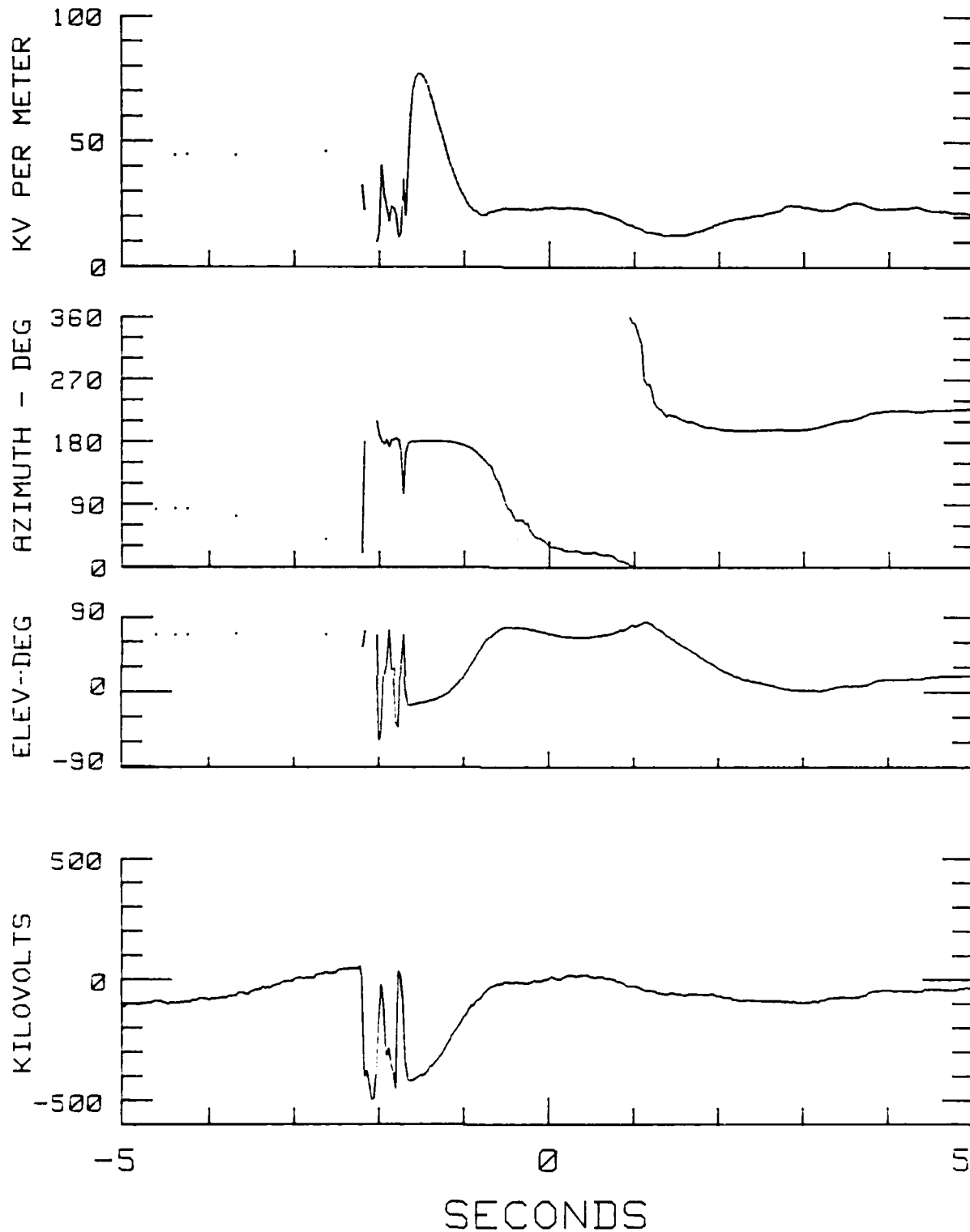


Fig. 69 — Vector field magnitude, azimuth, and elevation with aircraft potential



JUNE2685L3

2055:24.46

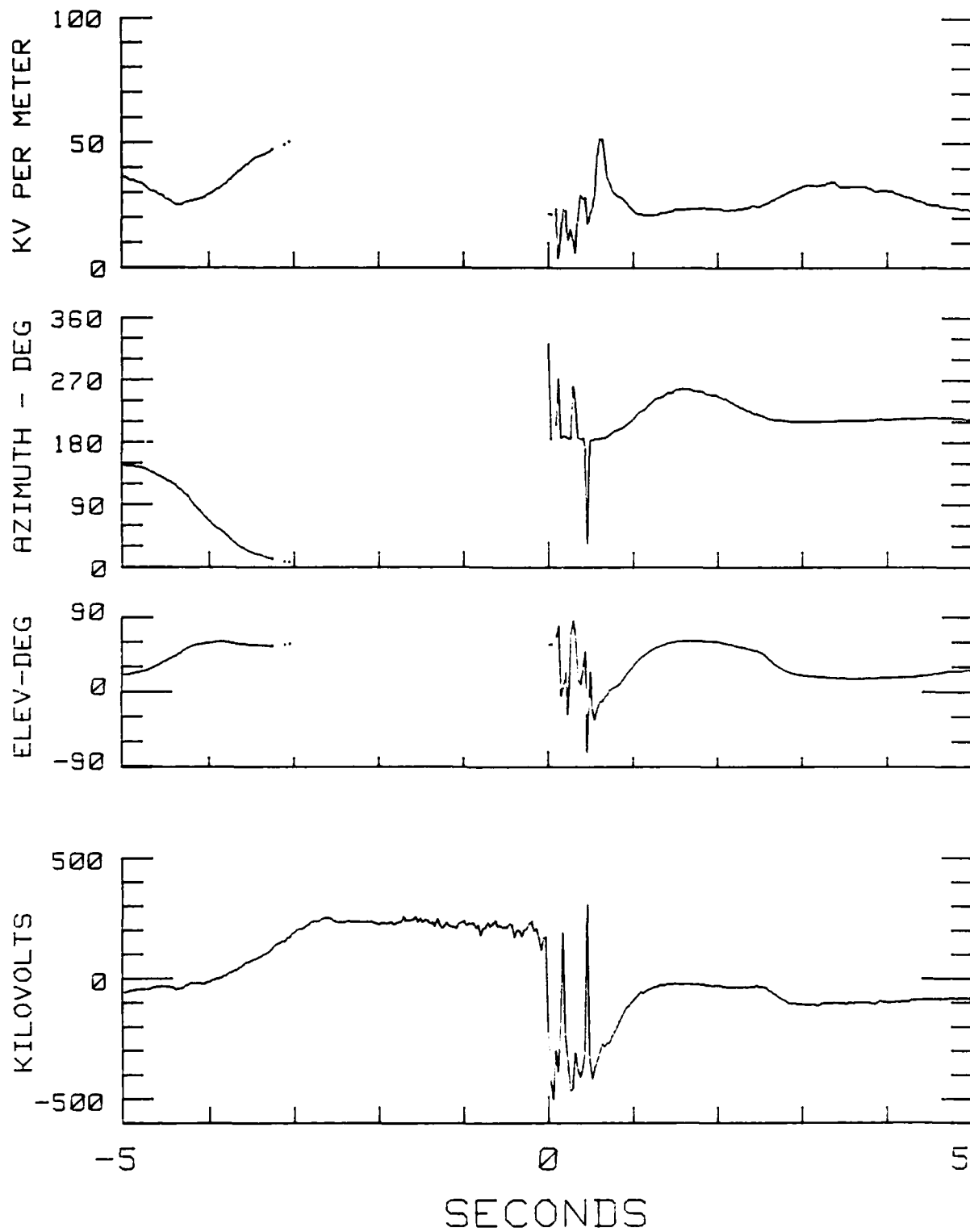


Fig. 70 — Vector field magnitude, azimuth, and elevation with aircraft potential

JUNE2685L3

2100:15.94

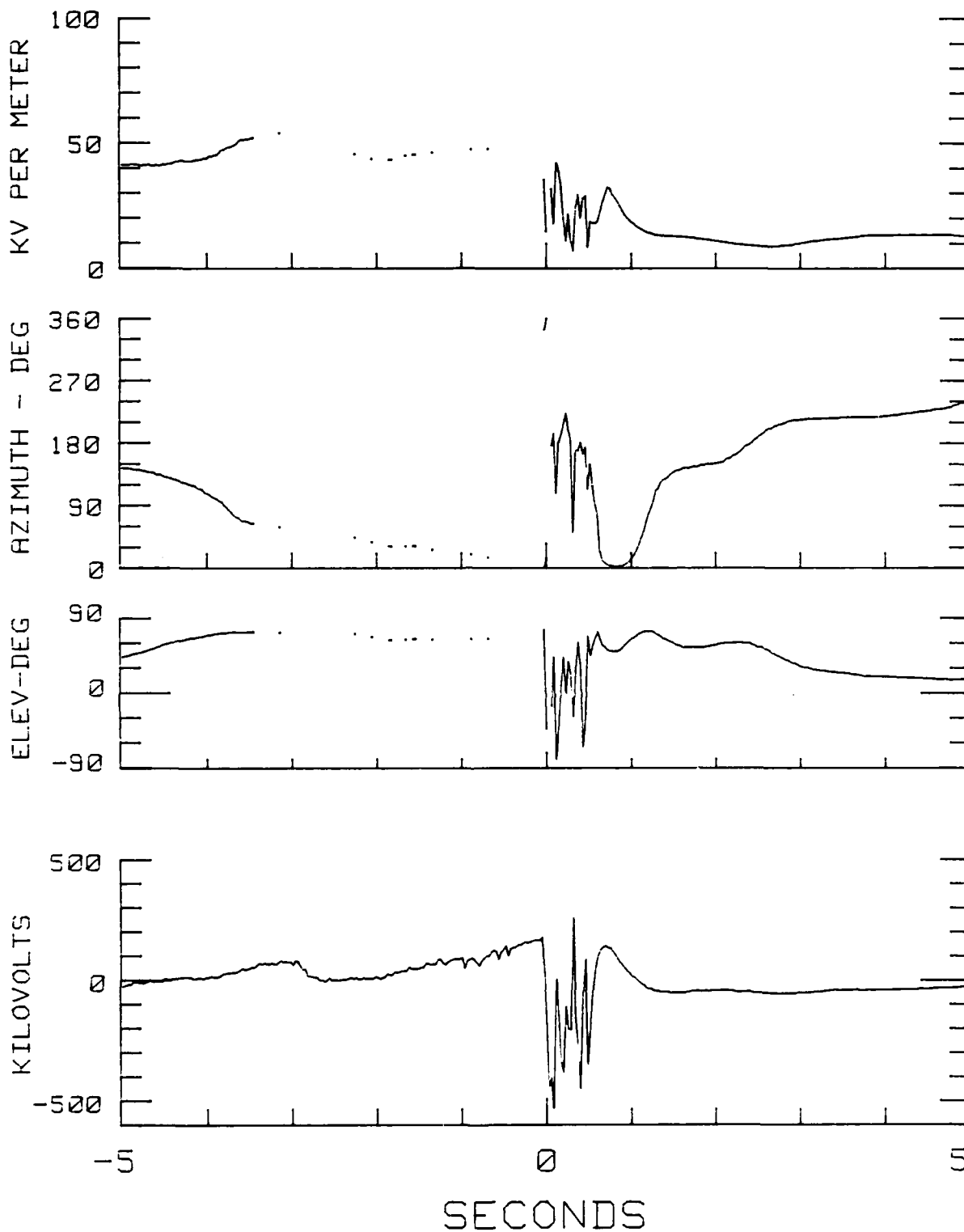


Fig. 71 — Vector field magnitude, azimuth, and elevation with aircraft potential

JUNE2785L2

1940:18.17

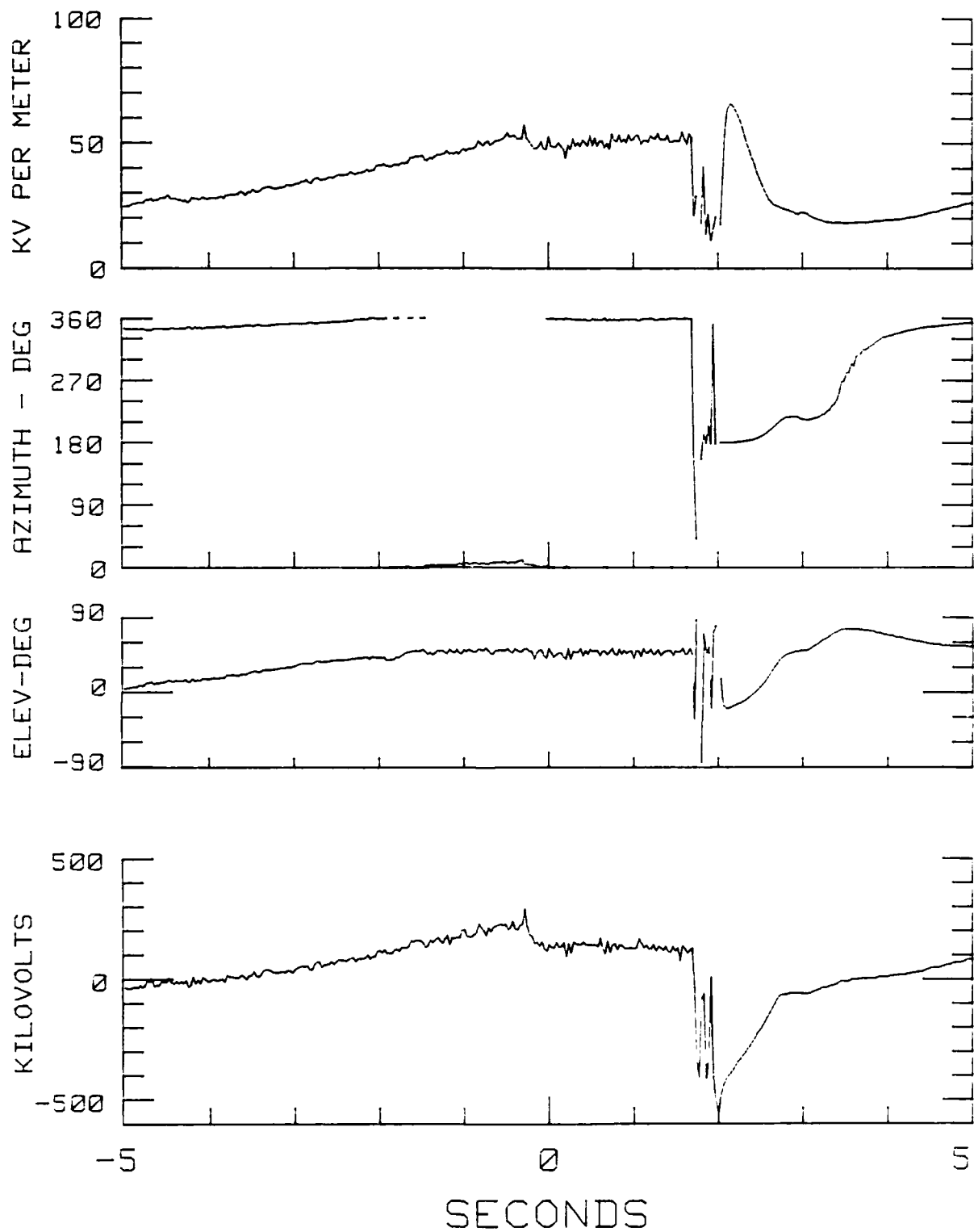


Fig. 72 — Vector field magnitude, azimuth, and elevation with aircraft potential

JUNE2785L2

2032:43.6

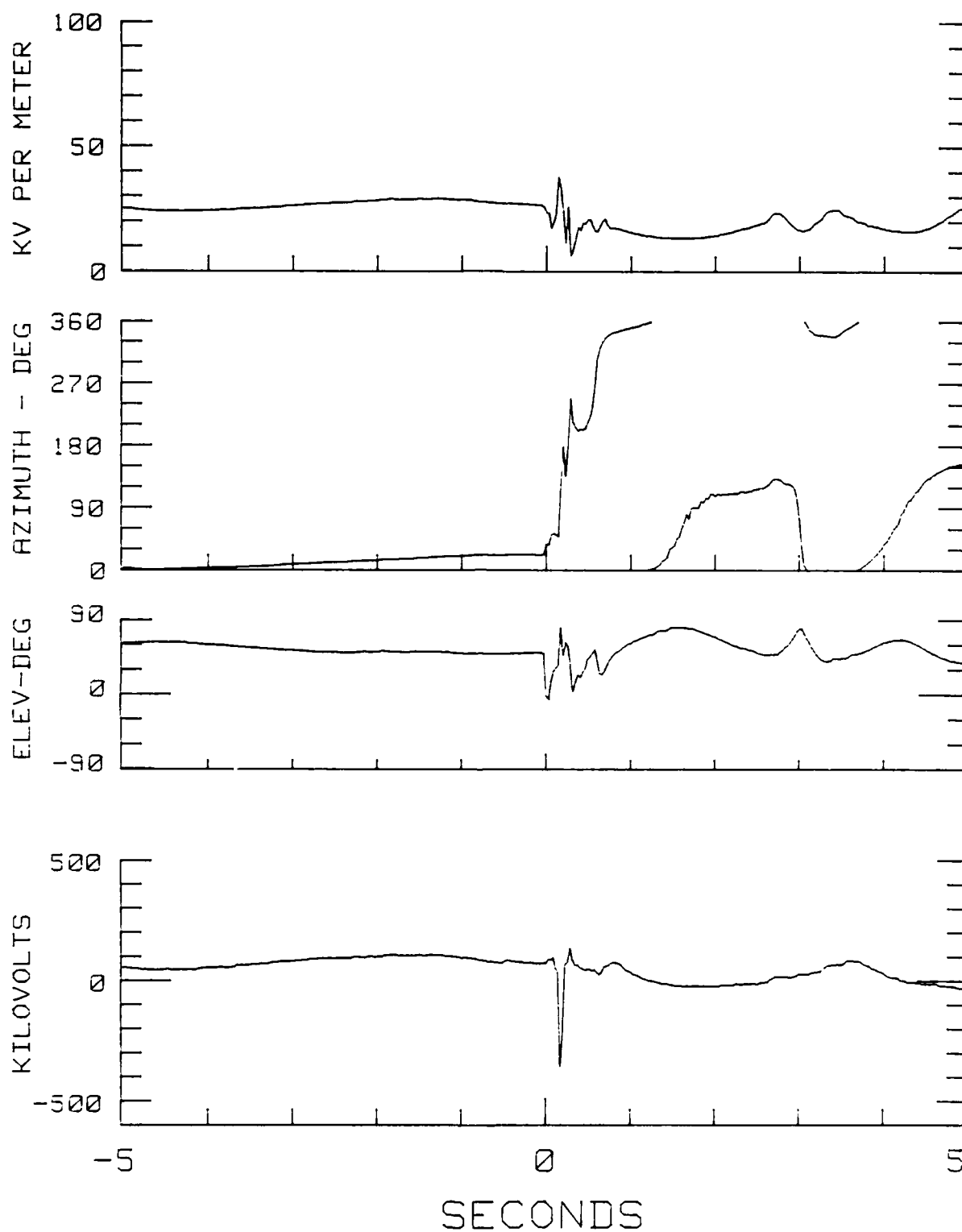


Fig. 73 — Vector field magnitude, azimuth, and elevation with aircraft potential

JUNE2985L2

1748:59

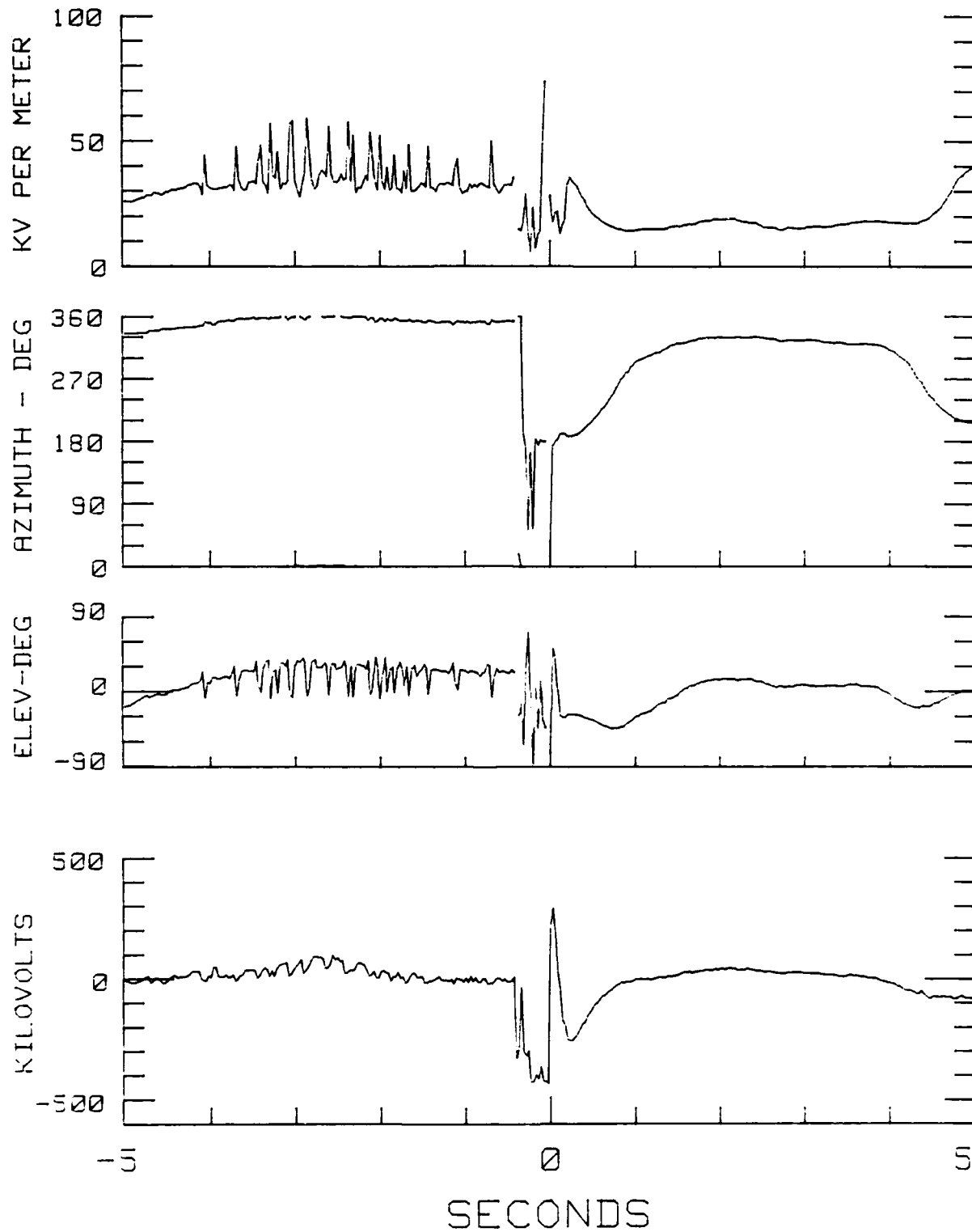


Fig. 74 — Vector field magnitude, azimuth, and elevation with aircraft potential

JULY0685L1

1940:10.03

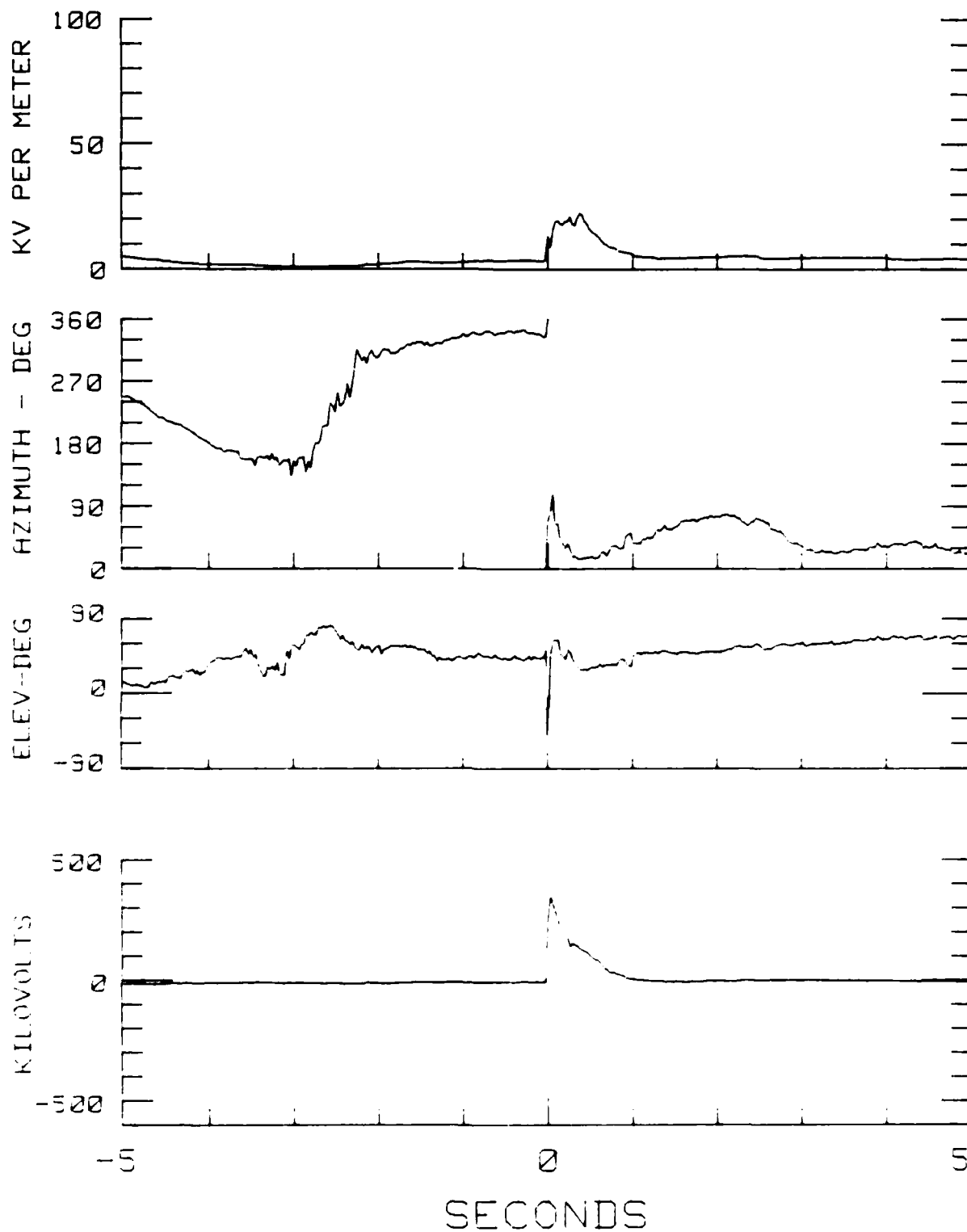


Fig. 75 — Vector field magnitude, azimuth, and elevation with aircraft potential

JULY 15 85L7

1738:44.06

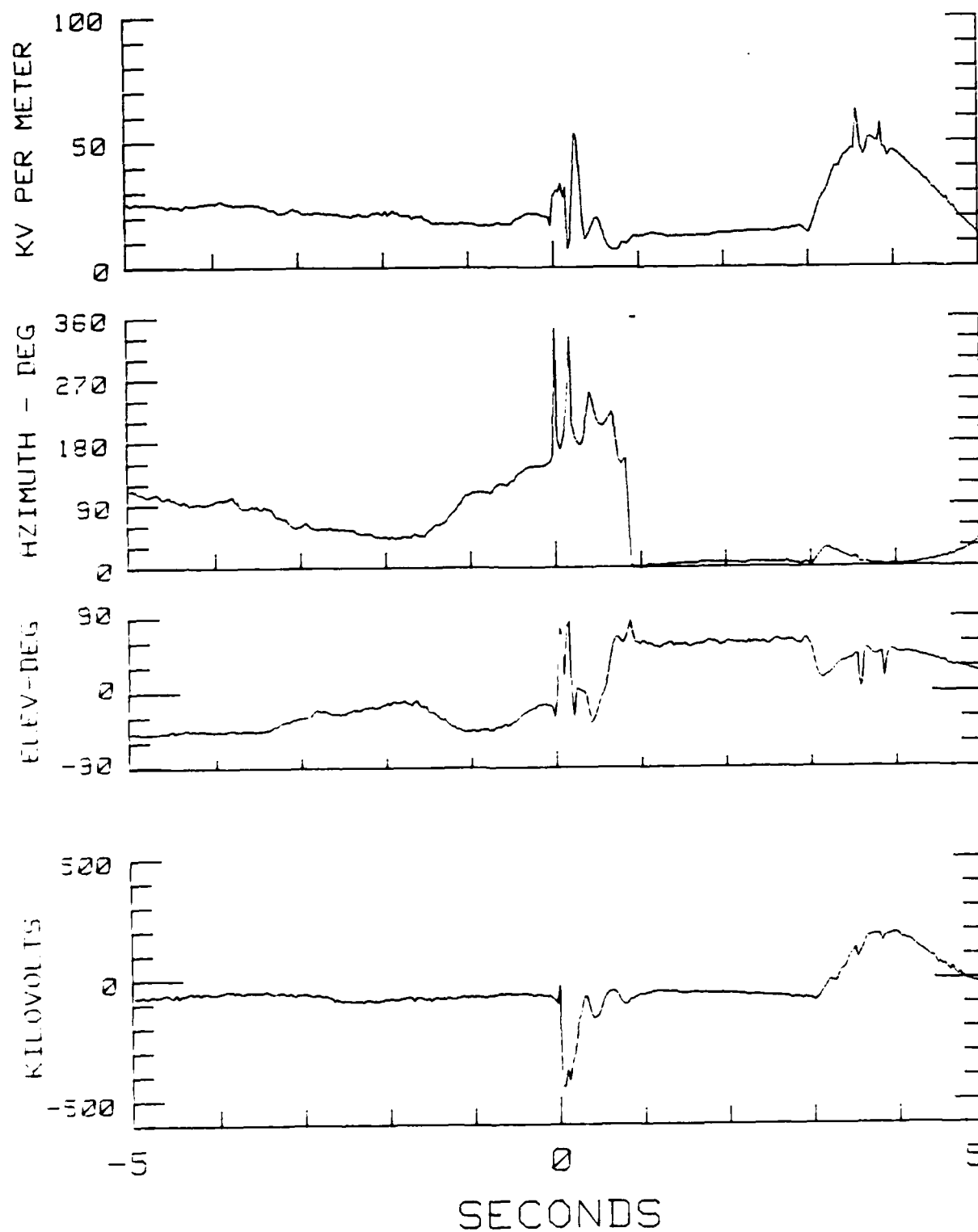


Fig. 76 - Vector field magnitude, azimuth, and elevation with aircraft potential

JULY 15 85 L7

1742:24.29

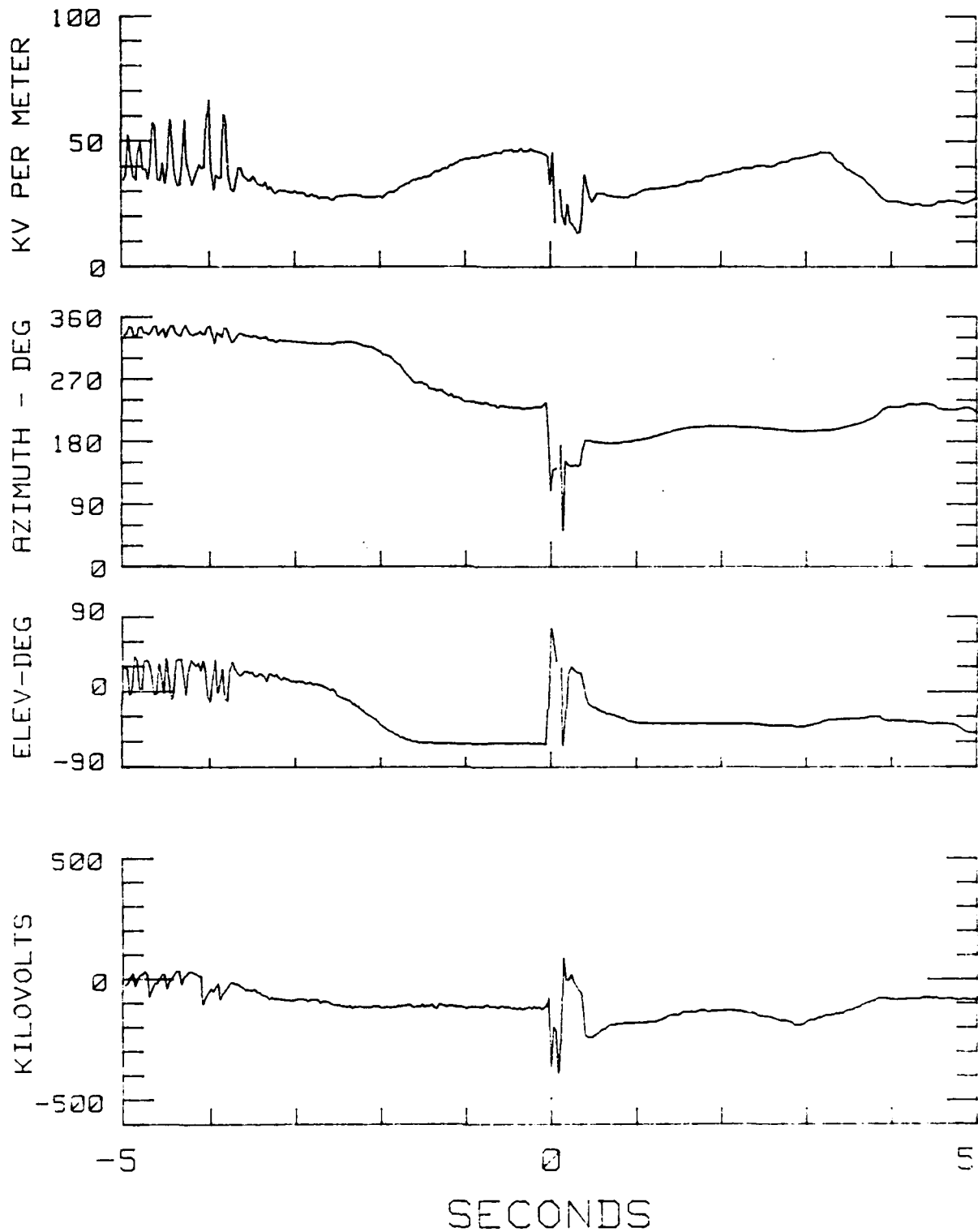


Fig. 77 — Vector field magnitude, azimuth, and elevation with aircraft potential



JULY 1585L7

1824:18.23

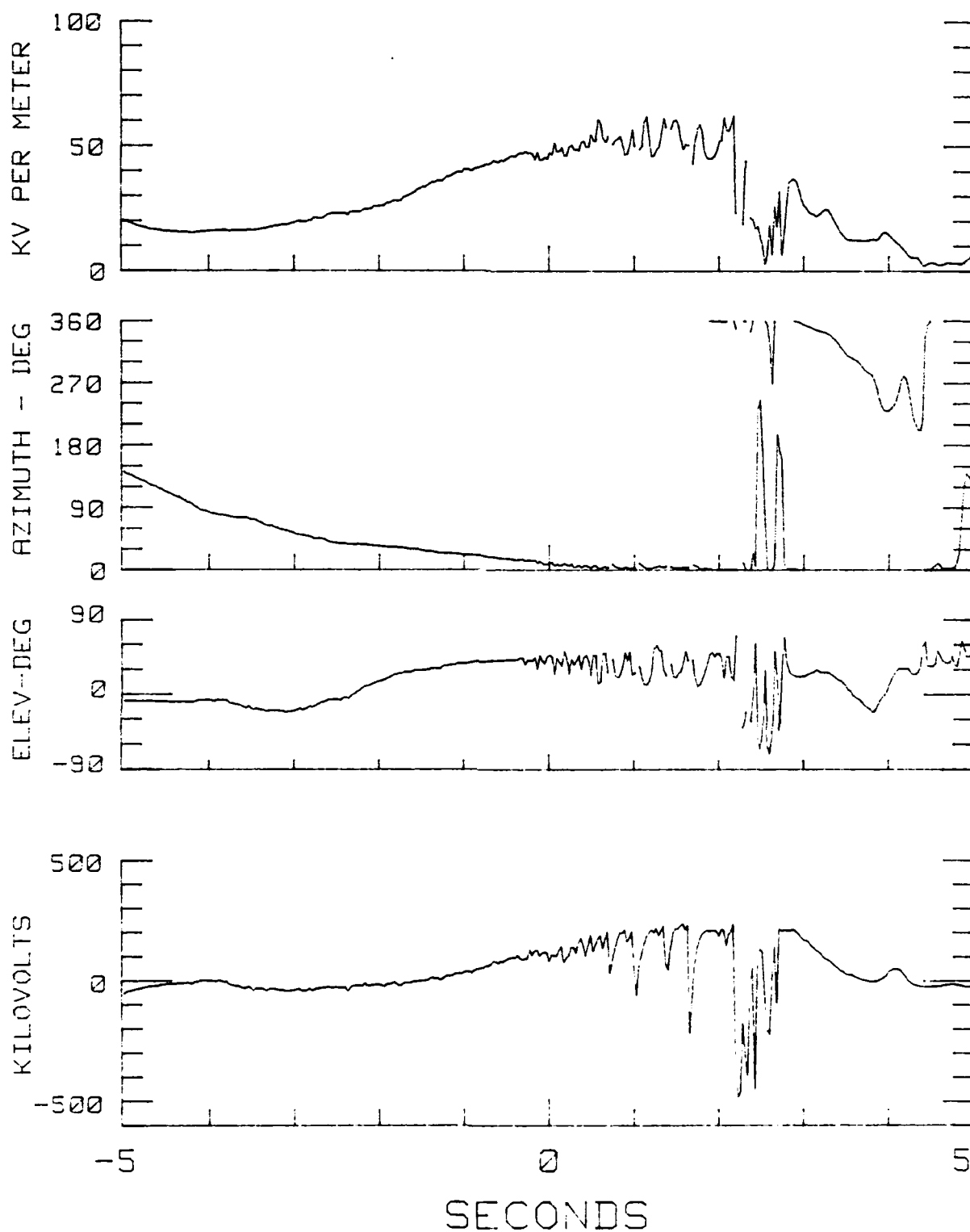


Fig. 78 — Vector field magnitude, azimuth, and elevation with aircraft potential

JULY 15 85L7

1854:39.89

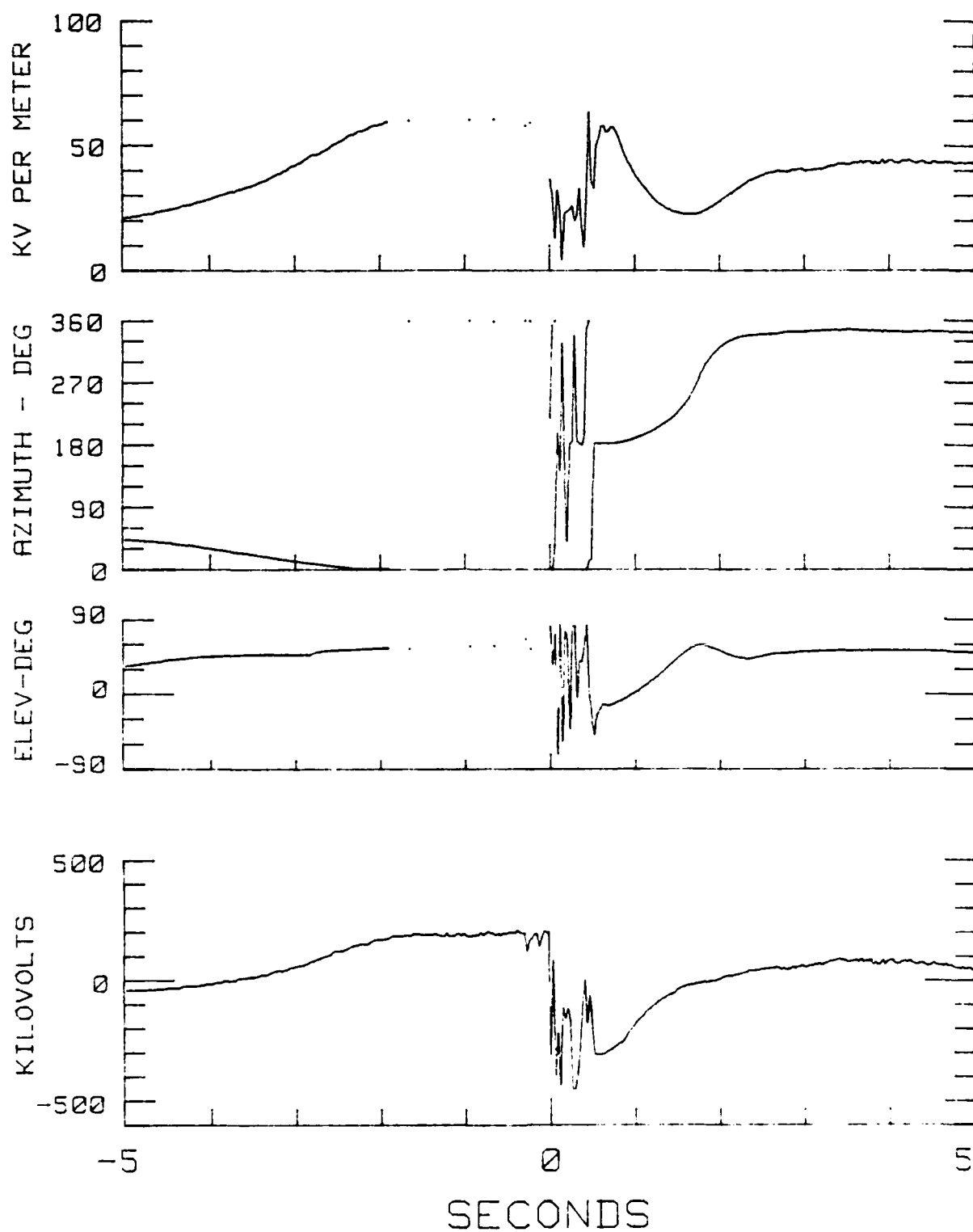


Fig. 79 — Vector field magnitude, azimuth, and elevation with aircraft potential

JULY 15 85L7

1940:56.51

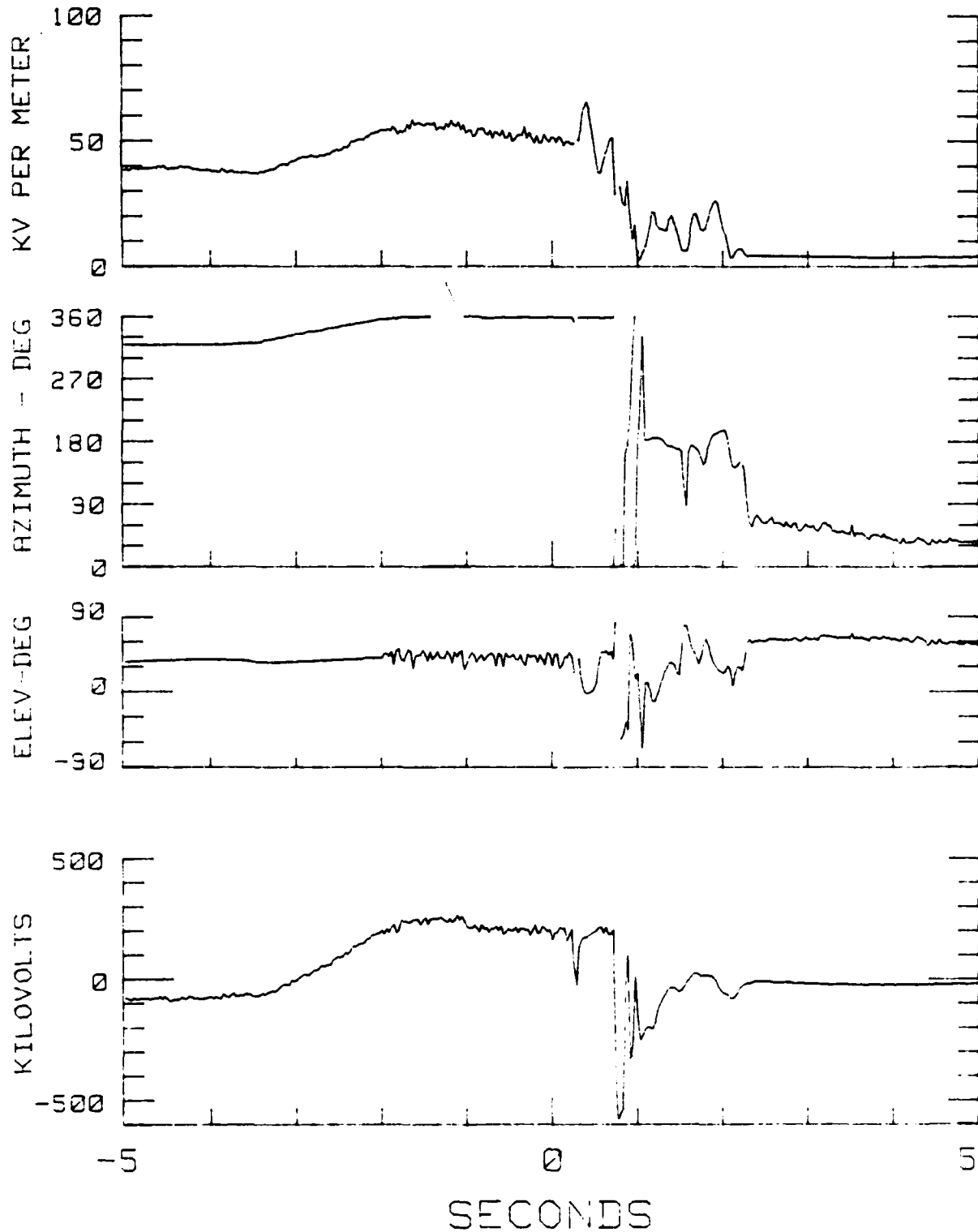


Fig. 80 — Vector field magnitude, azimuth, and elevation with aircraft potential

JULY 15 85L7

1944:34.71

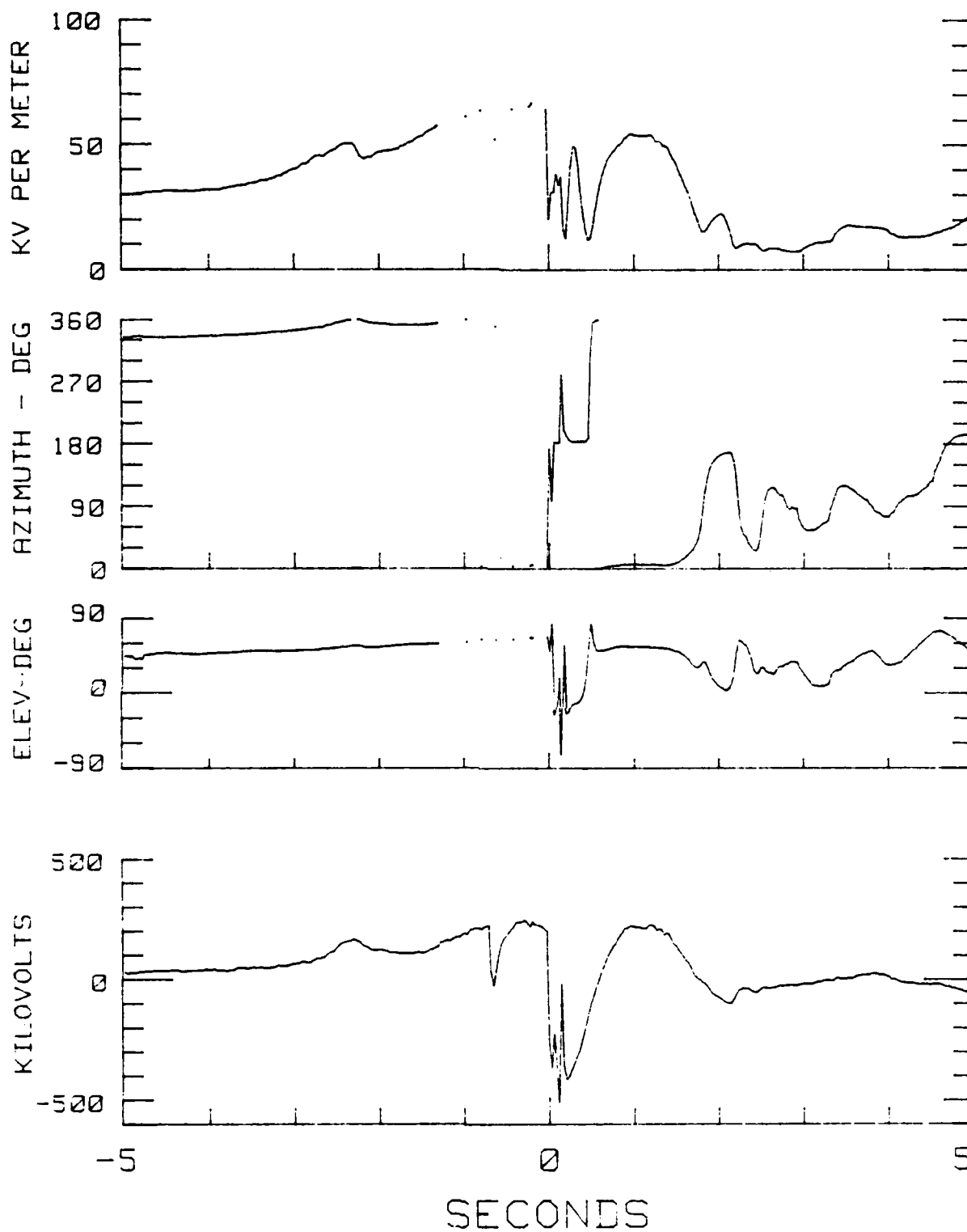


Fig. 81 — Vector field magnitude, azimuth, and elevation with aircraft potential

JULY 15 85L7

1949:16.74

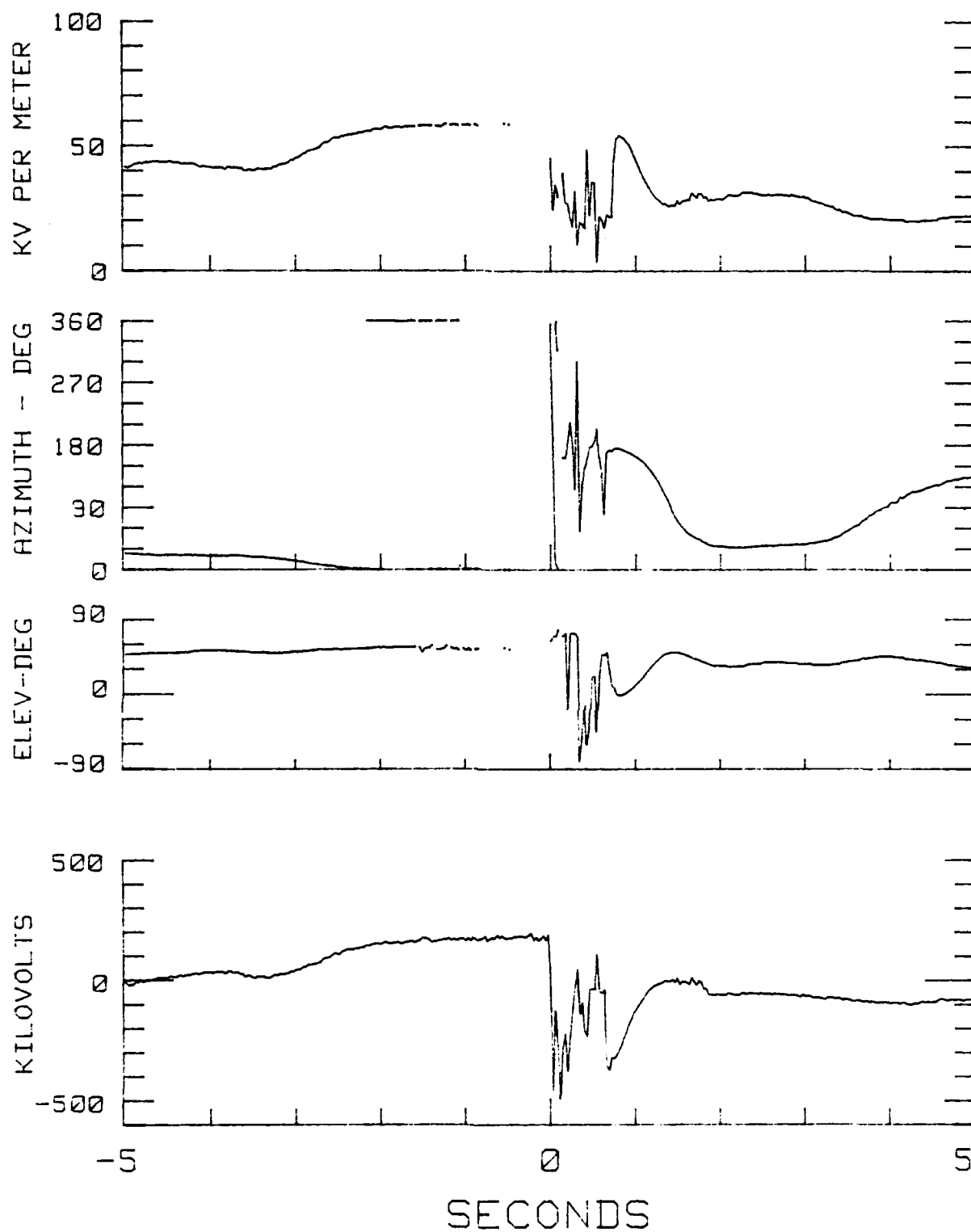


Fig. 82 — Vector field magnitude, azimuth, and elevation with aircraft potential

JUL 15 85 L1

2056:26.94

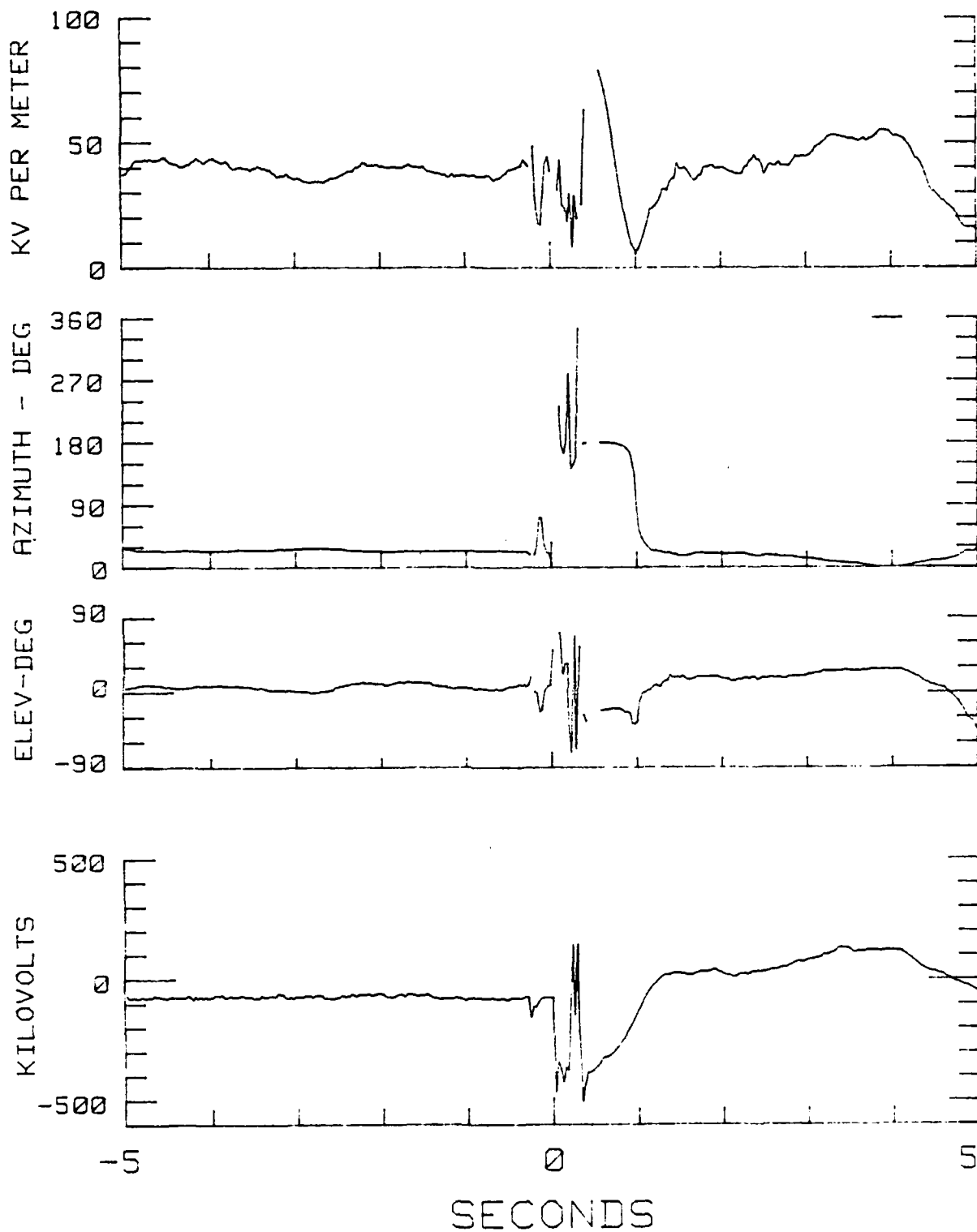


Fig. 83 — Vector field magnitude, azimuth, and elevation with aircraft potential

JULY2685L5

2321:20.91

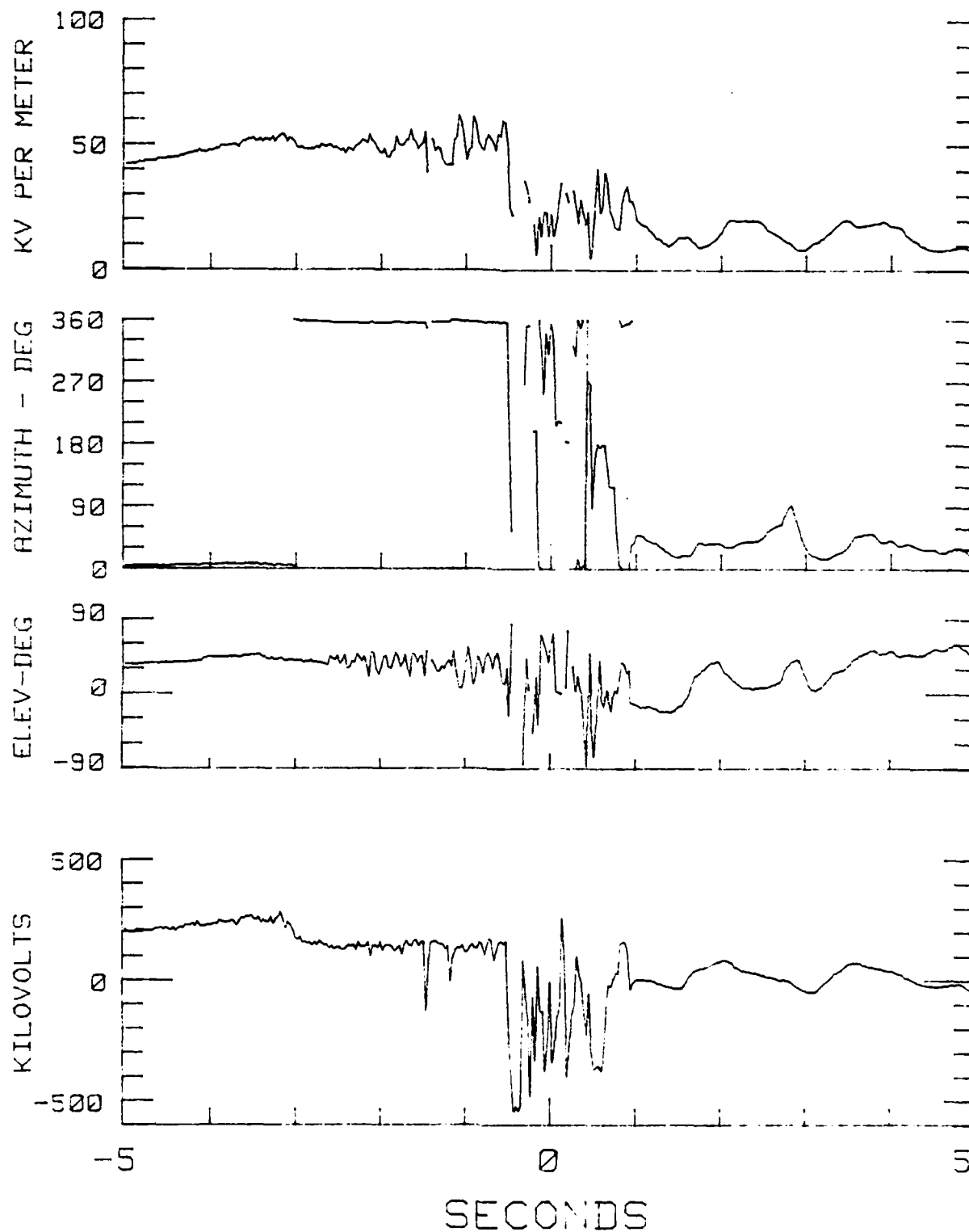


Fig. 84 — Vector field magnitude, azimuth, and elevation with aircraft potential

JULY2685L5

2333:23.34

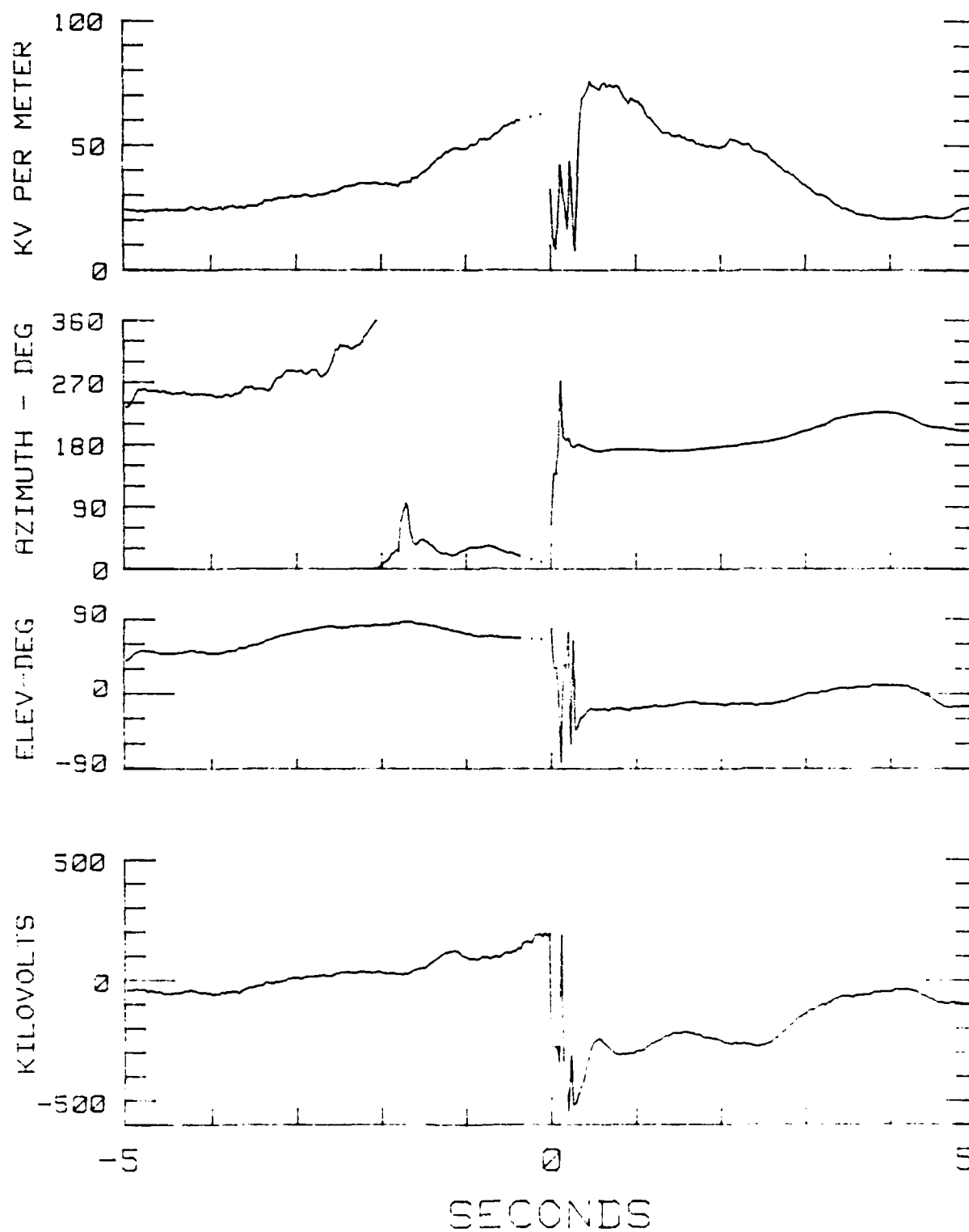


Fig. 85 — Vector field magnitude, azimuth, and elevation with aircraft potential



JULY2685L5

2351:58.13

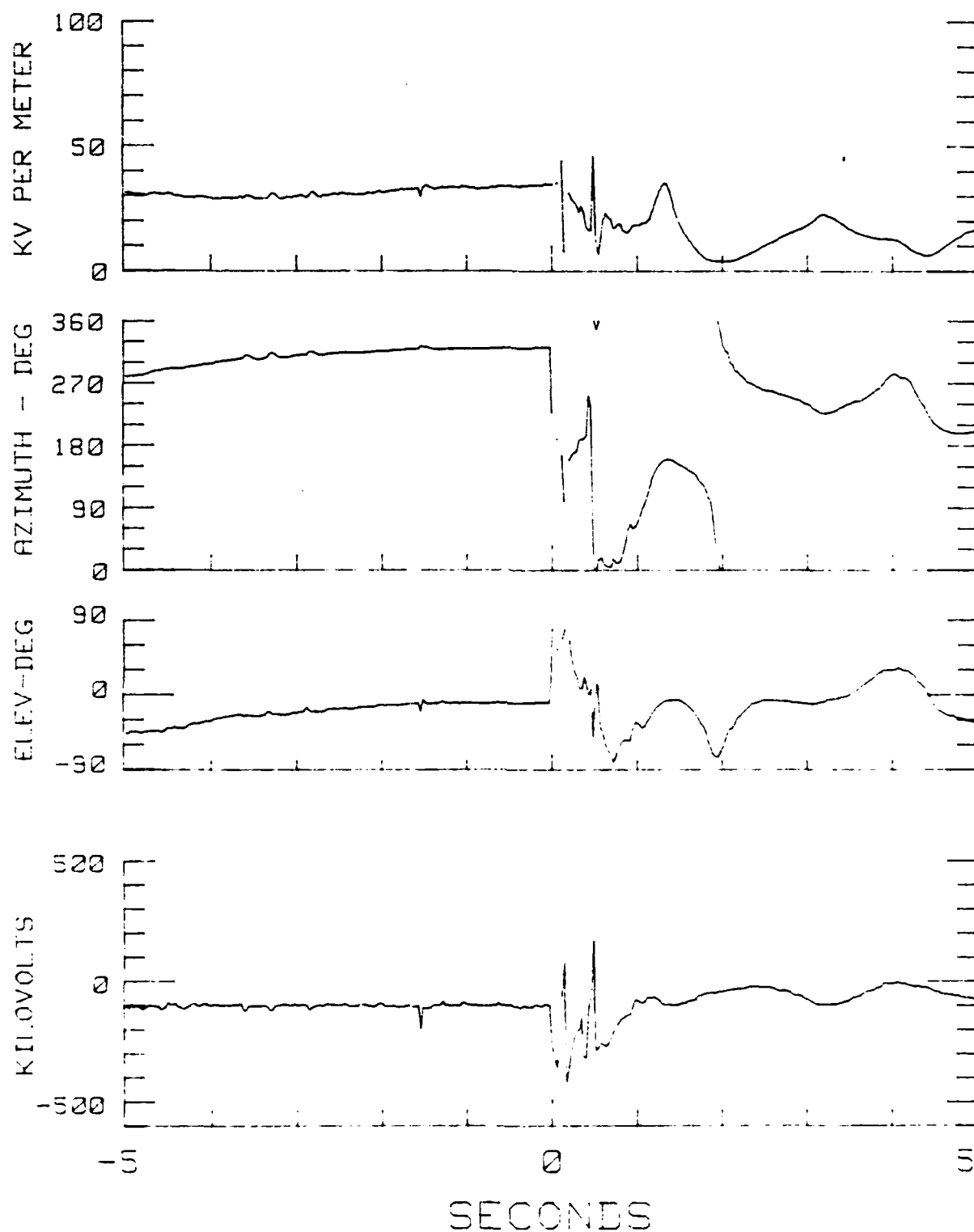


Fig. 86 — Vector field magnitude, azimuth, and elevation with aircraft potential

JULY2785L5

0004:19.72

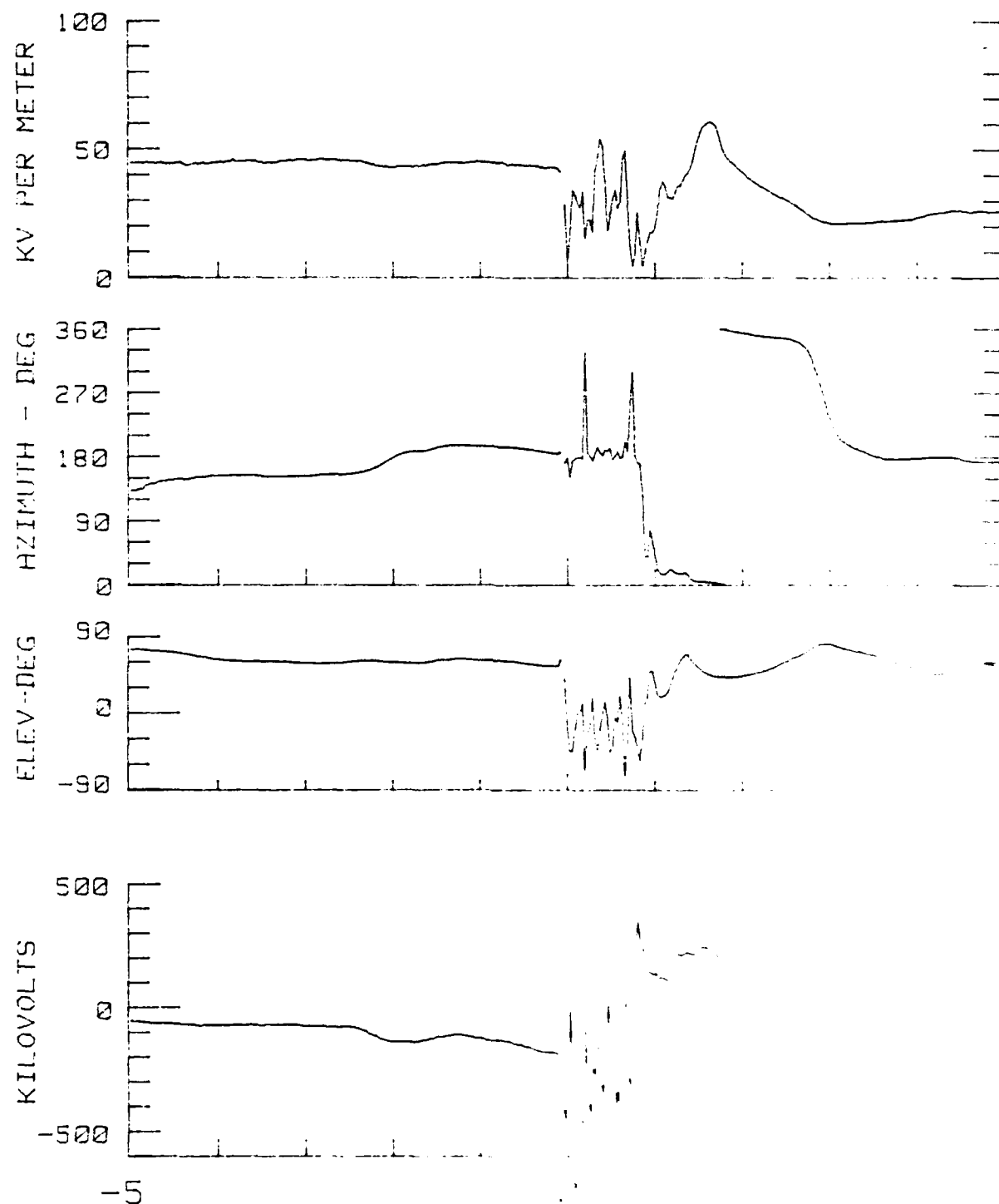


Fig. 87 — Vector field magnitude azimuth

AD-A188 012

VECTOR ELECTRIC FIELDS MEASURED IN A LIGHTNING  
ENVIRONMENT(U) NAVAL RESEARCH LAB WASHINGTON DC  
R V ANDERSON ET AL. 07 APR 87 NRL-NR-5899

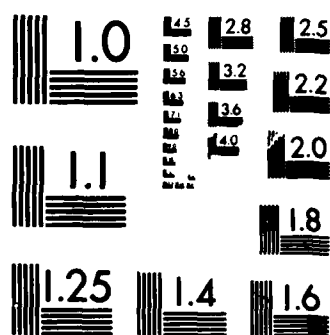
2/2

UNCLASSIFIED

F/G 4/1

NL





MICROCOPY RESOLUTION TEST CHART  
NATIONAL BUREAU OF STANDARDS-1963-A

JULY2785L5

0014:55

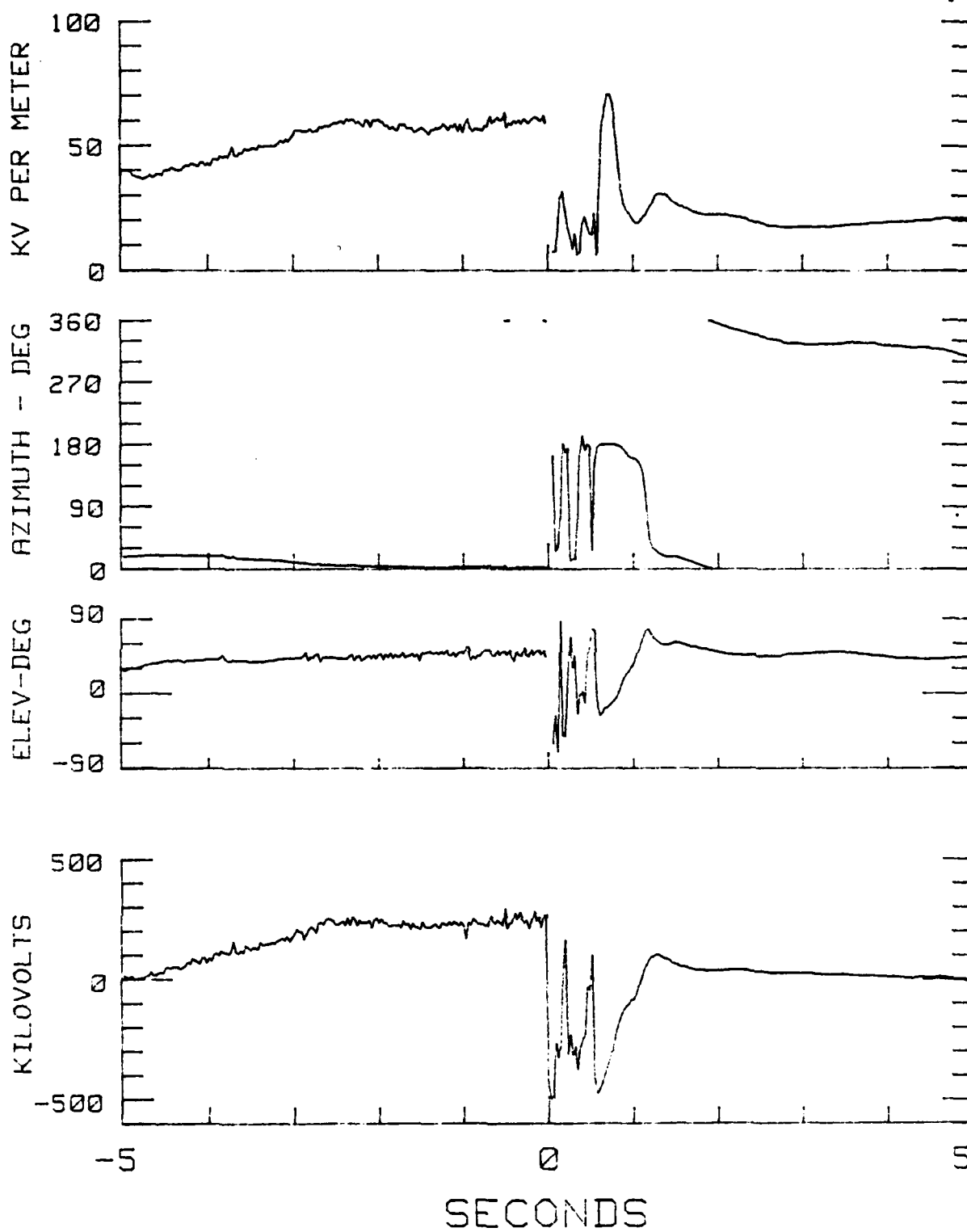


Fig. 88 — Vector field magnitude, azimuth, and elevation with aircraft potential

JULY3085L2

2028:18.51

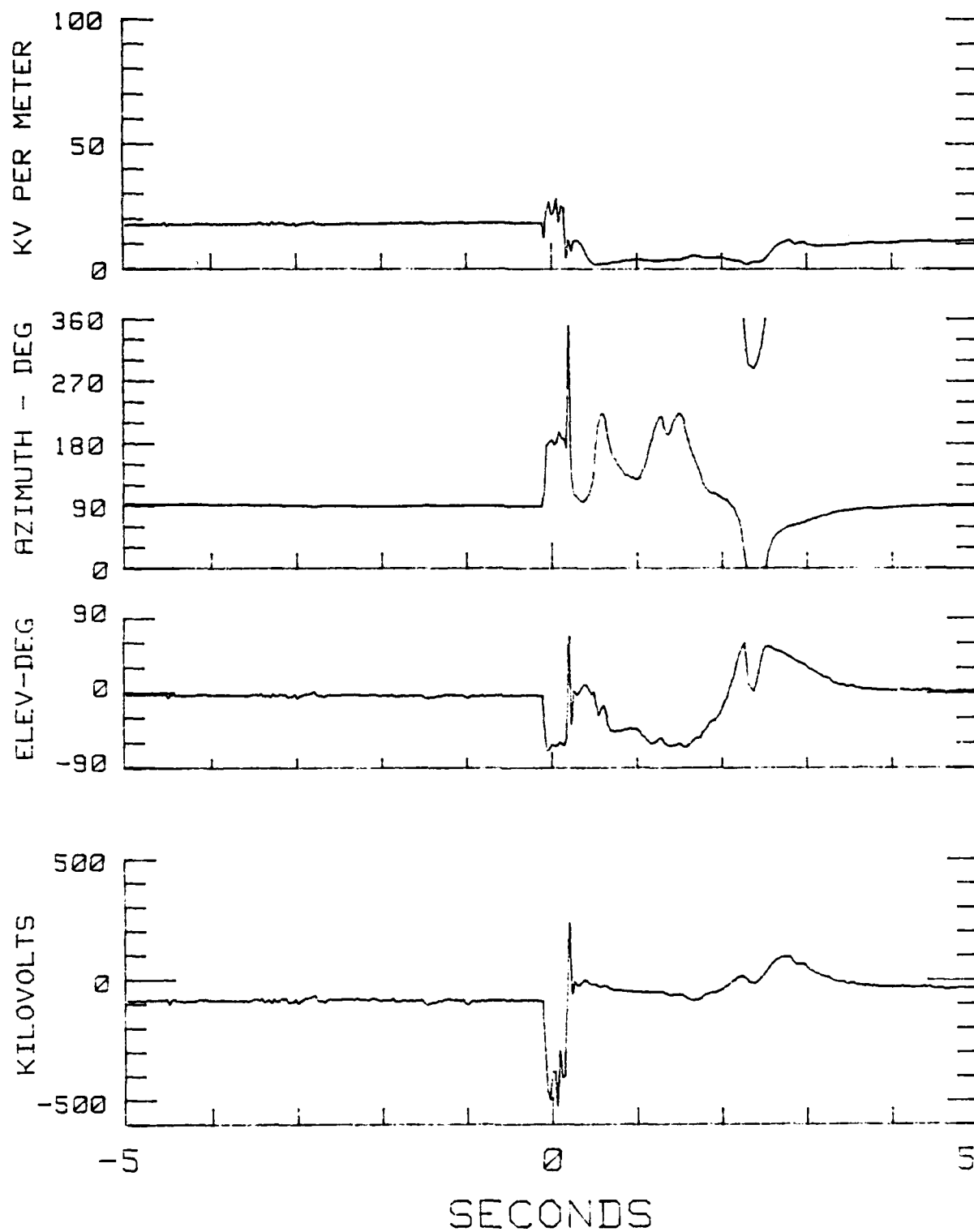


Fig. 89 — Vector field magnitude, azimuth, and elevation with aircraft potential

JULY3085L2

2118:33.37

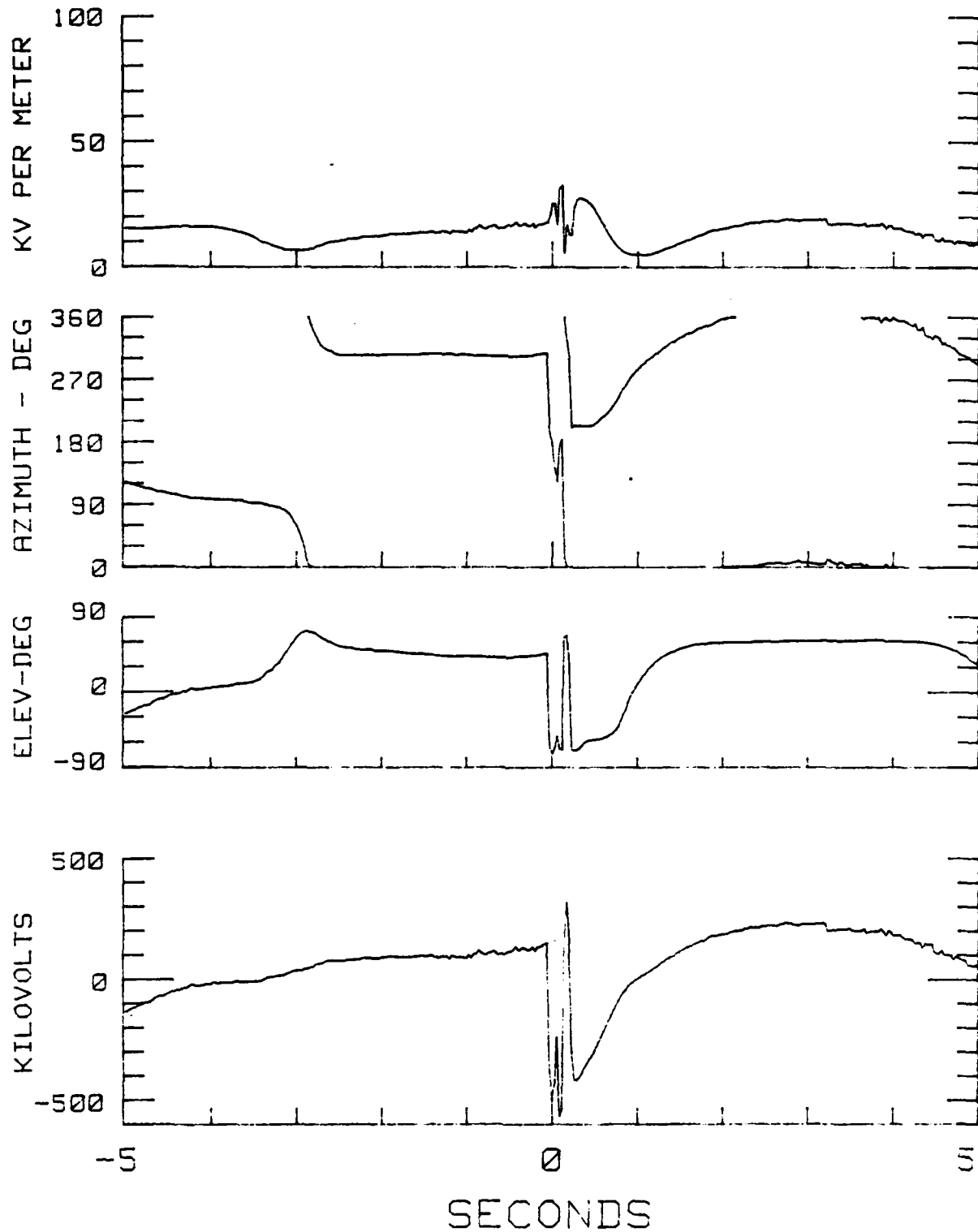


Fig. 90 — Vector field magnitude, azimuth, and elevation with aircraft potential

AUG0385L1

1946:08.31

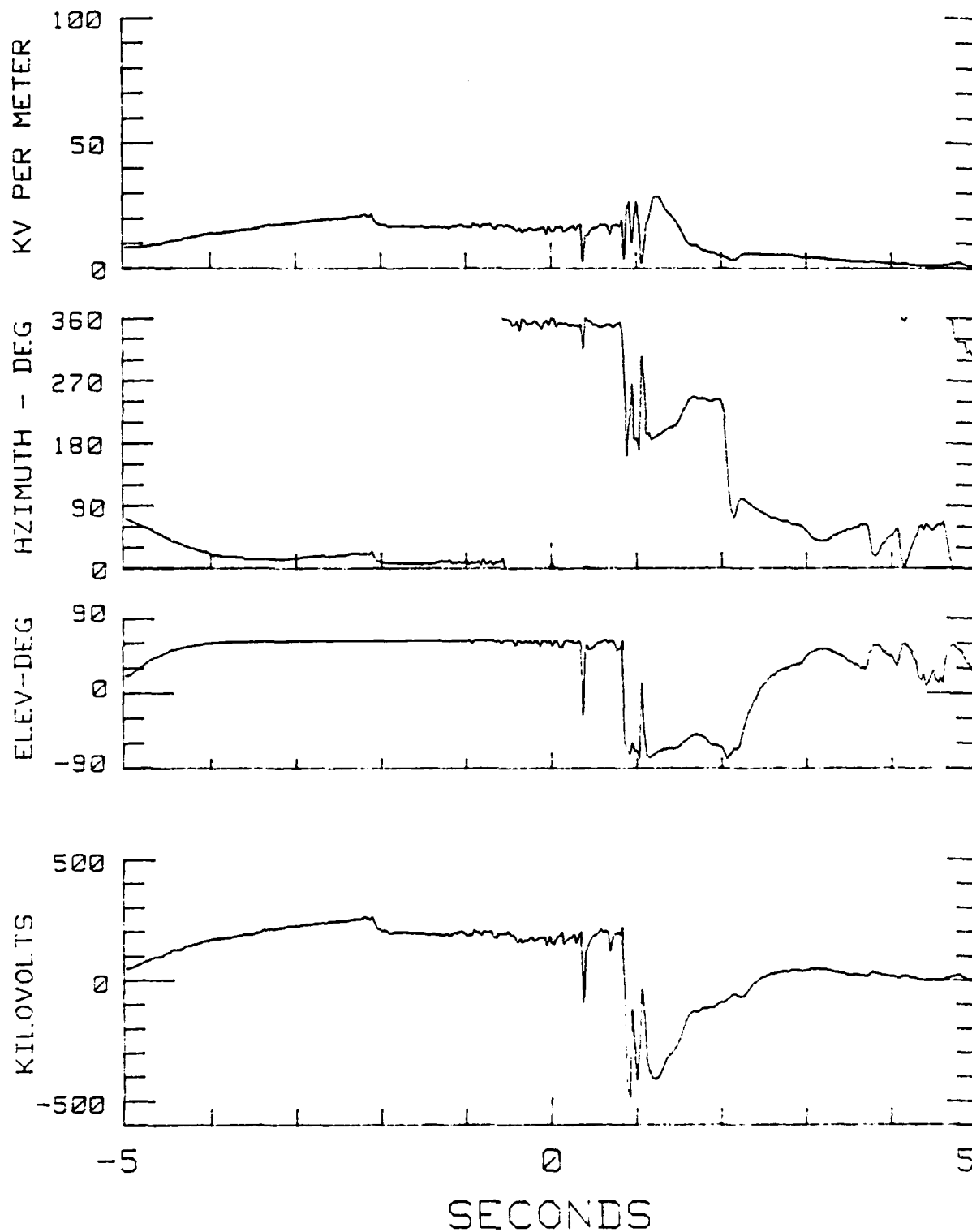


Fig. 91 — Vector field magnitude, azimuth, and elevation with aircraft potential



AUG0885L2

2033:32.77

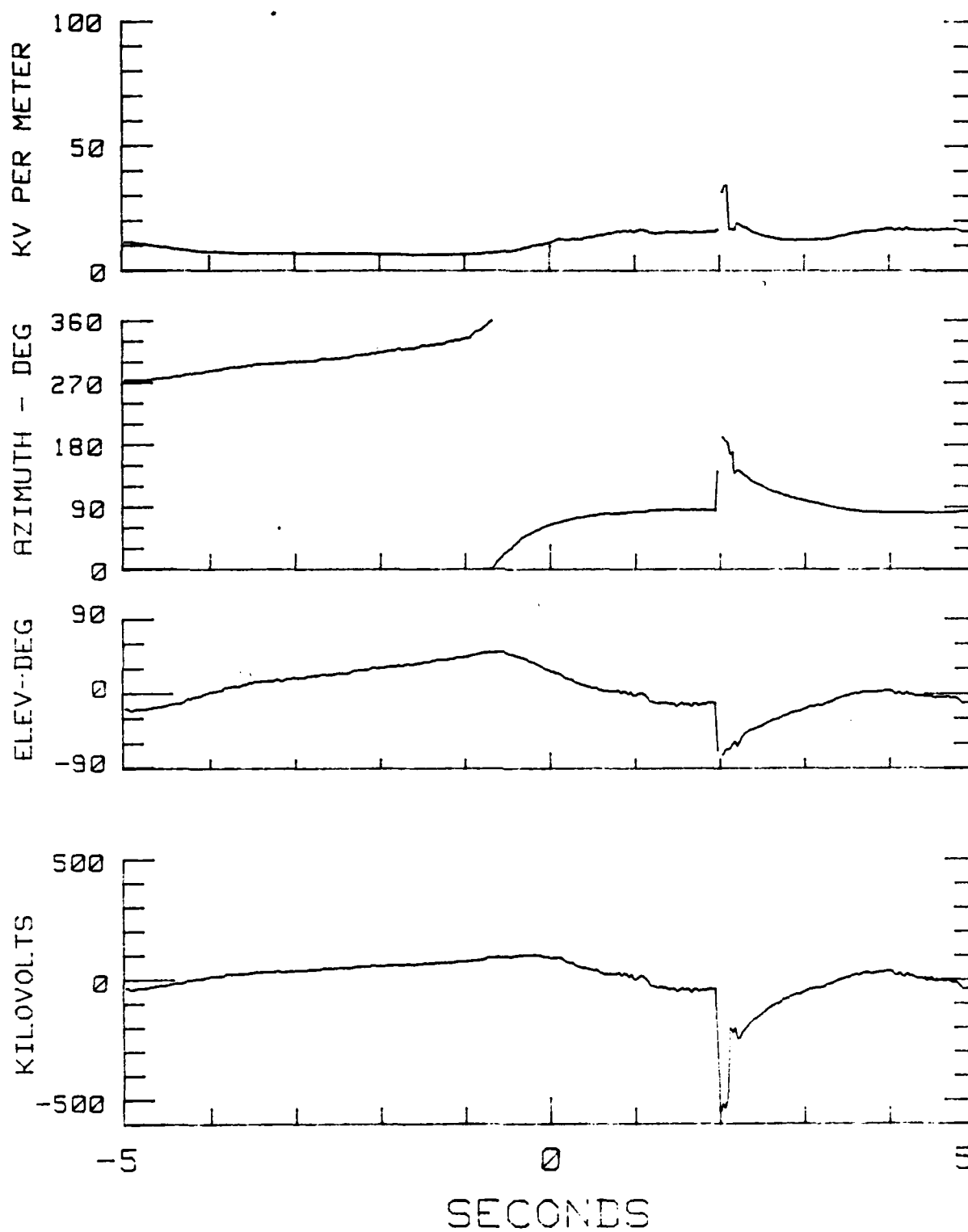


Fig. 92 — Vector field magnitude, azimuth, and elevation with aircraft potential

AUG0885L2

2049:46.63

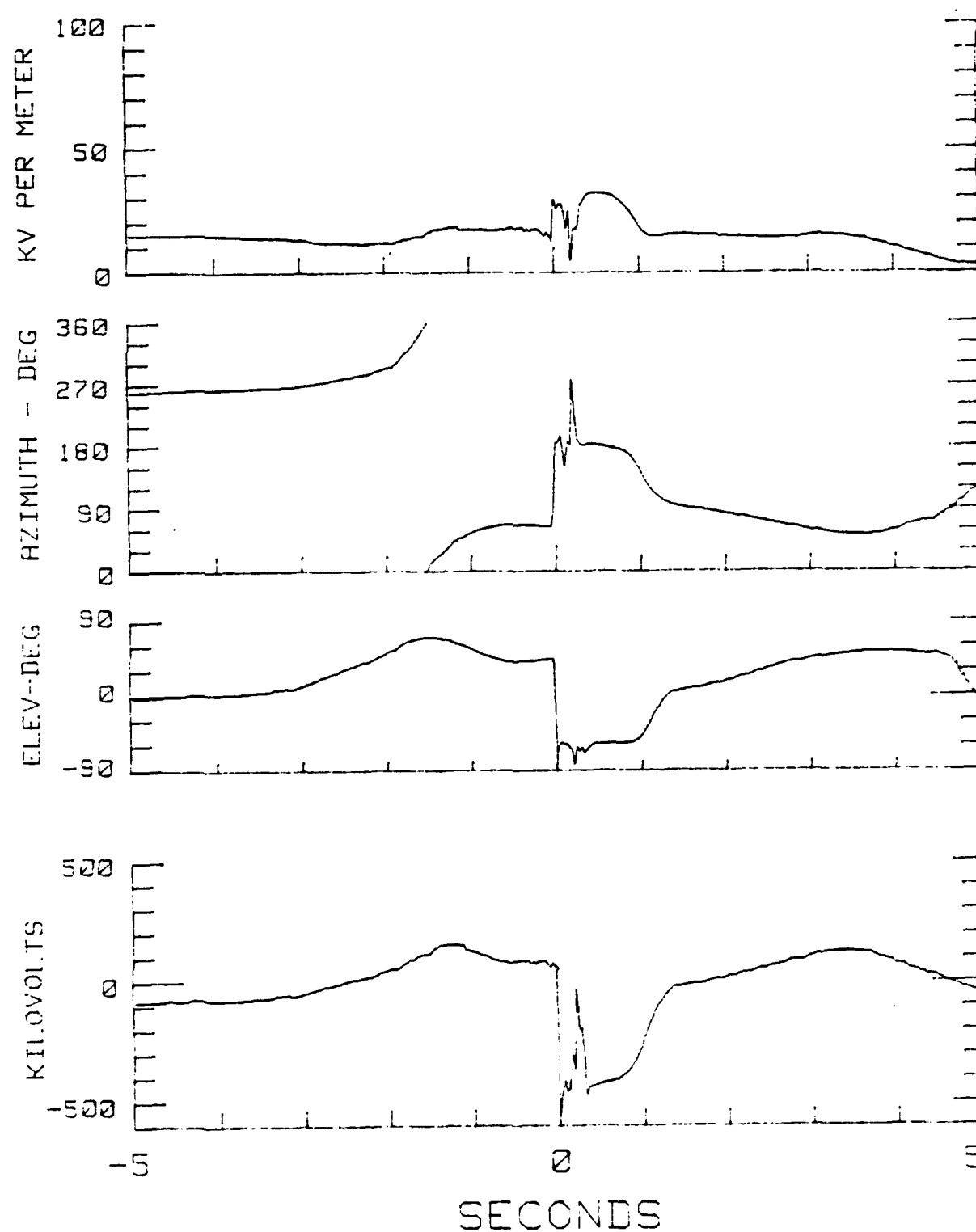


Fig. 93 — Vector field magnitude, azimuth, and elevation with aircraft potential

AUG3085L2

2227:08.29

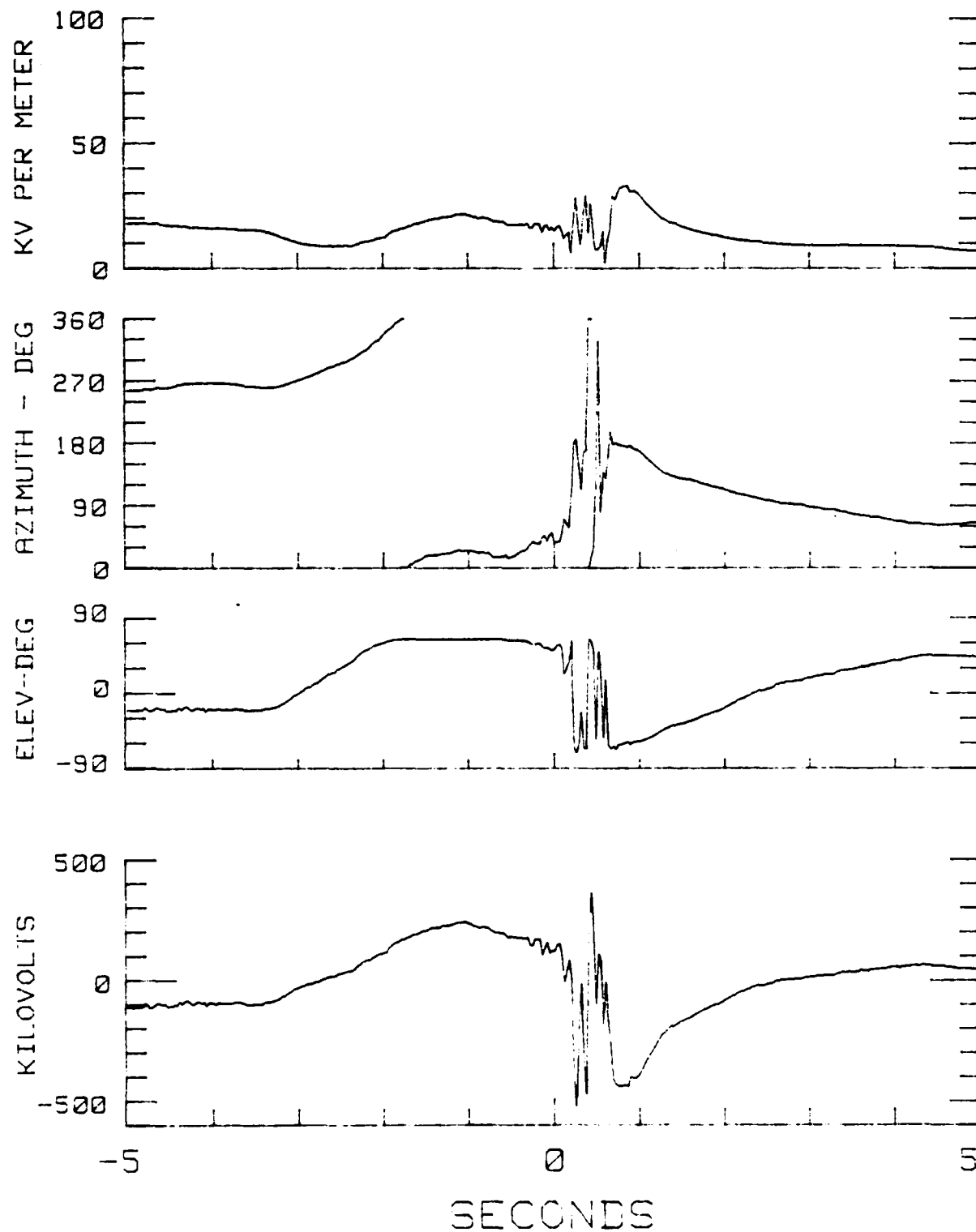


Fig. 94 — Vector field magnitude, azimuth, and elevation with aircraft potential

AUG3085L2

2234:42.74

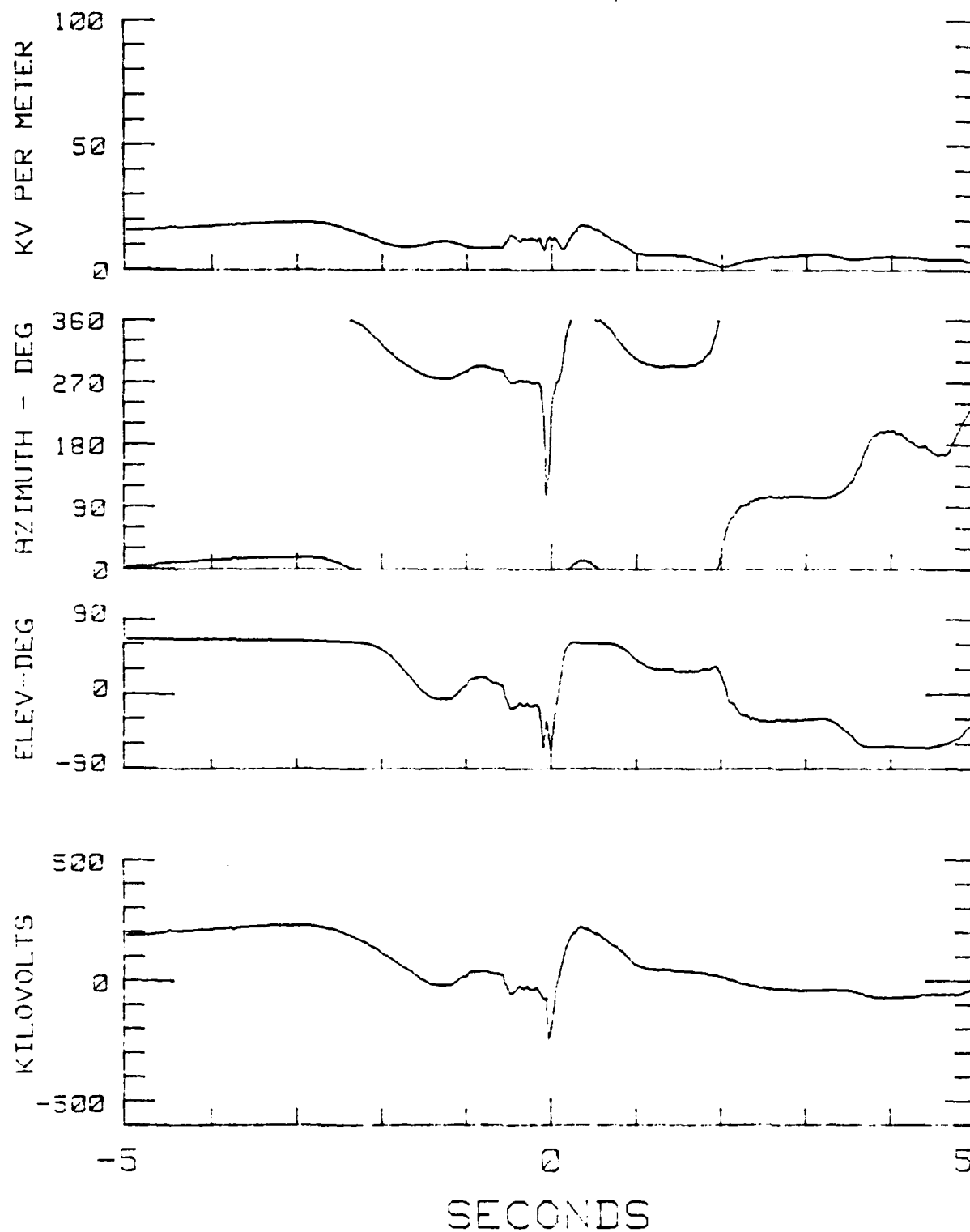


Fig. 95 — Vector field magnitude, azimuth, and elevation with aircraft potential

END

5-87

DTIC